

**TRIBOLOGY OF POLYMER FILM WITH HARD
INTERLAYERS ON SI SURFACE - ROLE OF SURFACE
ENERGY ON ADHESION AND STATIC FRICTION**

MYO MINN

NATIONAL UNIVERSITY OF SINGAPORE

2009

**TRIBOLOGY OF POLYMER FILM WITH HARD
INTERLAYERS ON SI SURFACE - ROLE OF SURFACE
ENERGY ON ADHESION AND STATIC FRICTION**



MYO MINN

(B. E., YTU, M. Sc., NUS)

**A THESIS SUBMITTED
FOR THE DEGREE OF DOCTOR OF PHILOSOPHY
DEPARTMENT OF MECHANICAL ENGINEERING
NATIONAL UNIVERSITY OF SINGAPORE**

2009

Preface

This thesis is submitted for the degree of Doctor of Philosophy in the Department of Mechanical Engineering, National University of Singapore under the supervision of Dr. Sujeet Kumar Sinha. All work in this thesis is to the best of my knowledge original unless reference is made to other work. No part of this thesis has been submitted for any degree or qualification at any other Universities or Institutions. Part of this thesis has been published/ accepted and under review for publication as listed below:

Journal articles

1. **Minn, M., Sinha, S. K., Lee, S.-K. and Kondo, H.** (2006) 'High-speed tribology of PFPEs with different functional groups and molecular weights coated on DLC', *Tribology Letters*, **24** (1), 67-76.
2. **Minn, M. and Sinha, S. K.** (2008) 'DLC and UHMWPE as hard/soft composite film on Si for improved tribological performance', *Surface & Coatings Technology*, **202**, 3698-708.
3. **Minn, M., Leong, Y. H. and Sinha, S. K.** (2008) 'Effects of interfacial energy modification on the tribology of UHMWPE coated Si', *Journal of Physics D: Applied Physics*, **41**, 055307.
4. **Minn, M. and Sinha, S. K.** (2009) 'Molecular orientation, crystallinity, and topographical changes in sliding and their frictional effects for UHMWPE film', *Tribology Letters*, **34**, 133-140.

-
5. **Minn, M. and Sinha, S. K.** (2010) 'The frictional behaviors of UHMWPE film with different surface energies at low normal loads', *Wear*, **268**, 1030-36.
 6. **Minn, M. and Sinha, S. K.** 'Tribology of UHMWPE film on Si substrate with CrN, TiN and DLC as intermediate layers', Accepted to be published in *Thin Solid Films*.

Book chapters

1. **Minn, M. and Sinha, S. K.** (2009) *Tribology of polymer thin films on modified Si substrate*, in *Polymer Tribology*, (Imperial College Press, London), 660-688.
2. **Satyanarayana, N., Minn, M., Samad, M. A. and Sinha, S. K.** (2009) *Polymer films*, in *Encyclopedia of Tribology*, (Springer).

Conference papers/presentations

1. **Minn, M. and Sinha, S. K.** (2007) 'Friction and wear properties of DLC/UHMWPE composite film', *STLE/ASME International Joint Tribology Conference*, 22-24 Oct., San Diego, California, USA, IJTC2007-44242-856.
2. **Minn, M. and Sinha, S. K.** (2008) 'Correlation between surface energy and friction on UHMWPE and silicon surfaces', *2nd International Conference on Advanced Tribology*, 3-5 Dec., Singapore, iCAT391.

3. **Leong, Y. H., Minn, M. and Sinha, S. K.** (2008) ‘Effects of surface wettability on tribology of UHMWPE film coated Si’, *2nd International Conference on Advanced Tribology*, 3-5 Dec., Singapore, iCAT392.
4. **Satyanarayana, N., Minn, M. and Sinha, S. K.** (2009) ‘Nano-lubrication of Si surface using dendrimer-mediated perfluoropolyether films for Micro-Electro-Mechanical systems applications’, Presented at *ICMAT2009*, 29 Jun.-3 Jul., Singapore, U54.
5. **Minn, M., Satyanarayana, N. and Sinha, S. K.** (2009) ‘Tribology of perfluoropolyether films on hydrogen-terminated Si surface’, Presented at *ICMAT2009*, 29 Jun.-3 Jul., Singapore, U55.
6. **Satyanarayana, N., Minn, M. and Sinha, S. K.** (2009) ‘Tribology of dendrimer-mediated perfluoropolyether films on Si surface for micro-electro mechanical systems applications’, *Proceedings of the World Tribology Congress IV*, 06-11 Sept., Kyoto, Japan, WTC2009-90849.
7. **Minn, M. and Sinha, S. K.** (2009) ‘The surface energy effects on static friction for soft and hard materials at low loads’, *Proceedings of the World Tribology Congress IV*, 06-11 Sept., Kyoto, Japan, WTC2009-91030.

Acknowledgements

This dissertation could not have been finished without the generous guidance, help and support from the following individuals. This is a great opportunity to express my sincere thanks to all I am deeply indebted. Without a doubt, the first person I would like to express my earnest gratitude is my supervisor, Dr. Sujeet Kumar Sinha for giving me a great opportunity to work with him, useful advice and guidance, encouragement and moral support through out my four years period of PhD. For not only giving advice in academic research but also in personal life, I am pleased to thank him again. I would also like to thank Dr. Satyanarayana Nalam for helping me whenever and whatever I needed since I joined to the current tribology group. I would like to say thanks to Prof. Seh Chun Lim and Dr. Zeng Kaiyang for their support while I am studying in NUS. This is also a great chance to express my respect to many scientists (Dr. P. H. Kasai, Dr. H. Kondo, Prof. N. Spencer, Prof. S. K. Biswas, Prof. D. Hargreaves, Prof. Z. Rymuza and Dr. S. Hsu) who visited to our Lab and shared their research ideas.

I am also grateful to the Material Science Lab staff, Mr. Thomas Tan Bah Chee, Mr. Abdul Khalim Bin Abdul, Mr. Ng Hong Wei, Mr. Maung Aye Thein, Mr. Juraimi Bin Madon and Mrs. Zhong Xiang Li for their continual support and assistance in many ways. It is also grateful to thank Ms. Shen Lu and Ms. Toh Mei Ling of IMRE (A-star) for their assistance in using Nano Indenter and FTIR.

I would like to thank all my friends in the Material Lab for their understanding and help especially Sandar.

Acknowledgements

I would also like to express my gratitude to all of my family members (including Ngadeelay) for their support and understanding, and at most my parents U Kyin Lwin and Daw Nang Htwan Yin for taking care of me throughout my life. Without their kindness and love, this work would not have been completed.

Table of Contents

Preface	i
Acknowledgements	iv
Table of Contents	vi
Summary	xiv
List of Tables	xvii
List of Figures	xix
List of Abbreviations	xxv
List of Symbols	xxvii
Chapter 1 Introduction	1
1.1 The importance of tribology	1
1.2 A brief history of tribology	2
1.2.1 Friction	2
1.2.2 Adhesion in friction	3
1.2.3 Wear	4
1.2.4 Lubrication	5
1.3 Solid lubricants	6
1.3.1 Inorganic and soft metal films	6
1.3.2 Polymeric films	7
1.4 Objectives of the thesis	10

1.5	Structure of the thesis	11
Chapter 2	Literature Review	12
2.1	General properties of polymers	12
2.2	Tribology of polymers	13
2.2.1	The friction mechanisms and types of wear of polymers	13
2.2.1.1	A brief summary of the friction mechanism of polymers	13
2.2.1.2	Types of wear	14
2.2.2	Tribology of bulk polymers	18
2.2.3	Tribology of polymer composites	19
2.2.4	Tribology of polymer thin films	21
2.2.4.1	Polymer film coating techniques	25
2.3	The properties of friction and wear resistance of bulk polymers	26
2.4	The effect of substrate hardness on the tribology of polymer film	29
2.5	The effect of surface wettability on the tribology of polymer film	30
2.6	The effect of sliding direction on friction in terms of crystallinity and molecular orientation	32
2.7	The relation between surface energy and friction	35
2.8	A summary of the research plans followed in the present thesis	37

Chapter 3	Materials and Experimental Methodologies	39
3.1	Materials	39
3.1.1	Silicon	39
3.1.2	UHMWPE	39
3.1.3	Perfluoropolyether (PFPE)	40
3.1.4	Silicon nitride ball	40
3.2	Preparation of UHMWPE film	41
3.2.1	Cleaning of Si substrate	41
3.2.2	Preparation and deposition of UHMWPE film	42
3.3	Surface analysis techniques	43
3.3.1	Contact angle	43
3.3.1.1	Types of surface wettability	43
3.3.1.2	Contact angle measurements	44
3.3.2	Nanoscratching and nanoindentation	45
3.3.3	X-ray photoelectron spectroscopy (XPS)	46
3.3.4	Fourier transform-infrared spectroscopy (FTIR)	47
3.3.5	Microscopy	47
3.3.5.1	Optical microscopy	47
3.3.5.2	Scanning electron microscopy (SEM)	48
3.3.5.3	Field emission scanning electron microscopy (FESEM)	49

3.3.6	Adhesion strength with a scratch tester	50
3.3.7	Friction and wear tests	50
Chapter 4	Tribology of DLC/UHMWPE as Hard and Soft Composite Film on Si	53
4.1	Materials and preparation of different layers	54
4.2	Experimental procedures	56
4.3	Results	57
4.3.1	Contact angle results	57
4.3.2	Roughness measurements using AFM	58
4.3.3	Nanoscratching and nanoindentation analysis	59
4.3.4	Comparison of UHMWPE film with and without DLC interface for friction and wear	61
4.3.5	Effect of UHMWPE thickness on the friction and wear	67
4.3.6	Wear mechanisms for different UHMWPE thicknesses	69
4.3.7	Discussion	70
4.4	Summary	76
Chapter 5	Tribology of UHMWPE Film with Different Hard Intermediate Layers	78
5.1	Experimental procedures	79
5.1.1	Materials	79
5.1.2	Preparation of different layers on Si substrate	79
5.1.3	Surface characterizations	80

5.1.4	Friction and wear tests	81
5.1.5	Scratch tests	82
5.2	Results and discussion	83
5.2.1	Surface analysis	83
5.2.2	Friction and wear results on hard intermediate layers	86
5.2.3	Friction and wear results of UHMWPE film with different hard intermediate layers	89
5.2.4	Polymer transfer mechanism	91
5.2.5	Critical load in scratch tests and film adhesion	93
5.2.6	Friction and wear results of Si/TiN/UHMWPE, Si/DLC57/UHMWPE and Si/DLC70/UHMWPE films at higher normal load	95
5.2.7	Effects of PFPE overcoat on composite films	95
5.3	Summary	99
Chapter 6	Effect of Interfacial Energy on the Tribology of UHMWPE Film on Si	101
6.1	Experimental procedures	102
6.1.1	Materials	102
6.1.2	Preparation of different interfaces on Si substrate	103
6.1.3	Surface characterizations	104
6.1.4	Friction and wear tests	104
6.1.5	Scratch tests	105
6.2	Results and discussion	105

6.2.1	Surface characterizations (nanoindentation and XPS peaks)	105
6.2.2	Friction and wear results	107
6.2.3	Study on wear track morphology	110
6.2.4	Optical microscopy: study of the transfer films	113
6.2.5	Effect of interfacial energy	114
6.2.6	Study of interfacial adhesive strength using scratch tests	116
6.3	Summary	121
Chapter 7	Molecular Orientation, Crystallinity, and Topographical Changes in Sliding and their Frictional Effects for UHMWPE Film	123
7.1	Experimental procedures	125
7.1.1	Materials	125
7.1.2	Friction measurements	125
7.1.3	Nanoscratching and nanoindentation	126
7.1.4	Measurement of molecular crystallinity of UHMWPE on the sliding track	127
7.1.5	Wear track profilometry	128
7.2	Results	128
7.2.1	Friction of UHMWPE film as a function of sliding cycles in the forward direction	128
7.2.2	Friction of UHMWPE film as a function of sliding cycles in the reverse direction	130
7.2.3	Friction of UHMWPE film as a function of scratch distance in nanoscratching	131

7.3	Discussion	134
7.4	Summary	141
Chapter 8	The Frictional Behaviors of UHMWPE Film with Different Surface Energies at Low Normal Loads	143
8.1	Experimental procedures	145
8.1.1	Materials and sample preparations	145
8.1.2	Contact angle measurements and surface energy analysis	146
8.1.3	Surface energy and attractive force between surfaces	148
8.1.4	Friction tests	148
8.2	Results and discussion	150
8.2.1	Surface energy and roughness	150
8.2.2	The relationship between the initial shear stress and the surface energy of UHMWPE film	153
8.2.3	The relation between the initial coefficient of friction and the surface energy on UHMWPE film	157
8.2.4	Material transfer between UHMWPE film and different surface energy balls	159
8.3	Summary	160
Chapter 9	Conclusions and Future Recommendation	162
9.1	General conclusions	162
9.1.1	Optimizing the parameters for UHMWPE film	162
9.1.1.1	Effect of thickness on tribology of UHMWPE film with and without DLC interface	163

9.1.1.2	Effect of hard intermediate layer on tribology of UHMWPE film	165
9.1.1.3	Effect of surface wettability on tribology of UHMWPE film	165
9.1.2	Effects of unidirectional dry sliding on the frictional behaviors of UHMWPE film	166
9.1.3	Effects of surface energy of UHMWPE film on friction, adhesion and wear	167
9.2	Future recommendations	169
References		170
Appendix A The Tribological Properties of Bulk Polymers		183

Summary

The shorter product life-span of most of the mechanical machine parts subjected to relative motion in sliding or rolling is due to a lack of or an improper protective coating or lubrication. Polymers are very promising materials as coatings because of their better tribological properties found in their bulk form. Though polymers have many advantages as tribological coatings, there are very limited number of research papers that have studied this important aspect of polymer films. The main objective of this doctoral research is to develop polymer thin films (with some pre-modifications) on Si in order to greatly enhance friction and wear properties of Si substrate. The choice of Si as the substrate material has been prompted because of the application of Si, a poor tribological material, in many microsystems such as micro-electro mechanical systems (MEMS).

In this study, ultra-high molecular weight polyethylene (UHMWPE) is selected as the polymer for depositing film because bulk UHMWPE has low coefficient of friction coupled with very high wear resistance among all other polymers. Direct coating of UHMWPE film onto Si surface can increase wear durability to some extent but it is not sufficient for industrial applications where the desired life of the products is in millions of cycles. There are two main reasons for low wear durability of UHMWPE film on Si. First, polymer film is soft and easy to get penetrated by hard asperities of the counterface that increase friction due to contact with the substrate and reduce wear durability. Second, the surface wettability of Si controls the adhesion of

the polymer film to the substrate and thus film can be easily removed (peeled) under continuous sliding if adhesion of the film with the substrate is poor.

Hence, as the first approach in this work, hard diamond-like carbon (DLC) is introduced as an intermediate layer between Si substrate and UHMWPE film in order to increase the load bearing capacity of the polymer film. DLC offers penetration resistance and promotes wear durability of soft UHMWPE film. DLC (with different hardness values) and some other hard intermediate layers, such as CrN and TiN, on Si have shown remarkable improvement (at least by ten orders of magnitude) in the wear durability of the UHMWPE film when the thickness of the polymer film is optimized.

In the second approach, the wettability (as controlled by the surface energy) of the Si surface is modified (using 3-Aminopropyltrimethoxysilane (APTMS) and Octadecyltrichlorosilane (OTS) SAMs, heating, -H termination etc) before UHMWPE is coated onto it, since the wetting property of Si is an important criterion in achieving strong adhesion and wear durability. Studies on a range of surface wettability of Si have shown that the existence of extreme hydrophilic or hydrophobic properties prior to film coating provides low wear durability. An optimized surface wettability between these two extremes provides high wear durability for the top UHMWPE film.

In the last part of this thesis, the effect of surface energy on the initial coefficient of friction (static friction) of the polymer film has been studied. The correlation between the initial coefficient of friction and surface energy is modeled and compared with the experimental results. Based on the experimental evidences, we propose an exponential relation between the initial coefficient of friction and the pull-

off force (or the attractive force due to surface energy difference between two solids) between surfaces.

The main conclusion drawn from this thesis is that the friction and wear durability of UHMWPE film (or any polymer film) can be improved by orders of magnitude by using different hard interface layers between Si substrate and UHMWPE film and by modifying the surface wettability of Si prior to film deposition. Further, low load tribological interactions involving polymer surfaces is greatly influenced by the surface energies of the interacting surfaces.

List of Tables

Table 2.1	Classifications of wear of polymers.	15
Table 2.2	Mechanical properties of bulk UHMWPE and PEEK.	27
Table 3.1	Physical properties of UHMWPE, as provided by the supplier.	40
Table 3.2	Physical properties of PFPE (Zdol 4000).	41
Table 4.1	Water contact angles of different surfaces on Si.	58
Table 4.2	Mechanical properties and other parameters for different samples.	61
Table 5.1	Water contact angles and nanohardness for different intermediate hard layers.	84
Table 5.2	The microhardness, critical loads in scratching and wear lives of UHMWPE with different intermediate hard layers. The applied load used for wear life determination is 40 mN.	85
Table 5.3	The initial coefficient of friction and wear durability of different intermediate layers. The ball and the film are worn at failure in all cases.	88
Table 6.1	Water contact angles and wear lives for different interfacial modifications on Si.	115
Table 6.2	The critical load as a function of different interfaces; the scratch length is 1 cm and the scratching velocity is 0.1 mm/s.	116
Table 7.1	The hardness and roughness of UHMWPE film with different number of sliding cycles.	136
Table 8.1	Surface tension component and parameters of distilled water, ethylene glycol, methanol and hexadecane in mJ/m^2 .	147

Table 8.2	A summary of surface roughness, treatments and surface energy of silicon nitride ball, UHMWPE film and Si surface. PFPE refers perfluoropolyether (Z-dol 4000) which was coated as 3-4 nm film on the solids mentioned.	151
Table 8.3	The attractive force, F_o between Si_3N_4 and UHMWPE film with different surface energies.	153
Table 8.4	The Poisson's ratio and elastic modulus for silicon nitride ball and UHMWPE film.	154
Table 9.1	The summary of the optimizing parameters of UHMWPE film thickness, interface layer thickness and surface wettability of Si substrate with respect to their wear durability. All tests were conducted with a normal load of 40 mN at a range of sliding (0.052 m/s to 0.1 m/s) except some cases that are mentioned in remarks.	164
Table A.1	Tribological properties of bulk properties.	183

List of Figures

Figure 1.1	A schematic diagram of the effect of hard and soft layers on the real contact area, A_r .	9
Figure 2.1	Schematic diagram of (a) adhesive, (b) abrasive and (c) fatigue wear mechanisms.	17
Figure 3.1	(a) Hydrophilic and (b) hydrophobic surfaces.	44
Figure 3.2	Experimental setup for measuring contact angle.	45
Figure 3.3	(a) Optical microscopy and (b) FESEM.	49
Figure 3.4	(a) Photographs and (b) schematic diagram of ball-on-disc tribometer.	51
Figure 4.1	Schematic diagram (not to scale) of different layers coated Si substrate.	54
Figure 4.2	A demonstration of the measurement of UHMWPE film thickness using FESEM.	56
Figure 4.3	A photograph of the contact point between the ball and the film. The radius of curvature of the ball was 2 mm.	57
Figure 4.4	(a) Scratch penetration depth as a function of progressively applied normal load and (b) SEM images of the scratch deformation for Si/UHMWPE and Si/DLC/UHMWPE films. The thickness of UHMWPE is 28 μm for both cases. The progressive scratch tests were conducted using a 5 μm -radius 90°-conical shape diamond tip with scratch velocity of 10 $\mu\text{m/s}$ for a scratch distance of 500 μm . Normal load varied from 0 to 250 mN and the scratching direction is from left to right.	60
Figure 4.5	Optical images of (a) wear track on bare Si and (b) counterface ball after five cycles. The scale bars are 100 μm .	62

Figure 4.6	(a) Coefficient of friction, (b) wear life (logarithmic scale) of bare Si and Si coated with different single and composite films and (c) coefficient of friction versus sliding cycles of some films at a normal load of 40 mN and at a rotational speed of 500 rpm (linear speed is 5.2 cm/s) where UHMWPE thickness is fixed as 28 μm for all coated samples. (A1 = bare Si, A2 = Si/UHMWPE, A3 = Si/UHMWPE/PFPE, A4 = Si/DLC, A5 = Si/DLC/UHMWPE, A6 = Si/DLC/UHMWPE/PFPE)	64
Figure 4.7	Optical images of Si/UHMWPE/PFPE (column 1) and Si/DLC/UHMWPE/PFPE (column 2) surfaces (a) before the test, (b) after sliding 100,000 cycles and (c) counterface ball after 100,000 cycles. The scale bars are 50 μm .	66
Figure 4.8	(a) Coefficient of friction with respect to sliding cycles in typical runs for different thicknesses of UHMWPE in composites films of Si/DLC/UHMWPE, (b) Wear life for different UHMWPE thicknesses for Si/DLC/UHMWPE. Data are averages of three repeated tests. For 12.3 μm thick film there was no failure at 300,000 cycles of sliding when the experiments were stopped due to long test duration.	68
Figure 4.9	Wear track optical images of 3.4 μm , 6.2 μm , 12.3 μm and 28 μm UHMWPE thicknesses for Si/DLC/UHMWPE (at a normal load of 40 mN, at a rotational speed of 5.2 cm/s (500 rpm) and test radius 1 mm) against Si_3N_4 counterface ball after 10,000, 50,000 and 100,000 sliding cycles. The scale bars are 50 μm .	69
Figure 4.10	Optical images of Si_3N_4 counterface ball against Si/DLC/UHMWPE with different polymer film thicknesses (a) 3.4 μm (b) 6.2 μm (c) 12.3 μm and (d) 28 μm after sliding 100,000 cycles. Figures (a, b and c) are magnified 500 times and Figure (d) is magnified 200 times. The scale bars are 50 μm .	71
Figure 4.11	Contact area and contact pressure vs. UHMWPE thickness for Si/DLC/UHMWPE where contact area and contact pressure are theoretically calculated using Hertzian equation and nanoindentation data presented in Table 4.2.	73

Figure 5.1	(a) Schematic (not to scale) diagram of different layers coated onto Si substrate and (b) FESEM image of the cross-section of UHMWPE (white region) film on Si substrate. The scale bar is 10 μm . The thickness of the polymer film is in the range of 4-5 μm .	80
Figure 5.2	A ball on disc tribometer with two laser sensors.	82
Figure 5.3	The variation of coefficient of friction with respect to the number of sliding cycles for Si/CrN, Si/DLC15, Si/TiN, Si/DLC57 and Si/DLC70.	87
Figure 5.4	The optical images of (a) CrN, (b) TiN, (c) DLC57 and (d) DLC70 films after sliding against Si_3N_4 ball with respective number of cycles mentioned in Table 5.3. The scale bars are 100 μm .	88
Figure 5.5	(a) Coefficient of friction and (b) wear life of Si substrate coated with different composite film. The applied load was 40 mN and the rotational speed was 500 rpm (linear speed = 0.052 m/s).	90
Figure 5.6	Optical microscopy images of (a) Si/TiN/UHMWPE, (b) Si/DLC57/UHMWPE and (c) Si/DLC70/UHMWPE films (first column) after sliding against respective Si_3N_4 balls (second column) for 300,000 cycles where the normal load is 40 mN and the linear sliding speed is 0.052 m/s. The vertical or horizontal scales correspond to 100 μm .	92
Figure 5.7	The FESEM image of a scratch on Si/DLC70/UHMWPE where the normal load was 80 mN and the scratching velocity was 0.1 mm/s. The Si peak seen in the EDS indicates film failure due to scratching.	93
Figure 5.8	(a) Coefficient of friction and (b) wear life of Si substrate coated with different composite layers (as mentioned in the figures). The applied load was 70 mN at a rotational speed of 500 rpm (linear speed = 0.052 m/s).	96

Figure 5.9	Optical microscopy images of (a) Si/TiN/UHMWPE/PFPE, (b) Si/DLC57/UHMWPE/PFPE and (c) Si/DLC70/UHMWPE/PFPE films (first column) after sliding against respective Si ₃ N ₄ balls (second column) for one million sliding cycles. The ball surfaces show transfer of PFPE molecules but very little of UHMWPE. The applied load was 70 mN and the linear sliding speed was 0.052 m/s. The vertical and horizontal scales correspond to 100 μm.	98
Figure 6.1	A schematic diagram of the Si/UHMWPE sample with different interfaces. Interfacial conditions used were bare Si (i.e. no interface modification), heated Si, APTMS, hydrogen-terminated Si and OTS.	104
Figure 6.2	XPS wide spectrum for (a) bare Si, (b) heated Si, (c) Si/APTMS, (d) Si-H and (e) Si/OTS surfaces.	106
Figure 6.3	Friction and wear properties of UHMWPE film with different interfaces where the normal load is 40 mN and sliding speed is 500 rpm (0.1 m/s). (a) Typical friction traces as a function of the number of sliding cycles for all samples. (b) Consolidated wear life data for all samples.	108
Figure 6.4	Optical microscopy images of (a) Si/UHMWPE film and (b) Si-H/UHMWPE film after sliding against Si ₃ N ₄ ball for 1,000 cycles where the normal load is 40 mN and the sliding speed is 500 rpm (0.1 m/s). (c) is the image of the ball after sliding against (a), and, (d) is image of the ball after sliding against (b). Solid arrows indicate the direction of sliding; white circles indicate the point of contacts.	111
Figure 6.5	Optical microscopy images of (a) Si-H/UHMWPE film after sliding against Si ₃ N ₄ ball for 250,000 cycles where the normal load is 40 mN and the sliding speed is 500 rpm (0.1 m/s). (b) is the image of the ball after sliding against the film shown in (a). Solid arrow indicates the direction of sliding. The white circle indicates the point of contact.	112
Figure 6.6	A diagrammatic model showing the interactions between the polymer molecules and the Si surface with different wettabilities as measured by water contact angle. θ_1 , θ_2 and θ_3 represent relative water contact angles of the interfaces before polymer coating where $\theta_1 < \theta_2 < \theta_3$.	115

Figure 6.7	The FESEM images of the scratches on (a) Si/UHMWPE and (b) Si/OTS/UHMWPE where the normal load is 20 mN and the scratching velocity is 0.1 mm/s.	117
Figure 6.8	The FESEM images of the scratches on Si-H/UHMWPE films where the normal loads are (a) 20 mN, (b) 40 mN and (c) 70 mN, and the scratching velocity is 0.1 mm/s.	119
Figure 7.1	UHMWPE curve with amorphous and crystalline peaks using FTIR.	127
Figure 7.2	Coefficient of friction of UHMWPE film plotted against cycles in forward direction. FD refers forward direction. 10000_FD means after sliding 10,000 cycles in forward direction, the counterface has been replaced with a new ball and continued on the same track in forward direction.	129
Figure 7.3	Coefficient of friction of UHMWPE film plotted against cycles in reverse direction. RD refers reverse direction. 10000_RD means after sliding 10,000 cycles in forward direction, the counterface has been replaced with a new ball and continued on the same track in reverse direction.	131
Figure 7.4	Coefficient of friction of UHMWPE film plotted against scratch distance in reverse direction. RD refers reverse direction. 10000_RD means after sliding 10,000 cycles in forward direction, the nanoscratching has been done on the same track in reverse direction.	132
Figure 7.5	The FESEM images of nano-scratches which were done on wear tracks after sliding (a) 10,000 cycles and (b) 100,000 cycles. The scratches were conducted from right to left that was opposite to the initial sliding direction.	134
Figure 7.6	Optical images of Si ₃ N ₄ ball surface after sliding (a) 10,000 cycles and (b) 100,000 cycles against UHMWPE film in forward direction. White circles show the contact points. The scale bars are 50 μm.	135
Figure 7.7	The relation between crystallinity and coefficient of friction (in reverse direction) as a function of sliding cycles.	139

Figure 7.8	The FESEM images of UHMWPE film (a) before sliding and after sliding (b) 10,000 cycles, (c) 30,000 cycles and (d) 100,000 cycles. Image (a) is taken with 4000 times and the rest are taken with 2000 times magnifications. Solid arrows show the sliding directions.	140
Figure 8.1	(a) Ball-on-disc tribometer, (b) larger view of the cantilever and the sample holder.	150
Figure 8.2	The water contact angle measurement on Si_3N_4 balls with different treatments.	151
Figure 8.3	The roughness measurement on UHMWPE film using DMEMS. (a) 2D and (b) 3D images where the scan size is $124 \mu\text{m} \times 93 \mu\text{m}$.	152
Figure 8.4	Shear stress versus contact pressure on UHMWPE film. For all F_o , there is a linear relation between the shear stress and the contact pressure.	154
Figure 8.5	The initial shear stress, τ_o as a function of the attractive force, F_o of UHMWPE film (a) with PFPE data and (b) without PFPE data. There is an exponential relation between the two.	156
Figure 8.6	The initial coefficient of friction of UHMWPE film versus F_o for different applied loads; (a) low loads and (b) higher loads.	158
Figure 8.7	(A1) and (B1) are FESEM images of UHMWPE films after sliding against (A2) PFPE coated Si_3N_4 and (B2) bare Si_3N_4 balls respectively, where the applied load is 15 mN.	159

List of Abbreviations

AFM	Atomic force microscopy
Al ₂ O ₃	Aluminum oxide
APTMS	3-Aminopropyltrimethoxysilane
CNT	Carbon nano tube
CrN	Chromium nitride
DLC	Diamond-like carbon
DMEMS	Dynamic microelectro-mechanical systems
FESEM	Field emission scanning electron spectroscopy
FTIR	Fourier transform infrared spectroscopy
HDPE	High density polyethylene
H ₂ O ₂	Hydrogen peroxide
H ₂ SO ₄	Sulfuric acid
LDPE	Low density polyethylene
MEMS	Microelectro-mechanical systems
MoS ₂	Molybdenum disulfide
NEMS	Nanoelectro-mechanical systems
OTS	Octadecyltrichlorosilane
PDMS	Polydimethylsiloxane
PE	Polyethylene
PEEK	Polyetheretherketone
PEI	Polyethyleneimine

PFPE	Perfluoropolyether
PI	Polyimide
PMMA	Polymethylmethacrylate
POM	Polyoxymethylene
PS	Polystyrene
PTFE	Polytetrafluoroethylene
RMS	Root mean square roughness
SAM	Self-assembled monolayer
SEM/EDS	Scanning electron microscopy coupled with Energy dispersion spectroscopy
SEBS	Poly[styrene- <i>b</i> -(ethylene-co-butylene)- <i>b</i> -styrene]
Si ₃ N ₄	Silicon nitride
UHMWPE	Ultra high molecular weight polyethylene
TiN	Titanium nitride
TiO ₂	Titanium oxide
XPS	X-ray photoelectron spectroscopy

List of Symbols

a	Contact radius
A	Contact area
A_r	Real contact area
d	Sliding distance
D	Track width
E_o	Energy of an x-ray
E_j	Energy of an ejected electron
F	Friction force
F_i	Initial friction
F_o	Friction force due to adhesion at no external load
H	Hardness
k	Dimensionless wear coefficient
L	Normal load
P	Contact pressure
V	Wear volume
α	Pressure coefficient
γ	Surface energy
τ	Shear stress
τ_o	Initial shear stress
μ	Coefficient of friction
μ_i	Initial coefficient of friction

Chapter 1

Introduction

1.1 The importance of tribology

Tribology is defined as the study of friction, wear and lubrication of interacting surfaces in relative motion [Jost 1966]. When two surfaces are in contact, there is usually an attractive force between them and is called adhesion. When they start to move relative to each other in shear, a force resists the movement which is called friction. Depending upon the attraction between surfaces and the nature of the surface materials, adhesion and friction can vary. For example, if the surface energy or surface tension of the sliding surfaces is high, the attraction becomes more and also the resulting friction will be higher. By changing the shape of the surfaces from flat in sliding to round in rolling, the friction can drop drastically as the rolling friction is usually much smaller than the sliding friction. Obviously, this understanding led to the invention of wheel in ancient times. Also, sliding objects on wax is much easier than that on wood because of the lubricating property of wax. This observation led to the use of wax as a lubricant in ancient time for chariots. Generally, high adhesion and friction tend to increase wear of surfaces by debris particle generation. The effective way to reduce adhesion and friction and thus also reduce wear is to provide a suitable lubricant, such as oil, grease or solid lubricant film, between sliding surfaces. Rolling elements also require similar protection against wear by surface fatigue.

In many engineering and industrial applications such as aerospace and land transportation, bearings, computer and electronic devices, domestic appliances, gears used in rolling and sliding, machining operations, power generation, vehicles where motion is encountered, tribology plays an important role for durability and reliability of the products. A small reduction in friction in bearings can save considerable amount of (frictional) power loss [Bowden and Tabor 1973]. Product failures, power wastage and maintenance problems related to tribology cost billions of dollars every year in industrialized nations [Devine 1976 and Peterson 1979]. Recent report stated that 1.3% to 1.6% of GDP (Gross Domestic Product) of a nation could be saved by giving proper attention to tribology [Jost 1990]. Saving, both in terms of energy and environment, can be tremendous if surfaces are designed to suit the application.

1.2 A brief history of tribology

The tribology is derived from the Greek word *tribos* which means rubbing. It was first recommended by Jost to use ‘tribology’ to cover the study of friction, lubrication and wear [Jost 1966]. Although the knowledge of tribology was limited in ancient time, people knew the use of lubricants as an easy way to drag things such as stones. Animal fats have been used in medieval time for the launching of ships into water by sliding it against a wooden ramp.

1.2.1 Friction

The scientific study of friction was first conducted by Leonardo da Vinci in the middle of fifteenth century. He discovered what is now known as the first law of

friction which states that the friction is proportional to the normal load. He also noticed that the friction was little dependent or independent of the contact area. This became the second law of friction. These two laws were rediscovered by Amontons in 1699 and today they are more popularly known as Amontons' laws of friction. In 1748, the famous mathematician Euler explained a clear distinction between the static and kinetic friction [Dawson 1998]. The force needed to initiate sliding is greater than the force needed to sustain sliding. Amontons' discoveries were verified by Coulomb in 1785. He also found that kinetic friction is independent of the sliding velocity which is known as the third law of friction or Coulomb's law of friction. Coulomb believed that the origin of the friction was only because of the interlocking between surface asperities. Early researchers assumed that the friction originated from the 'interlocking asperities' which were rigid. However, in real world, not all the asperities are rigid. The shape of the asperities can be changed by elastic or plastic deformation while applying load. In fact, adhesion is an important factor in friction.

1.2.2 Adhesion in friction

When two surfaces come into contact, there should be certain amount of interatomic forces between them, depending upon the adhesion properties of the surface materials. The basic model of adhesion contributing to friction was first proposed by Bowden and Tabor [1986]. Their model states that when two surfaces are pressed together, the asperities at the contact points undertake elastic and plastic deformations. These deformations generate a real area of contact, A_r between two sliding surfaces. Actually, atoms in the range of A_r attract each other by interatomic

forces. When a tangential force is applied to slide, the shear stress, τ at the asperity contacts (because of the adhesion or interatomic forces between the atoms) will prevent the movement. The movement will only begin when the applied tangential force overcomes the interatomic forces in the region of the real contact area, A_r . Therefore, the friction force, F can be expressed as

$$F = \tau A_r \quad (1.1)$$

The above explanation is also known as the junction growth model.

1.2.3 Wear

The understanding of wear mechanism is very important to prevent premature failure of products which brings economic loss. Though friction has been paid attention to and studied for centuries, a systematic study of the wear phenomenon has started only recently, largely due to the progresses made in the rail-road and surface transportation industry. The Organization of Economic Cooperation and Development (OECD) defined wear as the progressive loss of substance from the operating surface of a body occurring as a result of relative motion at the surface (OECD 1969). The mechanisms of wear can be divided into many factors notably: abrasion, adhesion, corrosion, delamination, erosion, fatigue and melting. It is difficult to separate contribution from each of wear mechanism in one wear process. Lim and Ashby constructed first 'wear maps' [1987 and 1990] which summarized the previous works of many researchers. Their wear maps are useful and easy tools to know the safe operating regimes of materials in which they operate. However, many problems are still remaining to solve as wear is not influenced by a single wear mechanism [Tabor

1995]. Many empirical equations to predict wear performance of specific materials and conditions have been proposed, and Archard equation [Archard 1953] is one of them. His equation is useful to estimate the dimensionless wear coefficient, $k = VH/Ld$ where V is the wear volume relates to sliding distance d , H is hardness of the wearing material and L is normal load. Archard's equation can be conveniently used to find out wear resistances of different materials if the sliding conditions and the counter surface material are fixed.

1.2.4 Lubrication

The effective way to reduce friction and wear in machines is to use a thin lubricating layer which prevents direct contacts between sliding surfaces. The history of lubrication goes back to 1400 BC where a lubricant was used on the axle of a chariot [Dawson 1998]. Although, people knew the usefulness of lubricant, only industrial revolution in the eighteenth century and further development of new technologies demanded advanced lubricants. Perhaps, it was Tower's experiment in [1883] that successfully led to the realization of hydrodynamic lubrication, an ultra low coefficient regime when certain conditions of lubricant viscosity, bearing pressure and the relative speed are maintained. In order to fulfill this demand, numerous tribological solutions such as hydrodynamic bearing design, synthesis lubricants, solid lubricants and wear resistant materials have been developed [Mate 2008].

1.3 Solid lubricants

The application of petroleum oil or grease as a liquid lubricant was widely used in the eighteenth century. The experimental study on the friction of oil-lubricated bearing was first conducted by Tower [1883]. He introduced the effect of hydrodynamic pressure on lubrication. Based on the experimental results of Tower, Reynolds derived the basic equation for the hydrodynamic lubrication [1886]. This idea leads to the application of various viscous liquids as liquid lubricants. These lubricants reduce friction by forming a thin adhered layer that lessens shear resistance and prevents direct contact between the sliding surfaces. It is known as hydrodynamic lubrication. Though the hydrodynamic lubrication is advantageous in many processes, there are many constraints, such as high load, low speed, low and high temperatures, misalignment, that hinder their applications. When the liquid lubricant is squeezed out due to any reason, the two surfaces come into direct contact through the liquid film. Because of some disadvantages of hydrodynamic lubrication in specific conditions, boundary or/and solid lubricants are used in conjunction with a liquid lubricant [Claus 1972].

1.3.1 Inorganic and soft metal films

Graphite and molybdenum disulphide are two most useful inorganic solid lubricants. Graphite is generally used as a dry powder or as dispersion in water, oil and various solvents. It is mainly applied in tools and dies in metal forming and in high temperature industrial applications. Molybdenum disulphide has replaced graphite in many applications due to its properties such as good lubrication, superior load carrying capacity, and more consistent properties [Lancaster 1984]. Some soft metals such as

gold, lead, silver, thallium and tin have low shear strength, high lubricity and good thermal conductivity. They can be easily bonded to metal surfaces as thin films.

1.3.2 Polymeric films

Polymers (especially linear thermoplastics) commonly have self-lubricating properties which allow them to be used as organic thin films in bearings and as binders for composites [Lancaster 1984, Loomis 1985, Gresham 1994 and Jamison 1994]. The polymers are used in powder or dispersion form and are coated onto the surface to provide lubricity, friction and wear resistance [Booser 1997]. The advantages of polymers are superior lubricity even under dry condition, low cost and weight, better corrosion and wear resistance, easy to coat onto different shapes and able to operate under low temperature and vacuum conditions. Because of their excellent lubrication properties under extreme conditions, polymers can be potential solid lubricating films.

The earliest and most extensively used polymer is polytetrafluoroethylene (PTFE). The coefficient of friction for PTFE is as low as 0.04 which is lower than any known solid lubricant. On the other hand, the wear rate of Teflon is inferior to comparison with those of some other polymers. Another promising polymer that can be used as a good solid lubricant is ultra-high molecular weight polyethylene (UHMWPE). The coefficient of friction of UHMWPE is a little higher than that of PTFE but its wear performance is far superior to that of PTFE or any other polymer. In addition to good wear resistance, UHMWPE has better abrasion resistance that is preferable for bearings, gears, bushings and many equipment parts [Clauss 1972].

Though UHMWPE has excellent properties to be used as a protective lubricating thin film, it has not been widely studied as alternative tribological film. Recently, a few groups have explored some ways to coat UHMWPE film. Bao *et al.* have deposited UHMWPE onto a substrate using thermal spraying method by controlling the composition and other process parameters [Bao *et al.* 2005]. Satyanarayana *et al.* have used decahydronaphthalin (decalin) as a solvent to dissolve UHMWPE powder [Satyanarayana *et al.* 2006]. After that, Si substrate was dipped into the solution and coated by the simple dip-coating method. The presence of UHMWPE film on Si provides a coefficient of friction in the range of 0.09 and wear durability of 12,000 cycles when slid against 4 mm diameter silicon nitride ball at a normal load of 70 mN and sliding speed of 0.042 m/s. These properties are superior to those of bare Si where the coefficient of friction is 0.65 and wear durability is only a few cycles at best.

Though UHMWPE film provides better tribological properties, it may still lack the product lifespan where the required wear durability is millions of cycles. Further research and development are necessary in the area of UHMWPE film to obtain high durability.

The UHMWPE film alone is relatively soft and easily gets penetrated by the hard sliding counterface and as a result, the real contact area is large as shown in Figure 1.1. As a way to increase the resistance to penetration and to reduce the real area of contact, a hard intermediate layer is proposed to be used between the substrate and soft UHMWPE film. By using hard (intermediate layer) and soft (UHMWPE) composite film, the hard layer decreases the contact area because of high load carrying

capacity whereas the soft layer reduces the shear stress. As a combined effect, the friction will drop as predicted by Equation (1.1) and the wear durability will increase. In this thesis, diamond-like carbon (DLC) is selected as a hard layer which is over-coated with soft UHMWPE film. This composite layer is evaluated for its tribological properties. In order to obtain an additional confirmation of the advantage of hard intermediate layer on the tribological properties, different hard intermediate layers such as chromium nitride (CrN), titanium nitride (TiN) are also used and their friction and wear performances evaluated.

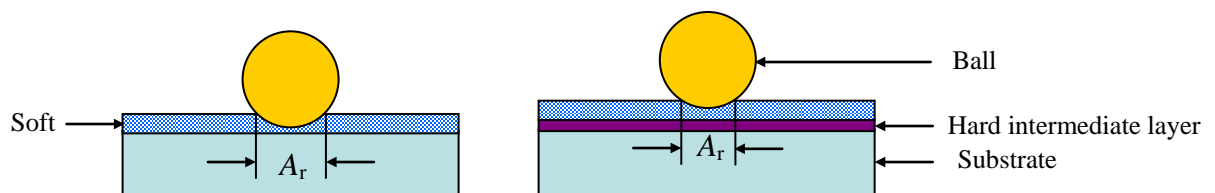


Figure 1.1: A schematic diagram of the effect of hard and soft layers on the real contact area, A_r .

Another important parameter that determines the wear property of the UHMWPE film is the adhesion strength of the UHMWPE film to the substrate. The adhesion is controlled by the surface wettability or the surface energy. By changing the surface wettability of the substrate, the substrate can attract or repel the water molecules which can affect the adhesion strength between the polymer film and the Si substrate, and the resulting tribological properties. The effect of the surface wettability of the substrate on the tribological properties of UHMWPE film is also investigated.

It is known that the frictional properties of UHMWPE film can be influenced by many factors such as the sliding direction, the crystallinity and molecular orientation, the surface energy etc. For example in a bearing or gear system, the relative motion between two sliding surfaces is not always unidirectional but

bidirectional. The crystallinity and molecular orientation of UHMWPE can change during sliding. The surface energy of the UHMWPE film depends on the environment. For instance, the humidity, temperature and presence of any organic molecule can change the surface energy. These mentioned factors are inevitable in actual working conditions. They can determine the coefficient of friction and the wear durability of UHMWPE film. Hence, it is important to study in a systematic way the effects of crystallinity, molecular orientation, surface energy and environment on the friction and wear characteristics of UHMWPE film.

1.4 Objectives of the thesis

The main objectives of this thesis can be classified into two parts. The first part focuses on the enhancement of the tribological properties of UHMWPE film using different intermediate layers and surface modifications of the Si substrate. Many hard layers such as CrN, TiN and DLC (of different hardness values) have been used as intermediate layers between Si substrate and UHMWPE film. The presence of hard layers provides high penetration resistance (load carrying capacity) and reduces the contact area which in turn increases the wear durability. The modification of surface wettability of the Si substrate varies the adhesion strength of UHMWPE film to the Si substrate and affects the wear life of the polymer film.

The second part presents the influences of sliding directions and surface energy on the friction characteristics of UHMWPE film. In the effect of sliding directions on friction, the mechanism of UHMWPE film is explained based on crystallinity and

molecular orientation. The effect of surface energy on friction, especially at low normal loads, is investigated using both theoretical and experimental methods.

1.5 Structure of the thesis

Chapter 2 presents a literature survey of different polymer films, coating techniques and their tribological properties.

Chapter 3 provides details of the materials, the experimental procedures and all the techniques used to characterize the surfaces employed in this thesis.

Chapter 4 explains the results and discussion of UHMWPE coated onto Si/DLC substrate. And then, the effect of UHMWPE film thickness on the wear durability of composite Si/DLC/UHMWPE film is explored.

The effects of different hard intermediate layers (CrN, TiN and DLC) on the tribological properties of UHMWPE film are provided in Chapter 5.

Chapter 6 focuses on the modifications of surface wettability (surface energy) of Si substrate. The effect of surface wettability of the Si substrate on the adhesion, friction and wear durability of top UHMWPE film is then studied.

In Chapter 7, changes in the crystallinity and molecular orientation of UHMWPE film are explored. The influence of those changes on friction is studied for different sliding directions.

Chapter 8 presents the frictional behaviors of UHMWPE film with different surface energies. The constructed model is compared with the experimental results.

Finally, Chapter 9 of the thesis summarizes the specific conclusions drawn from this work and suggests some future works.

Chapter 2

Literature Review

2.1 General properties of polymers

Polymers are organic compounds composed of many repeating molecules known as 'mer' (unit). The molecules in polymers have a few thousands to millions of mers depending upon the molecular weight of the polymers and they are usually referred to as macromolecules. These molecules are composed of covalently bonded, elements such as C, H, O and N.

“Natural polymers” such as cotton, rubber, silk and wood have been used for many centuries. Scientists have developed synthetic polymers such as fiber, plastic and rubber after World War II. With the development of synthetic polymers, the polymers became an important area for tribological applications such as ball bearings, cams, gears, journal bearings, seals of shafts and other mechanical parts, sliders, tires and so on [Suh 1986]. The advantages of polymers over metals or ceramics in tribological perspective are as follows:

1. Easy to fabricate into complex shapes
2. Eco-friendly and less contamination (when compared with the use of lubricants for metals)
3. Low cost
4. High impact resistance

5. Self-lubricity: Many polymers have low coefficient of friction even under dry and extreme conditions (for example low speed, low and high temperature)
6. Wear durability and corrosion resistance

2.2 Tribology of polymers

This section will present the mechanisms of friction and types of wear of polymers. It will review the historical background of the tribology of polymers in bulk, composite and thin film forms.

2.2.1 *The friction mechanisms and types of wear of polymers*

2.2.1.1 *A brief summary of the friction mechanism of polymers*

The friction force (F) in polymers is the result of plowing of the asperities of the surfaces (F_p) and the adhesive interaction between the two surfaces in contact (F_a) [Bowden and Tabor 1986]. The first term, plowing is important if a hard body is sliding against a relatively soft surface. The second term, adhesion depends on the interfacial shear stress of the two surfaces in the absence of hard asperities. The shear stress, τ is directly proportional to the contact pressure, P [Bowden and Tabor 1986] as

$$\tau = \tau_0 + \alpha P \quad (2.1)$$

where τ_0 is the initial or intrinsic shear property and α is the pressure coefficient. τ can be calculated as the friction force, F divided by the real contact area, A which can be measured on the sliding track [Briscoe *et al.* 1973 and Briscoe and Tabor 1978]. P is the ratio of the applied normal load, L to the real contact area, A .

The Equation (2.1) can be re-written as

$$F/A = \tau_0 + \alpha (L/A) \quad (2.2)$$

The initial shear stress, τ_0 is often neglected and assumed zero when the applied load is too high [Briscoe and Tabor 1975]. Therefore, for higher applied loads, Equation (2.2) becomes

$$F = \alpha L \text{ or } \mu = \alpha \quad (2.3)$$

as the coefficient of friction is the friction force divided by the applied normal load.

The frictional behavior of polymers is not as simple as that of metals or ceramics. Because of the visco-elastic nature of polymers, many factors such as load, geometry and loading time affect the friction. For example, if the geometry and the loading time are fixed, the contact area of polymers is not proportional to the applied normal load, L , as it is so for metals. The friction force F for polymers is found to be proportional to L^n where n is nearly 0.75 for polymers [Bowden and Tabor 1986].

2.2.1.2 Types of wear

Classifications of wear of polymers are shown in Table 2.1 [Briscoe and Sinha 2002]. In the first generic scaling approach, wear is divided into cohesive and interfacial components which are a result of the two-term friction model of bulk and interfacial frictional work dissipations. In the phenomenological approach, which is based on the mechanism of material removal, the types of wear are abrasive, adhesive, chemical, delamination, erosive, fatigue, fretting and transfer. The last classification of wear is based on the material characteristics in which wear is divided into polymer classes as elastomers, glassy polymers, semi-crystalline polymers and thermosets.

Table 2.1: Classifications of wear of polymers.

Generic scaling approach	Phenomenological approach	Material response approach
Two-term interacting model: <ul style="list-style-type: none"> ▪ Cohesive wear ▪ Interfacial wear 	Origin of wear process model: <ul style="list-style-type: none"> ▪ Abrasive wear ▪ Adhesive wear ▪ Chemical wear ▪ Delamination wear ▪ Erosive wear ▪ Fatigue wear ▪ Fretting wear ▪ Transfer wear 	Polymer class model: <ul style="list-style-type: none"> ▪ Elastomers ▪ Glassy polymers ▪ Semi-crystalline polymers ▪ Thermosets

Details of some mechanisms such as adhesive, abrasive and fatigue wear that occurs in most polymer wear [Opondo and Bessell 1982], as they do in metals, are explained below.

Adhesive wear is a very common form of wear as it cannot be eliminated when two surfaces slide against each other [Rabinowicz 1976]. Adhesive wear often leads to the transfer of the material from worn part to the wearing surface. Depending on the geometry of the counterface, the load and the surface energy of the two mating surfaces, the amount of transfer layer to the counterface can vary. The nature of the transfer layer greatly affects the steady-state coefficient of friction and wear rate of polymers. If the transfer film is thin enough to shield the counterface and if the polymer has linear molecules, the friction and wear rate reduce as the sliding is between polymer and polymer with easy shear. In addition, the molecular orientation can align along the sliding direction which can reduce the coefficient of friction.

However if the sliding direction is perpendicular or reversed to the orientation, the frictional behaviors change. If the transfer film is thick, back to back polymer transfer mechanism may occur that leads to high wear rate. Further, the intrinsic properties of the polymer such as molecule type and glass transition temperature have great influence on the tribological properties of the bulk polymers and the transfer layer.

Abrasive wear is another important mechanism in polymer. It has two types based on the type of interfaces: two-body and three-body abrasive wear. Only the polymer surface and the counterface involves in the case of two-body. When the hard debris, if any, or foreign particles are trapped between the two sliding surfaces, it becomes a three-body abrasive wear process. The wear rate can increase or decrease in abrasive manner. If the loose particles form a thin layer on either of the two sliding surfaces or both, the nature of the sliding mechanism may change from abrasive to a transfer layer dominated.

The abrasive wear can be related to the bulk mechanical properties as proposed by Ratner *et al.* [1964] and Lancaster [1969 and 1973], and the relation is given as,

$$V \propto \frac{K \mu L v}{H S e} \quad (2.4)$$

where V is the wear volume, K is the proportionality constant, L is the normal load, v is the sliding velocity, H is the hardness of the polymer, S is the ultimate tensile stress and e is the % elongation to break. Many researchers have experimentally proved the validation of Equation (2.4) and they have observed a linear relation between V and $\frac{1}{S e}$ [Ratner *et al.* 1964, Briscoe 1981 and Shipway and Ngao 2003].

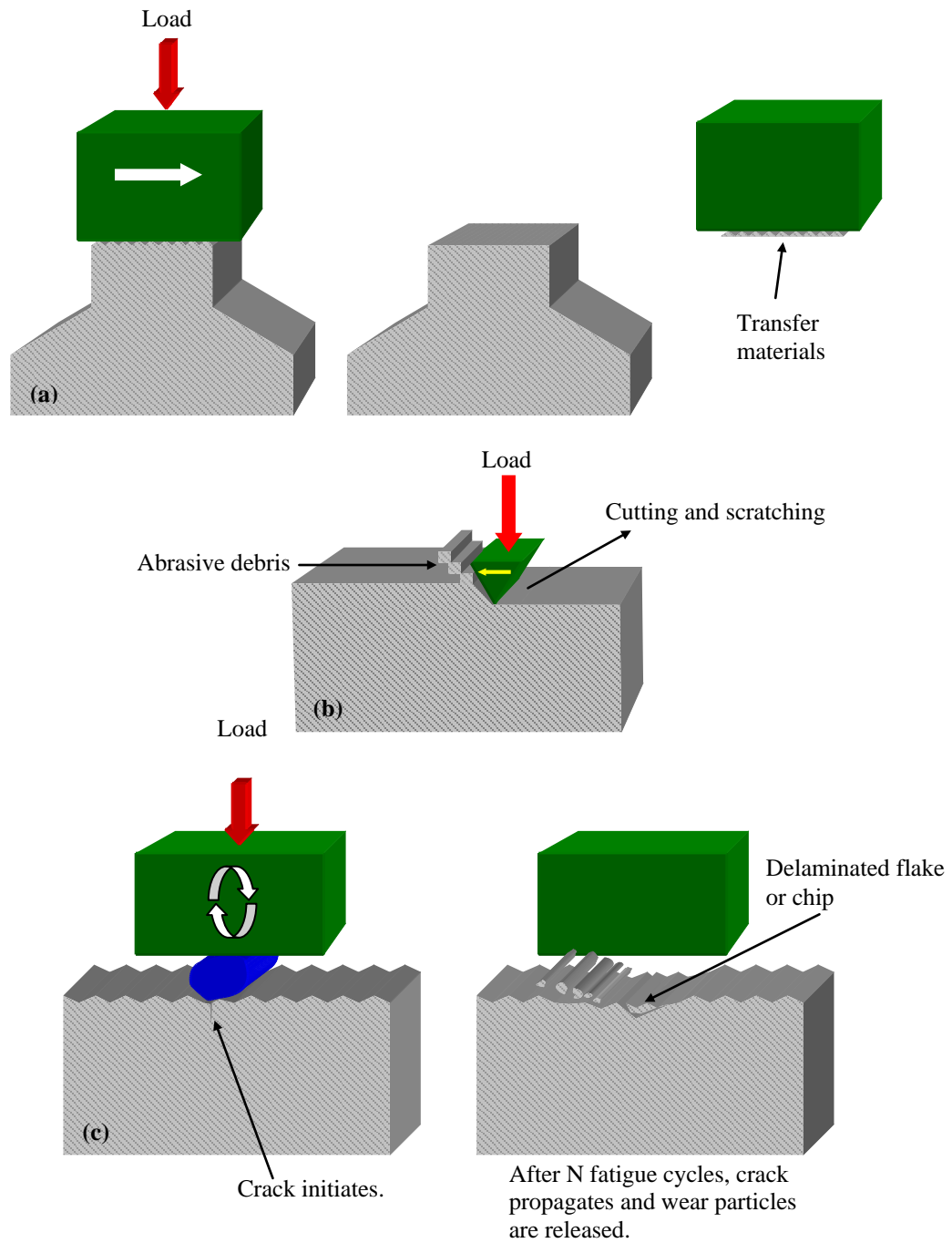


Figure 2.1: Schematic diagram of (a) adhesive, (b) abrasive and (c) fatigue wear mechanisms.

Fatigue wear occurs from repetitive cyclic loading with compressive and tangential contact stresses where wear particles come out after fatigue crack growth [Opondo and Bessell 1982] in the form of delaminated flakes. It is comparatively

smaller in comparison to the wear by adhesive or abrasive but the effect can be very damaging to the mechanical component such as bearing.

2.2.2 Tribology of bulk polymers

The first widely recognized bulk polymer in applications is rubber. Rubber is extensively used as tyres in automobile industry. The unique characteristic of rubber is its elastic deformation to high strain under small loads. It can retain elasticity as the load is removed. The friction of rubber increases rapidly with the sliding speed in a creep region and reaches a maximum limit. And then the friction drops as the sliding speed increases [Gough 1958 a, b]. Since rubber has poor thermal conductivity, the high frictional heat generated at the interface between a tyre and the road especially at high speeds affects the frictional properties. Ettles and Shen have studied the effects of frictional heat on the friction of rubber [Ettles *et al.* 1987]. It is also found that the friction of rubber is independent of applied load and decreases with temperature [Extrand *et al.* 1990].

The scientific study of the tribological properties of non-elastomeric (thermoplastics and thermosets) polymers was studied by Shooter and Thomas [Shooter and Thomas 1949]. They investigated the frictional behavior of different polymers such as PE, PMMA, PS and PTFE by sliding the polymer against a steel counterface. Their work concluded that the friction of linear polymers (PE and PTFE) were very low which was the beginning of the tribological applications of these two polymers in modern technology. The extensive study of tribology on bulk polymers have been reported since late 1950s. Many researchers have reported the frictional

properties of PTFE and other thermoplastics in 1960s and 1970s [Grosch 1963, Makinson and Tabor 1964, Ludema and Tabor 1966, Steijn 1968, Schonhorn and Ryan 1969, Pooley and Tabor 1972, Tanaka *et al.* 1973, Tanaka and Miyata 1977]. Another interesting polymer, UHMWPE has also been studied because of its high wear durability in comparison with other thermoplastic polymers [Tetrault 1989, Fisher *et al.* 1994]. Currently, it is the only polymer suitable for hip, knee and total joint replacements [Livermore *et al.* 1990, Amstutz *et al.* 1991].

2.2.3 Tribology of polymer composites

With the successful applications of bulk polymers, many new polymer composites with fibers, fillers, hard ceramic particles and lubricating particles have emerged. They have been used on a large scale in industrial applications because of their remarkable properties such as high specific strength (strength/density), high specific stiffness (modulus/density) and mechanical properties are adjustable by controlling the amount and the type of fillers or fibers through processing [Friedrich 1984]. The early scientific investigation on the tribological advantages of polymer composites was conducted by Ricklin *et al.* in 1954 [Ricklin *et al.* 1954]. Followed by this observation, many research groups have been working thoroughly on polymer composites. For example, the role of the filler shapes on the tribological properties of PTFE was conducted [Speerschneider and Li 1962]. Their results showed that the presence of spherical shaped Al_2O_3 fillers could drastically enhance the abrasion resistant of PTFE composite. Briscoe *et al.* have studied the friction and wear properties of HDPE with lead oxide (Pb_3O_4) and copper oxide (CuO) as fillers

[Briscoe *et al.* 1974] and PTFE with carbon filler [Briscoe *et al.* 1977]. They observed that the addition of fillers helped to reduce the wear rate with optimum filler content. The effect of PTFE filler on the tribology of POM (polyoxymethylene) was investigated by Kar and Bahadur [1974]. They confirmed that the addition of PTFE filler considerably reduced the wear rate of POM as PTFE filler helped to reduce the coefficient of friction. In the 1980s and 1990s, Friedrich's group has reported the tribological properties of PEEK by adding different types and amounts of particles or short-fiber reinforcements and tested them in a wide range of temperature [Friedrich *et al.* 1987 a, b, 1988, 1991 and 1996]. Bijwe's group has studied the tribological properties of polyetherimide (PEI) and polyimide (PI) composites using carbon and glass fibers with different weight percentages [Bijwe and Tewari 1989 and 1990, Bijwe *et al.* 1990, Tewari and Bijwe 1991, Bijwe and Rattan 2007 a and b, and Rattan *et al.* 2008]. All the scientific investigations on polymer composites show that a combination of optimum amounts of fillers, fibers or particles, is helpful in improving the performance in terms of friction and wear.

In 1990s, Bahadur and colleagues studied the advantages of micro size particles as reinforcements in polymer composites [Bahadur and Gong 1992, Bahadur *et al.* 1993, Van de Voort and Bahadur 1995, Bahadur and Polineni 1996, Yu and Bahadur 1998, Zhao and Bahadur 1999, Schwartz and Bahadur 2001]. Their results have shown that the wear rate depends on the particle size. Smaller particle size provides lower wear rate than larger size. These observations give an encouragement to use nano size particle in polymer composites for better efficiency [Wang *et al.* 1996, Xue and Wang 1997]. From then on, many successful polymer composites with nano

fillers have been introduced [Ng *et al.* 1999, 2001, Petrovicova *et al.* 2000, Reynaud *et al.* 2001, Seigel *et al.* 2001, Sawyer *et al.* 2003, Lee and Lim 2004, Burris and Sawyer 2006].

In summary, researchers have been successful in altering the bulk compositions of polymers for controlling the tribological performances. This has resulted in many industrial applications of polymer composites.

2.2.4 Tribology of polymer thin films

The surface properties of the products can be improved by using a thin polymer film which prevents a direct interaction of the products to the environments that leads to longer product life-span.

The earliest study on the tribological performance of polymer film was that on PTFE (Teflon) [Fitzsimmons and Zisman 1956, 1958] where the thickness of the film was 15.2 μm to 17.8 μm . It was applied as protective coating film for aircrafts, ammunition cartridges, submarines and weapons. It is also applicable for bearings, gears, hinges, piston rings, shafts, valves and other industrial applications [Claus 1972]. Though PTFE film can reduce the friction, as mentioned in Table 1.1, its wear resistance is poor when compared to other polymers. Thus, PTFE film is most suitable for the following conditions: low sliding speed and/or low to moderate the applied load, and presence of an effective coolant such as air, oil or water [Fitzsimmons and Zisman 1958].

Harrop and Harrop [1969] have studied the frictional behavior of sputtered PTFE film on mild and silver coated steel rods. The film thickness was in the range of

0.01 μm to 12 μm and it was observed that the friction varied with the film thickness. Between 2 μm to 12 μm , the coefficient of friction, μ increases (from 0.09 to 0.1) with thickness due to an increased volume of polymer. Below 0.5 μm thickness, μ rises (0.13 at 0.5 μm thickness to 0.2 at no PTFE film) due to the high shear property of the hard metal substrates. The coefficient of friction, μ also decreases with increasing load for any given thickness.

Kitoh and Honda [1995] have investigated the tribological performance of sputtered polyimide film (20 nm thickness) on Si substrate. The results show that the abrasion resistance of PI film is three to five times better than that of PTFE film under a normal load of 0.49 N and a sliding velocity of 80 mm/s.

Tsukruk and colleagues [Luzinov *et al.* 2001 and Sidorenko *et al.* 2002] have used thermoplastic elastomeric composite film (20 nm thickness) which consists of two parts: an elastomeric and a reactive interfacial. The elastomeric layer has the properties of largely reversible deformation and low shear stress. The reactive interfacial layer serves as an anchor between the elastomeric layer and the Si substrate. In their composite film, they selected tri-block polymer, poly [styrene-b-(ethylenecobutylene)-b-styrene] (SEBS) functionalized with 2% of maleic anhydride (MA) as the elastomeric film and epoxy-terminated SAM as a reactive anchoring interface on Si substrate. The MA groups from elastomeric react with the epoxy groups of the monolayer, thus enabling anchoring of the elastic blocks to the Si substrate. The friction and wear tests were conducted under a constant pressure of 1.2 GPa with a 3 mm diameter steel ball. The wear durability of trilayer film is 3,300 cycles where the bare Si has failed within a few cycles.

Liu *et al.* [2002] have prepared a polydimethylsiloxane (PDMS) film about 180 nm thick on Si substrate using spin coating. The frictional behaviors of film were evaluated by sliding against an AISI-52100 steel ball of 3 mm diameter under a normal load of 0.5 N. The results showed that the wear resistance of PDMS film on the hydrophilic substrates (hydroxylated Si or vinyl terminated Si) was the best. They have summarized that the chemical characteristic of the substrate is an important factor for longer wear life of the PDMS film. Yamada [2003] has studied the effect of PDMS multi layers on the friction properties. He found that when there were three or more PDMS layers or above, the first layer adjacent to the Si substrate was strongly adsorbed onto the substrate surface and was immobile during sliding; the low shear stress was accomplished by the slipping of mobile middle layers and the friction reduced. He has shown that the magnitude of friction of two layer PDMS films (no mobile layers) is 6-8 times larger than that of the films having mobile middle layers.

Ren *et al.* [2004] have investigated the tribological properties of a composite film consisting of C₆₀ (fullerene) film onto polyethyleneimine (PEI) coated Si substrate. The coefficients of friction are 0.65 and 0.22 for bare Si and Si/PEI respectively. Si/PEI shows low friction but it fails instantly in sliding test as does bare Si sample. The presence of PEI film obtains amino-groups on Si surface that could undergo reaction with C₆₀. Once C₆₀ is coated onto Si/PEI, the friction is lowered to 0.13~0.17 and wear life increases to 10,000 cycles under normal the load of 0.5 N.

Sakata *et al.* [2005] have shown that PMMA brush on Si substrate has better wear resistance when slid against a stainless steel ball under a normal load of 0.49 N, when compared to the spin-coated PMMA film on bare Si. Sun *et al.* [2006] have

studied the effect of chemisorption of PI films on Si via reactive polymer layer (polyglycidyl methacrylate, PGMA). It is observed that the wear performance increases to 25,000 cycles whereas PI film on Si without the intermediate reactive polymer layer has failed at 800 cycles under the same test conditions. It proves that the chemical bonding between the polymer film and the substrate is important in enhancing the wear resistance of the polymer film.

In a recent paper, Satyanarayana *et al.* [15] have used UHMWPE as a protective coating on Si by dip-coating method and showed that the coefficient of friction of Si/UHMWPE was 0.09 while that of bare Si was 0.65. In addition, after coating UHMWPE, the wear life of Si/UHMWPE increased more than 4000 times in comparison with that of bare Si.

From the literature review of the tribology of polymers, it is obvious that the tribology of bulk polymers and polymer composites are well studied and understood. Though the polymer films are very useful for many engineering applications, their tribological properties have not been studied and optimized as much as those of bulk polymers and polymer composites. It is well understood that the tribology of polymer films is different from that of bulk or composite polymers. The film coated onto a hard substrate gives lower coefficient of friction than the bulk polymer value because of the efficient heat dissipation rate if the substrate is metallic. Another advantage of polymer films is easy change of its tribological performances by giving different treatments to the substrates or to the surface of the films and by adding fillers such as CNT (carbon nano tube) or nanoclay particles. It is obvious that this field is largely unexplored from engineering and scientific perspectives. Many researchers working in this area have

obtained ultra-thin polymer films which provide low friction but most of them are not durable in term of wear resistance for the total product lifespan.

2.2.4.1 Polymer film coating techniques

In a solution-based coating technique, polymer molecules are adsorbed from the solution and the solvent evaporates during the coating process. The polymer molecules are attached to the substrate by means of either physisorption or chemisorption depending on the coating technique. The attraction between the polymer molecules and the substrate greatly influences the overall tribological properties of the polymer film. The following solution-based techniques [Advincula *et al.* 2004] are widely used in applications in which molecules are physically attached to the substrate:

- printing/droplet evaporation
- spray coating
- spin coating
- dip-coating
- doctor blading

The extremely thin and good homogeneous films (starting from nanometer to micrometer thickness) can be obtained in dip-coating or spin coating processes with an appropriate control of the parameters such as the polymer concentration, the dipping or spinning speed and time, the post-heating temperature and post-heating time.

2.3 The properties of friction and wear resistance of bulk polymers

The friction and wear properties of some polymers that are widely used in many applications are summarized in Appendix A. The study of the tribology properties of bulk polymers is helpful in selecting a suitable polymer to be used as a film. Often, there are two important requirements for a better tribological performance of polymers: low or optimum friction and high wear resistance. Hence, the primary focus in this thesis will be on these two requirements.

The glassy polymers, such as PC, PMMA and PS are transparent and widely used in optical applications. The bulky molecular structure and inability to deform plastically make glassy polymer prone to wear by fracture at the contacting surface. Friction coefficient is also generally high because of high surface energy and the surface deformational work [Briscoe and Sinha 2002]. The semi-crystalline polymers with linear structure such as PTFE and UHMWPE have the lowest kinetic friction with PTFE showing the coefficient of friction as low as 0.04 (detailed properties are provided in Appendix A). Though linear structure is an important factor for low friction, it alone is not enough for excellent tribological performances. Except for PEEK and UHMWPE, the others polymers have either high kinetic friction or relatively high wear rate. Though UHMWPE has higher kinetic friction than PTFE, its wear rate is much lower than all other polymers. The wear rate of UHMWPE is an order of magnitude lower than that of PEEK which has the second lowest wear rate [Lubricomp 1998]. Some mechanical properties of bulk UHMWPE and PEEK are provided in Table 2.2 for reference.

The above studies have shown that the bulk UHMWPE has lower coefficient of friction and comparatively higher wear resistance than any other polymer. From the perspectives of both friction and wear rate, UHMWPE is the most promising polymer to be used as a film. In spite of having superior wear performance in bulk form, the application of UHMWPE as a film is restricted due to its high viscosity in the melt form and inability to dissolve in most of the common solvents.

Table 2.2: Mechanical properties of bulk UHMWPE and PEEK.

Property	UHMWPE ^a	PEEK ^b
Molecular weight (10 ⁶ g/mole)	2-6	-
Melting temperature (°C)	125-138	340-343
Poisson's ratio	0.46	0.4
Tensile modulus of elasticity (GPa)	0.8-1.6	1.1
Tensile yield strength (MPa)	21-28	91
Tensile ultimate strength (MPa)	39-48	70.3-103
Tensile ultimate elongation (%)	350-525	30-150
Impact strength, Izod (J/m of notch; 3.175 thick specimen)	>1070	85
Degree of crystallinity (%)	39-75	-

^aEdidin and Kurtz 2000 and ^bCallister 2007.

In a recent paper, Bao *et al.* [2005] have applied UHMWPE coating by thermal spraying method in which the coatings were deposited by combustion using acetylene as the fuel gas and compressed air as the oxidant. This method consists of injecting powdered UHMWPE particles into a hot jet in which the particles melt and is projected onto a substrate to form a coating. An important requirement of this process is that the polymer particles must flow extensively upon impact on the substrate. This

enables them to make close contact with the surface irregularities of the underlying substrate and form denser coating. Therefore a well uniform coating by thermal spraying is difficult to form and it depends on many parameters such as molecular weight, particle size, additional binder and flame temperature as well as the impact velocity. Satyanarayana *et al.* [2006] have found that decahydronaphthalin (decalin) solvent can dissolve UHMWPE if the solvent temperature and the dissolution process are carefully controlled. Their UHMWPE film was relatively uniform and the RMS roughness was 0.556 μm . As observed by other researchers, the tribological behavior of film is different from that of the bulk polymer. The coefficient of friction of UHMWPE film (0.09) [Satyanarayana *et al.* 2006] is lower than that of bulk UHMWPE (0.25). The wear durability of UHMWPE film on Si is 12,000 cycles whereas that of bare Si is only a few cycles when tested in sliding against a 4 mm diameter silicon nitride ball at a normal load of 70 mN and a sliding speed of 0.042 m/s.

The results of Satyanarayana *et al.* have shown ways to use UHMWPE as a film with good tribological performances. However, the wear life of this UHMWPE film is still low if the product life-cycle involves millions of cycles of sliding or revolution. Further research and developments are necessary to improve the wear durability of UHMWPE film. In the following sections, different modification techniques and concepts will be reviewed that are aimed at improving the wear durability of any tribological film.

2.4 The effect of substrate hardness on the tribology of polymer film

Bowden and Tabor [1986] showed that the influence of hardness on friction is rather small by using tin on hard steel where the difference in the hardness values is by a factor of 100. When a soft material is slid against a hard counterface, though the shear stress, τ is small, the area of contact, A increases due to the low load carrying capacity of soft material. On the other hand, when a hard material is slid against a hard counterface, though the contact area, A is small, the shear stress, τ eventually increases again.

The tribological requirements of high load carrying capacity and low shear stress can be obtained using a thin film of soft metal bonded to a hard substrate. For example, lead or silver coatings have been applied to bearing steels for shear stress and low coefficient of friction.

Bowden and Tabor [1943] were some of the leading researchers who studied the effect of soft metallic film on the tribological properties of hard substrates. They demonstrated the role of soft film in reducing the friction using copper, indium and lead. Tsuya and Takagi [1964] have studied the frictional behavior of soft lead film with a thickness of 0.1 to 130 μm on hard copper substrate and they found that the presence of lead film could reduce the friction to 0.5 whereas the friction of uncoated copper was more than 1. Sherbiney and Halling [1977] have reviewed the tribological behaviors of soft metallic films (indium, lead and silver) on steel substrates. They observed that the tribological properties of the soft film depend on the coating technique and the film material, and greatly influenced by normal load, sliding velocity and film thickness. Spalvins and Buzek [1981] have observed similar

tribological advantage of soft gold and lead films deposited on stainless steel. They also investigated the effect of film thickness on the friction. Ajayi *et al.* [1991] have observed that the coefficient of friction was reduced by 50 % and the wear rate by one or two orders in magnitude in the presence of soft silver film (1 μm thickness) on silicon nitride ceramic substrate. Jang and Kim [1991] have studied the frictional properties of gold and silver films (less than 1 μm) deposited on Si substrate under normal loads of 100 mg and 1 g using pin-on-disc method. Their results showed that the coefficient of friction reduced from 0.38 (bare Si) to 0.21.

The above literature review confirms that applying a soft film on a hard substrate can considerably improve the tribological performances of the hard substrate.

UHMWPE film can reduce the shear stress and the friction if coated onto a substrate. However, UHMWPE film has low load carrying capacity and is easy to be penetrated in sliding against a hard counterface which will result poor wear durability. A thin hard intermediate layer can improve the load carrying capacity of UHMWPE film. By doing this, both the friction and wear durability of UHMWPE film can be extended to a desired level. It is noted that if UHMWPE film is carefully optimized, this polymer has the potential of providing extremely high wear resistant film as seen in its bulk form.

2.5 The effect of surface wettability on the tribology of polymer film

The adhesion between the polymer film and the substrate is an important factor in obtaining better tribological performances. However, polymers are difficult to adhere strongly to a substrate since many of them have no functional groups unless

they have been chemically functionalized. Some basic techniques to gain strong adhesion are wettability (increasing hydrophilic behavior) of the substrate, cohesion strength of the polymer films and removal of stress concentration in the coating films [Ryntz 1994].

Surface wettability is measured by contact angle which is directly correlated to the free energy of the substrate. Higher contact angle means lower surface energy and poor wetting. For instance, poly(olefins) have lower surface energy which is difficult to adhere to substrates. It can achieve better adhesion using silicone agents which can effectively promote the surface wettability [Ryntz 1994]. Rauhut [1969] has presented the effect of different pre-treatments such as UV light, flame, UV light in the presence of solvent and etched in chromic acid etc on the changes in the surface energy of the substrate and the final adhesive strength of polyethylene. He has observed that etching with chromic acid is the most effective way to attain higher surface energy. Increasing the oxidation layers on the substrate is one of the ways to enhance the surface wettability and adhesion.

The presence of condensed water on the substrate due to high surface wettability strongly dominates the adhesion strength of the film [O'Brien *et al.* 2006]. Moy and Karasz [1980] and Lee and Peppas [1993] have observed that the presence of water molecules on the substrate deteriorates the film properties. Water molecules can create some cracks or voids on the coating [Wong and Broutman 1985 and Xu and Ashbee 1991]. The adhesion loss of the coating is inevitable if water or other chemicals can reach the substrate through the cracks or voids. Under sliding condition,

these cracks are the potential sites for stress concentration and delamination of the film.

From the above literature review, it is clear that the surface wettability is an important factor in determining the adhesive strength of a polymer film. Higher surface wettability of the substrate is desirable for better adhesion of the polymer film, but at the same time, it can attract water molecules from atmosphere to condense on the substrate and can weaken the adhesion. Depending upon the coating film and the substrate material, the wettability of a substrate needs to be optimized for better adhesion.

2.6 The effect of sliding direction on friction in terms of crystallinity and molecular orientation

As mentioned before, the sliding on UHMWPE film in real applications is rarely unidirectional but bidirectional. It is interesting to explore the frictional properties of the film in changing sliding direction. The crystallinity and molecular orientation of the film especially for semicrystalline UHMWPE is clearly affected by the number of sliding cycles. Deeper understanding of the effect of sliding direction on the frictional behaviors of UHMWPE film with different number of sliding cycles is essential in order to use the film efficiently in applications. As the study of the tribology of the polymer film has started only recently, there is limited literature on the effect of sliding direction on the friction in terms of changing crystallinity and molecular orientation. Hence, the literature review is made on semicrystalline bulk

polymers that will be helpful in the understanding of the effect of crystallinity and molecular orientation on friction in the case of polymer films.

The early investigation on the effect of molecular orientation on friction for PTFE was conducted by Tabor and Williams [1961]. They found dependency of friction on the sliding direction. They also observed that when two oriented PTFE surfaces were slid against, the friction was approximately 30% higher when sliding across than when sliding in the direction of orientation. This was attributed to the molecular orientation prior to the sliding process.

Gorokhovskii and Agulov [1966] have studied to correlate the crystallinity and wear rate of PTFE as a function of sliding velocity and applied load. Their results showed that the wear rate reduced with increasing % crystallinity up to a certain amount of crystallinity. Beyond that limit, the wear rate increased again. In addition, they observed higher wear rate with higher sliding velocity and applied load at a given % crystallinity. For example, for 90 % crystallinity and 8 kg/cm² applied pressure, the wear rate increased from 75 mg to 250 mg as the sliding velocity varied from 1.5 cm/s to 5 cm/s.

Pooley and Tabor [1972] have investigated the frictional behavior of PTFE slider and the effects of orientation and sliding direction on friction by sliding PTFE against a glass plate. The static friction of a fresh PTFE slider showed 0.2 for the first slide but it dropped to 0.07 when the slider is moved to a new glass plate and slid again parallel to the first track. When the slider was rotated by 90° angle and made a new track parallel to the previous tracks, a high static friction was observed. These results showed the importance of molecular orientation on friction of PTFE.

Extensive studies on the frictional behaviors of semicrystalline polymers such as PTFE, HDPE and UHMWPE have been conducted by Tanaka and Miyata [1977]. Similar results were found in their observations also and the static friction was very sensitive to the sliding direction as it was much smaller in sliding parallel to the initial orientation than that in sliding perpendicular to it. The molecular orientation was parallel to the sliding direction during the initial sliding process. Effect of degree of crystallinity on the friction and wear of PET was studied by Yamada and Tanaka [1986] under water lubrication. The tests were conducted using the pin-on-disk method under a normal load of 10 N. The coefficient of friction was little dependent on the degree of crystallinity under water lubrication. However, the higher degree of crystallinity reduced the wear rate with water lubrication. The results were in contrast to the wear rates under dry condition. The reason is water and some aqueous solutions inhibit the formation of transfer film on the counterface and as a result the wear rate is higher than that under dry condition [Lancaster 1972].

Eleiche and Amin [1986] reported that the wear rates of PVC and PC decreased with increasing molecular orientation under a sliding speed of 27.5 cm/s and a normal load of 49 N tested by the pin-on-disc method.

In recent papers, Aoike *et al.* [2007] and Kanaga Karuppiah *et al.* [2008] have controlled the crystallinity of UHMWPE by giving different temperature treatments and studied the effect of crystallinity on friction. The results showed that the higher degree of crystallinity provides low friction (from 0.39 to 0.28), shallow wear depth (from 0.21 μm to 0.12 μm) and high scratch resistance.

The role of crystallinity and molecular orientation on friction of different bulk polymers have been studied and reported by many researchers. However, their effects on friction of polymer films have never been investigated. Moreover, in studying the effect of sliding direction, many researchers have conducted the tests in parallel and perpendicular directions. It is also important to understand the frictional behavior of polymer films in both forward and reverse directions on the same track.

2.7 The relation between surface energy and friction

It was earlier believed that the friction was only controlled by the geometry of the asperities of the surfaces involved. The Amonton's Laws state that the friction force is directly proportion to the applied normal load. However, it was observed later that if two surfaces have adhesive interaction between them at rest, there is a finite value of friction even at no externally applied load. That means, friction is decided by not only the geometry of the asperities but also the surface energies or adhesion forces of the surfaces. If the effect of surface energy is taken into account in the JKR [Johnson *et al.* 1971] and DMT [Derjaguin *et al.* 1975] models and the contact radii in static condition from both models are derived, there is a deviation from the Hertzian contact radius. Israelachvili and Tabor [1972] experimentally measured the contact radius with adhesion effect. Both theoretical and experimental results proved that the role of surface energy on friction is not negligible especially when the applied load is very small. Thus, for two adhering surfaces, the total friction force can be expressed as

$$F = \mu (L_o + L) = F_o + \mu L \quad (2.5)$$

where F_o is a constant friction force due to adhesion at no external applied load.

Erhard [1983] and Lavielle [1991] used different polymer pairs and correlated the surface energies of different pairs with their frictional behaviors. Depending upon the surface energies of two sliding polymers, the frictional value has changed. They observed that the coefficient of friction increases with increasing surface energy and the relationship is exponential.

Yoshizawa *et al.* [1993] have studied the correlation between friction and adhesion by means of adhesion energy hysteresis using the surface force apparatus. Their results show that the friction force is directly proportional to the adhesion hysteresis. In a recent paper, Corwin and de Boer [2004] have investigated the effect of adhesion on static and dynamic frictions on Si substrate. They observed that the interfacial adhesion due to surface energy has affected static and dynamic coefficient of friction at zero applied loads. The adhesive force is the same for both static and dynamic conditions.

Recent molecular dynamics computer simulations by Robbins and co-workers have shown that the coefficient of friction is strongly dependent on the surface energy [He *et al.* 1999, He and Robbins 2001, Müser *et al.* 2001 and Rotter and Robbins 2001].

Though the effect of surface energy on friction of different polymers have been studied and reported, the actual relation between surface energy and friction is not well understood in term of surface forces. Therefore, in the last part of the thesis, this correlation will be studied by varying the surface energies of UHMWPE film and the counterface ball along with the effect of applied load. The validity of theoretical model will be confirmed with our experimental results.

2.8 A summary of the research plans followed in the present thesis

From the literature review on the tribology of polymers, it is clear that bulk polymers and polymer composites have been widely explored and used in industrial applications. Polymer films are potentially useful in enhancing the product lifespan especially where the bodies are sliding or rolling. The polymer used as film must fulfill the requirements of low friction and high wear durability. From the results of previous studies, UHMWPE is one of the most suitable polymers for coatings. However, more research on the fundamental understanding and property enhancing strategies of UHMWPE films are still necessary to explore in terms of friction and wear durability.

Therefore, the following research plans have been adopted in the present thesis:

1. Enhancement of the friction and wear durability of UHMWPE thin film by using hard intermediate layers (such as CrN, TiN and DLC) and optimization of UHMWPE film thickness
2. Enhancement of the friction and wear durability of UHMWPE thin film by optimizing the surface wettability (surface energy) of the Si substrate
3. Understanding the effect of crystallinity and molecular orientation on the frictional properties of UHMWPE thin film with different sliding directions and number of sliding cycles
4. Correlation between the surface energy of UHMWPE thin film and the coefficient of friction as a function of the applied normal loads

Si is used as the substrate in this work because of the importance Si as micro-electro mechanical systems (MEMS). Si is a very poor tribological material and hence

a research on improving the tribological properties of Si surface would have great technological impact for the future growth of microsystems.

The motivation, background and detail procedures of each study are provided in the respective Chapters.

Chapter 3

Materials and Experimental Methodologies

In this Chapter, the general materials used in the present research work, the preparation of UHMWPE film and various common methods used to characterize the chemical, mechanical, physical and tribological properties of the polymer films will be described. Additional information on specific materials, preparation methods, characterization techniques and calculation procedures will be provided in the respective Chapters.

3.1 Materials

3.1.1 Silicon

Polished n-type Si (100) wafers (obtained from Engage Electronics (Singapore) Pte Ltd), about 455–575 μm in thickness and hardness of 12.4 GPa, were used as the substrate. Roughness of the Si wafers was measured with an atomic force microscopy (AFM) and given as 0.41 nm. Various modifications and additional intermediate layers were deposited on Si wafers before UHMWPE film was deposited as the top layer.

3.1.2 UHMWPE

Ultra high molecular weight polyethylene (UHMWPE) powder (Grade: GUR X143) was (supplied by Ticona Engineering Polymers, Germany) dissolved in

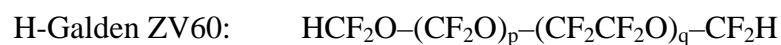
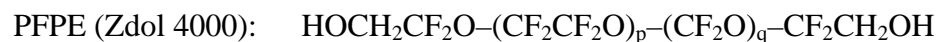
decahydronaphthalin (decalin) and deposited onto Si substrate. The physical properties of UHMWPE used in this study are provided in Table 3.1.

Table 3.1: Physical properties of UHMWPE, as provided by the supplier.

Properties	Units	Value
Melt index MFR 190/15	G/10 min	1.8 ± 0.5
Bulk density	g/cm^3	0.33 ± 0.03
Average particle size d50	μm	20 ± 5

3.1.3 Perfluoropolyether (PFPE)

In order to extend the wear durability of UHMWPE film, a commercial perfluoropolyether (PFPE) Z-dol 4000 (dissolved into H-Galden ZV60 purchased from Ausimont INC) was overcoated onto UHMWPE film. Chemical formulae of Zdol and H-Galden ZV60 are



where the ratio p/q is $2/3$. The physical properties of PFPE (Zdol 4000) used in this study are provided in Table 3.2.

3.1.4 Silicon nitride ball

A silicon nitride (Si_3N_4) ball of 4 mm diameter was used as the counterface in determining the tribological properties of UHMWPE films. The hardness and roughness (RMS) of the ball are 1500 HV and 5 nm respectively. Young's modulus and Poisson's ratio of Si_3N_4 used in this research are 310 GPa and 0.22 respectively.

Table 3.2: Physical properties of PFPE (Zdol 4000).

Properties	Units	Value
Functional group	-	Alcohol (-OH)
Appearance	Visual	Clear liquid
Color	APHA	Colorless
MW (NMR)	Amu	4000
Difunctional content (NMR)	%	90
C2/C1 ratio (NMR)	-	1
Kinematic viscosity	cSt	100
Density @ 20°C	g/ml	1.82
Vapor pressure @ 20°C	Torr	1 x 10 ⁻⁸
Vapor pressure @ 100°C	Torr	1 x 10 ⁻⁴
Refractive index @ 20°C	-	1.296
Surface Tension @ 20°C	dyne/cm	22
Polydispersity @ 20°C	Mw/Mn	1.15

3.2 Preparation of UHMWPE film

3.2.1 Cleaning of Si substrate

The removal of contaminants and undesired particles from Si substrate is the most important and an essential step in the coating procedure. A proper cleaning process provides better bonding of the coated films to the substrate. In the cleaning process, Si substrates were rinsed for 1 minute and ultrasonically cleaned for 15 minutes in soap water, distilled water and acetone, respectively. Ultrasonic energy can remove loose surface materials and organic contaminants. The cavitation bubbles produced from the change in pressure during ultrasonication have the capacity of blasting contaminants away from the surface [Dunbar 1994]. The cleaned substrates

were blow-dried with pure nitrogen gas and immersed into a piranha solution (70 vol.% H₂SO₄ and 30 vol.% H₂O₂) at a temperature of 70 °C for an hour. The objectives of piranha treatment are hydroxylation and removal of any organic/inorganic contaminants present on Si substrate. The measured RMS roughness of piranha treated Si surface was 0.3~0.5 nm. After piranha treatment, the substrates were rinsed again with distilled water and acetone for 1 minute each and finally dried with nitrogen gas.

3.2.2 Preparation and deposition of UHMWPE film

UHMWPE powder was dissolved in decahydronaphthalin (decalin) at a temperature of 150 °C for 30 minutes and 250 °C for another 30 minutes with a magnetic stirrer. The purpose of using a magnetic stirrer was to fasten the dissolution rate. After UHMWPE powder was completely dissolved, the cleaned Si substrate was immersed in the solution for 30 seconds and withdrawn at a speed of 2.4 mm/s. After that, the samples coated with UHMWPE were given heat treatment in a clean air oven at 100 °C for 15 hours. After heat treatment, the samples were cooled to room temperature in the same oven. The measured RMS roughness of UHMWPE films coated on Si was 0.56 μm, measured within a scan area of 10 μm × 10 μm using AFM.

In order to understand the effect of residual solvent in UHMWPE film, if any, both bulk UHMWPE powder and coated UHMWPE film were examined using differential scanning calorimetry (DSC60, Shimadzu) under an argon gas flow with a heating rate of 20 °C/min. No additional peak corresponding to the decalin (solvent) was observed in UHMWPE film. This suggested that the solvent must have evaporated completely from UHMWPE film during the heat treatment. The results confirmed that

there was no effect of the solvent on the mechanical or tribological properties of the coated polymer film.

3.3 Surface analysis techniques

3.3.1 Contact angle

A common method to estimate the surface energy is to measure the wetting property using solid-liquid contact angle method. This technique uses the spreading ability of a liquid in response to the surface tension generated due to the difference in the surface energies at the solid and liquid interface. Depending on the interfacial surface energy, the profile of a liquid droplet on the surface can change. The simplest relationship between the contact angle and the surface free energy is stated by Young's equation as,

$$\gamma_{SV} = \gamma_{SL} + \gamma_{LV} \cos \theta \quad (3.1)$$

where γ is the surface free energy and the subscripts *SV*, *SL* and *LV* represent surface-vapor, surface-liquid and liquid-vapor interfaces, respectively. Therefore, γ_S can be calculated from Equation (3.1) if γ_{SL} , γ_L and θ are known. γ_L is generally known from data source and θ from contact angle measurement. In the later part of the thesis, detailed calculation procedures of γ_{SL} and γ_S will be presented.

3.3.1.1 Types of surface wettability

Based on the profile of a droplet on the surface, the surface wettability can be classified as [Mate 2008]

- Wetting - The contact angle of the droplet on a surface is zero or close to zero.
- Partial wetting - The contact angle is greater than zero.
- Non-wetting - A subset of partial wetting where the contact angle is greater than 90° .

Surfaces can also be described as

- Hydrophilic - A surface with a low water contact angle (generally less than 90°) which attracts water.
- Hydrophobic - A surface with a high water contact angle ($\sim 90^\circ$ or more) which repels water.

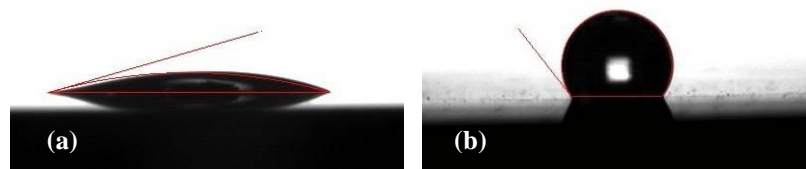


Figure 3.1: (a) Hydrophilic and (b) hydrophobic surfaces.

3.3.1.2 Contact angle measurements

The contact angle measurements were conducted using VCA Optima Contact Angle System (AST product, Inc., USA) machine (Figure 3.2) with a distilled water droplet of $0.5 \mu\text{L}$. The contact angle is measured at the edge of the droplet on a surface. A droplet is placed on the surface using a syringe and a microscope is used to examine the edge of the droplet. The contact angle is typically measured by capturing a video image or manual examination through the microscope eyepiece and determining θ with the computer software.

In this thesis, the contact angle is reported as an average value of at least five independent measurements for three different samples. The variation in the contact angles at various locations of a sample is $\pm 2^\circ$ and measurement error is $\pm 1^\circ$.

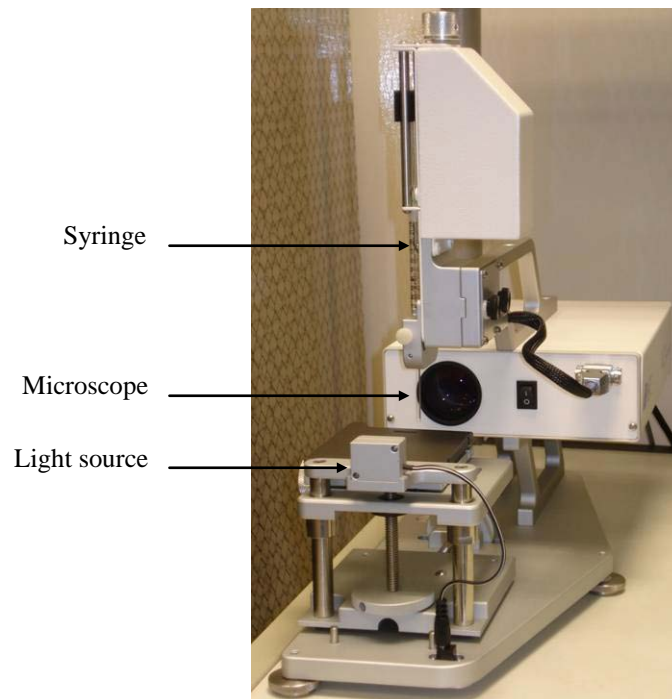


Figure 3.2: *Experimental setup for measuring contact angle.*

3.3.2 Nanoscratching and nanoindentation

The nanoscratch resistance of Si/UHMWPE and Si/DLC/UHMWPE was measured using MTS Nano Indenter XP machine. The indenter used for nanoscratching was a conical shape diamond tip with 90° cone angle and a tip radius of $5\ \mu\text{m}$. The scratch tests were conducted using a ramp loading setup from 0~250 mN at a constant velocity of $10\ \mu\text{m/s}$. The topography of the nano scratches was studied with a JEOL JSM-5600 LV scanning electron microscope (SEM).

Nanoindentation is widely used to characterize the surface mechanical properties of thin polymer films or thin surface layers [Zeng 2009]. It is applicable to determine the elastic modulus and hardness of the polymer film at submicron or nanometer levels. Nanoindentation tests were conducted using the MTS Nano Indenter XP machine. A triangular pyramid Berkovich diamond tip was used for nanoindentation tests with a fixed maximum normal load of 40 mN. The average hardness and elastic modulus values were calculated from the data of a total of 10 indentations made on different random surface locations.

3.3.3 X-ray photoelectron spectroscopy (XPS)

The chemical state of Si surface after modifications was studied by XPS which is a useful technique for quantitative analysis of the surface chemical composition. XPS is sensitive to the chemical environment of an atom. In the XPS measurement, a sample surface is exposed to a monochromatic X-ray radiation that is generated either by Mg or Al source. If E_o is the energy of an X-ray, and E_j is the binding energy of the electron in the atom, $E_o - E_j$ is the energy of the ejected electron. In other words, the difference between the energy of X-ray, E_o (1253 eV for Mg and 1486 eV for Al) and the binding energy of the electron, E_j gives the valuable information of the ejected electron.

In the present research, XPS measurements were conducted with a Kratos Analytical AXIS HSi spectrometer with a monochromatized Al $K\alpha$ X-ray source (1486.6 eV photons) at a constant dwell time of 100 ms and pass energy of 40 eV. A photoelectron take-off angle of 90° (with respect to the sample surface) was applied to

obtain the core level signals. All binding energies (BE) were referenced to the C1s hydrocarbon peak at 284.6 eV.

3.3.4 *Fourier transform-infrared spectroscopy (FTIR)*

FTIR technique is used to measure the absorption or transmission of infrared radiation with respect to the wavelength. The infrared absorption bands identify molecular components and structures. The absorbed IR radiation at the sample surface generally excites molecules into a higher vibrational state. The absorbed or transmitted wavelengths are due to the molecular structure of the sample.

An interferometer with a broadband infrared source is used to modulate the wavelength. The intensity of the reflected or transmitted light is recorded with a detector as a function of its wavelength. The recorded data are analyzed with a computer using Fourier transforms to obtain a single-beam infrared spectrum.

The percent crystallinity of UHMWPE film inside the wear tracks was measured using Fourier Transform Infrared Spectroscopy (FTIR, Spectrum 1000, Perkin Elmer Life and Analytical Sciences, Boston, MA, USA). The spectra were obtained with an accumulation of 16 scans in transmission mode with a spot size of 100 μm diameter.

3.3.5 *Microscopy*

3.3.5.1 *Optical microscopy*

Olympus microscope was used to study the polymer transfer mechanism between the ball and the polymer film, the extent of polymer transfer and the surface

morphology. It uses monochromatic light source to enhance the contrast between light and dark regions.

3.3.5.2 Scanning electron microscopy (SEM)

In an electron microscopy, an electron beam is produced from a tungsten filament which is focused by magnetic lenses in a high vacuum chamber. The electron beam is composed of the primary electrons that are reflected from the surface without any energy change. As the energy of the primary electrons are much higher than the energy of the electrons which are bound to the nucleus, the electrons of the atoms from the sample can be knocked out easily. These knocked out electrons are called secondary electrons.

The intensity of the secondary electrons is basically used in the SEM technique [Barraud *et al.* 1974 and Janssen *et al.* 1980]. When some of the secondary electrons re-combine with ions at the surface, some photons are released. Depending on the intensity of the photons; the SEM image capability can vary. SEM is widely used in the study of interface and sub-surface morphology, defects, patterns, pinholes etc [Ulman 1991].

In the present research, the surface morphologies of the nano scratches were observed with a JEOL JSM-5600 LV scanning electron microscope (SEM) coupled with energy dispersive spectroscopy (EDS).

3.3.5.3 Field emission scanning electron microscopy (FESEM)

The surface topography of the scratches and the thickness of the polymer film are examined with a field emission scanning electron microscope (FESEM) (Hitachi S4300) machine coupled with an energy dispersive spectrometer (EDS). Before taking FESEM images, gold coating was performed on the tested polymer films at 10 mA for 40 seconds (JEOL, JFC-1200 Fine Coater) to impart conductivity to these films. EDS tests were performed on the scratches with gold coating to identify and to record carbon and silicon peaks.

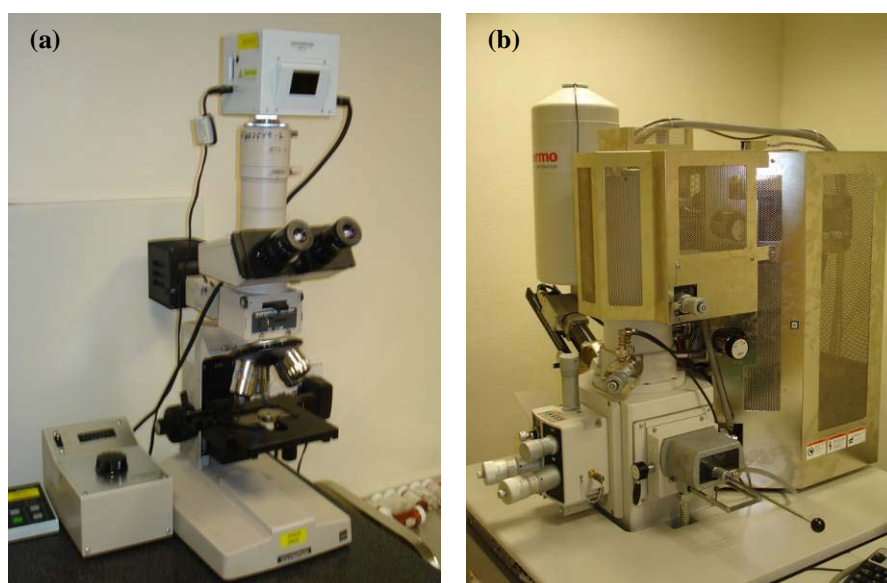


Figure 3.3: (a) Optical microscopy and (b) FESEM.

The samples coated with UHMWPE films were cut and mounted with their cross-sections horizontal under FESEM to measure the thickness. At least ten measurements were randomly carried out for each film and an average value was reported. The thickness variation of the film is within $\pm 1 \mu\text{m}$.

3.3.6 Adhesion strength with a scratch tester

The study of the adhesion strength of UHMWPE film on differently modified Si substrates was conducted using a scratch tester with a diamond tip of 2 μm tip radius. The scratching velocity and the linear scratch distance were fixed at 0.1 mm/s and 1 cm respectively. The applied normal load was varied from 10 mN with an increment of 10 mN. The critical load of each film was determined by measuring Si peak inside the scratches using EDS or by observing debris particles or delamination of the film. In these tests, the critical load was defined as the applied normal load at which the film failed during scratching.

3.3.7 Friction and wear tests

The friction and wear tests were conducted on a ball-on-disc tribometer (Figure 3.4 a). A 4 mm diameter silicon nitride (Si_3N_4) ball was chosen as a stationary counterface whereas UHMWPE coated samples acted as the rotating disc. Before the tests, Si_3N_4 balls were cleaned with acetone to remove any contaminant. The wear track radius and the normal load were 1~2 mm and 40 mN respectively. The rotational speed chosen for the tests was 500 rpm giving a linear speed in the range of 0.052~0.105 m/s. A schematic diagram of the cantilever for normal and frictional force measurement is given in Figure 3.4 (b). The normal load was converted from the vertical displacement of the double cantilever that was measured using a laser displacement sensor. The friction force was continuously measured using four strain gauges attached to the cantilever arms. The sampling rate used to measure the friction data was 5 Hz. The tests were carried out in a class 100 clean booth environment at a

temperature of 25 ± 2 °C and a relative humidity of $55 \pm 5\%$. The initial coefficient of friction was taken as an average value of the first 4 seconds of sliding. In this study, the wear life of UHMWPE film is defined as the number of cycles when the coefficient of friction exceeds 0.3 or large fluctuations of the coefficient of friction (indicative of film failure) occur continuously, whichever happens first. This definition of wear life is consistent with previous studies dealing with thin films.

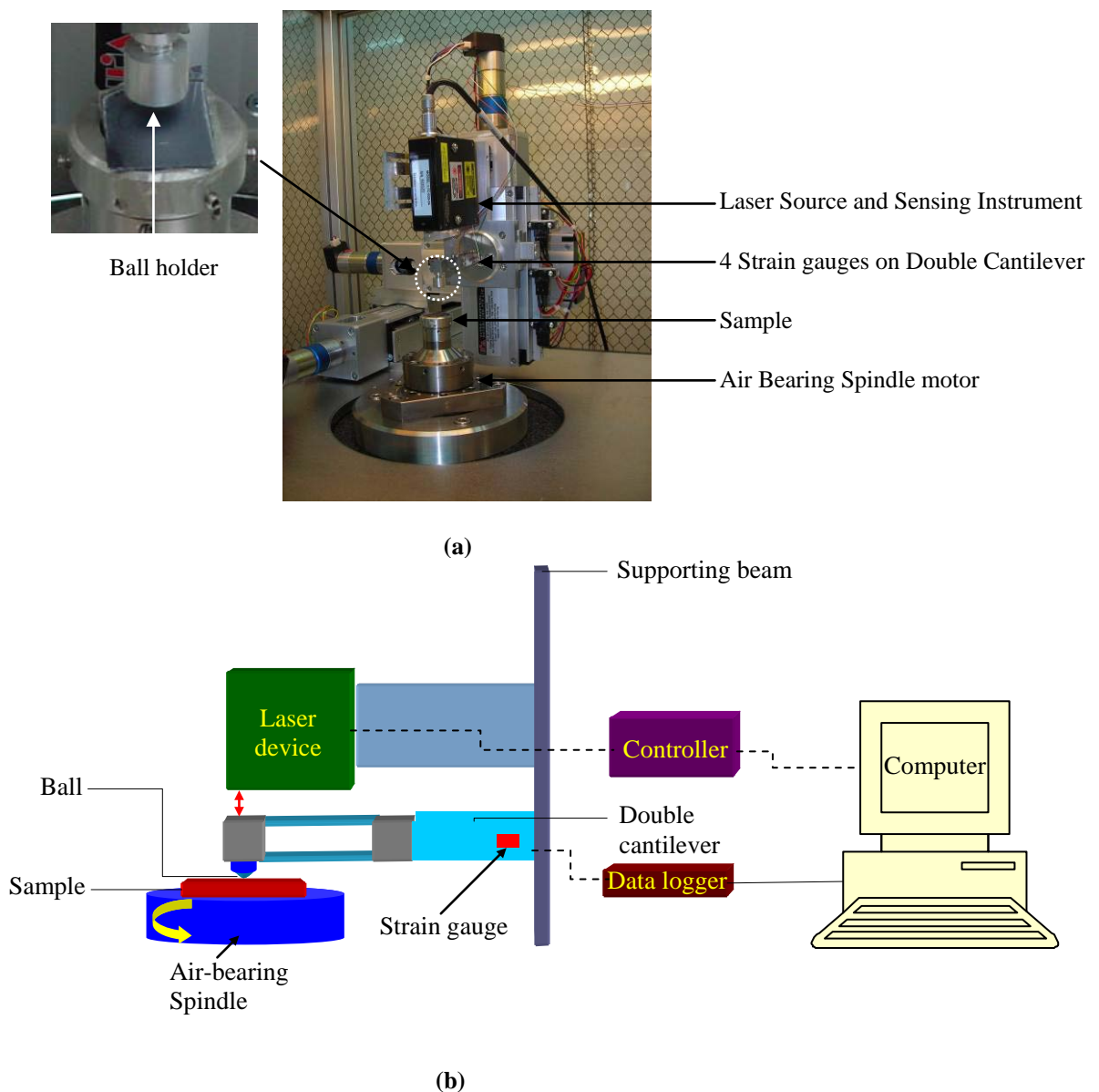


Figure 3.4: (a) Photographs and (b) schematic diagram of the ball-on-disc tribometer.

Energy dispersive spectroscopy (EDS) (Hitachi S4300 FESEM/EDS system) tests were conducted on every wear track in order to confirm the failure of the film by observing the presence of Si peak. Both the coefficient of friction and the wear life data reported are averages of at least three repeated tests.

The specific materials, experimental procedures and instruments of certain research environments will be presented in the respective Chapters.

Chapter 4

Tribology of DLC/UHMWPE as Hard and Soft Composite

Film on Si

In this Chapter the evaluation of the tribology of UHMWPE film (28 μm thickness) on Si with and without DLC (diamond like carbon) film as an intermediate layer will be presented. Perfluoropolyether (PFPE) is applied onto UHMWPE film to further extend the wear durability and results will be discussed. The effect of UHMWPE film thickness on the tribology of Si/DLC/UHMWPE will also be presented in the later part of the Chapter.

As mentioned in Chapters 1 and 2, bulk UHMWPE is a very promising polymer to be used as a solid lubricant in relative sliding components. It has been found that UHMWPE film provides a very low coefficient of friction because of the low shear strength of the polymer. However, the main disadvantage is its low load carrying capacity that leads to large contact area, high friction and failure after a few thousand cycles of sliding. One solution to reduce the contact area is the application of a hard layer between the soft UHMWPE film and the Si substrate. By introducing a new hard intermediate layer, the top polymer film help to reduce the friction whereas the underlying hard layer provides the load bearing capacity and thus longer wear life. In a recent paper, Gadow and Scherer [2002] have coated polymer film on hard coatings such as Al_2O_3 or TiO_2 which showed longer wear durability coupled with low coefficient friction by pin-on-disc method. Jiang *et al.* [2007] have proved the

tribological advantage of soft MoS₂-PTFE top layer on hard cBN-TiN substrate in reducing the friction in a ball-on-disc test.

In selecting a hard layer, DLC film is found to be an excellent medium from tribological perspective because of its chemical inertness, corrosion resistance [Liu *et al.* 1998 and 1999], high hardness, high wear resistance [Robertson 1992] and low surface energy [Grill and Patel 1993]. A very wide range of the coefficient of friction (0.001~0.7) of DLC has been reported [Erdemir and Donnet 2000] which depends not only on the chemical and structural properties of carbon contents but also on the test conditions such as the applied load, chemistry of the environment, counterface material, humidity, rotational speed and the substrate etc [Erdemir and Donnet 2006]. In this work, DLC is chosen as an intermediate layer schematically as shown in Figure 4.1. The high load carrying capacity of DLC would help in reducing the contact area between UHMWPE film and the counterface because of the substrate effect and finally promote the wear resistance.

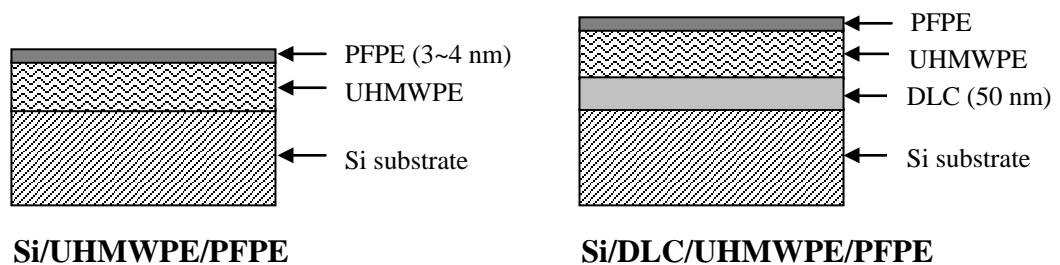


Figure 4.1: Schematic diagram (not to scale) of different layers coated on Si substrate.

4.1 Materials and preparation of different layers

Tetrahedral amorphous carbon, ta-C, (non-hydrogenated DLC) film was deposited onto n-type Si substrate by Filtered Cathodic Vacuum Arc (FCVA) technology (Nanofilm Technologies International Pte. Ltd, Singapore) and the detailed

deposition procedure can be found in Tay *et al.* [2000]. The thickness of DLC is in the range of 50 nm and hardness is 57 GPa, as provided by the supplier. Before UHMWPE was coated onto the samples, Si/DLC samples were ultrasonically cleaned in ethanol for 30 minutes whereas Si samples were cleaned as mentioned in Section 3.2.1.

The cleaned samples were then dip-coated using an UHMWPE solution of 5 wt.% (that gave approximate film thickness of 28 μm). And then, the tribological results for UHMWPE films with and without DLC intermediate layer are compared. For further enhancement on the wear durability, PFPE (0.2 wt.% in H-Galden ZV60) was dip-coated onto UHMWPE film with and without the intermediate DLC film, at dipping and withdrawal speeds of 2.4 mm/s with a fixed dipping duration of 30 seconds. This coating condition is expected to give a few (3~4 nm) nanometers PFPE film thickness.

To explore the effect of UHMWPE thickness on the tribological properties of Si/DLC/UHMWPE films, Si/DLC samples were dipped into 0.5 wt.%, 1 wt.%, 3 wt.% and 5 wt.% UHMWPE solutions at the same dipping/withdrawal speeds and dipping duration. The UHMWPE film thicknesses after dip coating into different weight concentrations were found to be approximately 3.4 μm , 6.2 μm , 12.3 μm , 28 μm respectively. The reported UHMWPE thickness was measured using the Field Emission Scanning Electron Microscopy (FESEM, Hitachi S4300). The samples were cut and mounted with their cross-sections horizontal under the FESEM to measure the polymer thickness as shown in Figure 4.2. At least ten independent measurements on three samples were carried out for each film and an average value is reported. The thickness variation is within $\pm 1 \mu\text{m}$ which is expected because of the roughness of the

polymer film after coating. The UHMWPE coatings on Si or Si/DLC substrates were of uniform thickness with no sign of uncoated area or pinholes in the film. However, when the thickness was brought down to below 3 μm , the film showed patchiness and non-uniformity. The UHMWPE coated samples were kept in a clean room for 24 hours before any test was carried out.

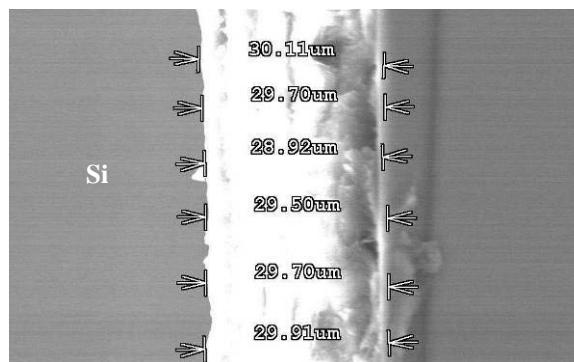


Figure 4.2: A demonstration of the measurement of UHMWPE film thickness using FESEM.

4.2 Experimental procedures

The surface analyzing techniques such as contact angle measurement, AFM topography, nanoscratching and nanoindentation were used to characterize the surface properties of UHMWPE film with and without DLC intermediate layer. The friction and wear durability were measured using ball on disc method with a custom-built tribometer. The contact point between the ball and the film was shown in Figure 4.3 where the diameter of the ball was 4 mm. Detailed characterization procedures have been explained in Chapter 3.

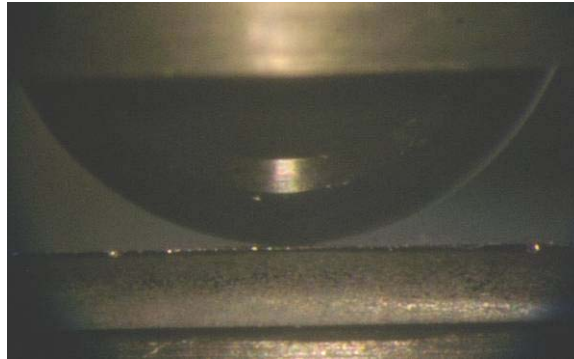


Figure 4.3: A photograph of the contact point between the ball and the film. The radius of curvature of the ball was 2 mm.

4.3 Results

4.3.1 Contact angle results

The water contact angles of bare Si, Si/UHMWPE, Si/UHMWPE/PFPE, Si/DLC, Si/DLC/UHMWPE and Si/DLC/UHMWPE/PFPE (28 μm UHMWPE thickness) are shown in Table 4.1 where the water droplet size was 0.5 μL . Bare Si substrate was hydrophilic with a contact angle of 21° . After giving the piranha treatment to bare Si, hydroxyl groups (OH) form on Si which can react with water molecules to form hydrogen bonds. The hydrogen bonds tend to be in hydrophilic in nature [Good 1993]. The contact angle of Si/DLC was 81° . The DLC film used in this study is non-hydrogenated and has only sp^3 hybridized carbons which are less reactive with water molecules. This is the possible reason for a higher contact angle. After coating UHMWPE film onto bare Si and Si/DLC, the surfaces became more hydrophobic with water contact angle of 93° and 91° respectively. When PFPE is applied as a top layer, the contact angles further increased to 95° and 102° for Si/UHMWPE and Si/DLC/UHMWPE, respectively. The hydrocarbons in UHMWPE and the fluorocarbons in PFPE do not form hydrogen bonds and thus their surface

tensions are low, in other words, their water contact angles are high [Good 1993]. The increasing contact angle is desirable in eliminating the stiction or adhesion problem arising from the capillary forces at the contact points [Mastrangelo 1997 and Maboudian and Howe 1997]. The differences in the contact angles for UHMWPE and PFPE layers on bare Si and Si/DLC are nearly the same and the variations are within the measurement error. This shows that there is no influence of the intermediate layer on the water contact angle of the top layer.

Table 4.1: Water contact angles of different surfaces on Si [Minn and Sinha 2008 a].

Surface	Contact Angle, θ ($^{\circ}$)
Bare Si	21
Si/DLC	81
Si/UHMWPE	93
Si/DLC/UHMWPE	91
Si/UHMWPE/PFPE	95
Si/DLC/UHMWPE/PFPE	102

4.3.2 Roughness measurements using AFM

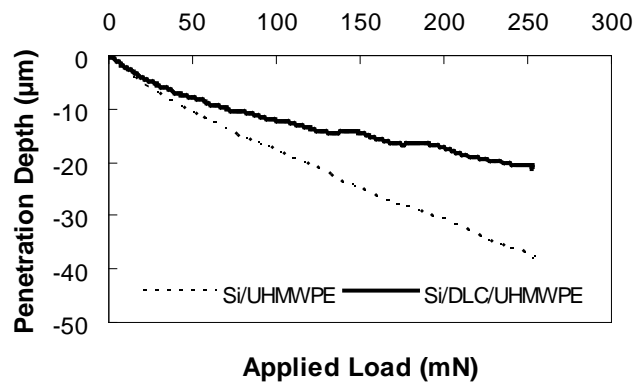
RMS roughness measurements were conducted using AFM (atomic force microscopy) within a scan area of $10 \mu\text{m} \times 10 \mu\text{m}$. The measured roughness of Si and Si/DLC surfaces are 0.41 nm and 34.8 nm respectively whereas that of UHMWPE films coated on both Si and Si/DLC are 0.56 μm . The roughness values for UHMWPE films measured within the $10 \mu\text{m} \times 10 \mu\text{m}$ scan area did not change for different film

thicknesses. Since the thickness of PFPE overcoat is in the range of a few nanometers, it does not affect much on the roughness of UHMWPE film which is in micron scale. Therefore, the roughness of Si/UHMWPE/PFPE and Si/DLC/UHMWPE/PFPE was also found to be same as 0.56 μm .

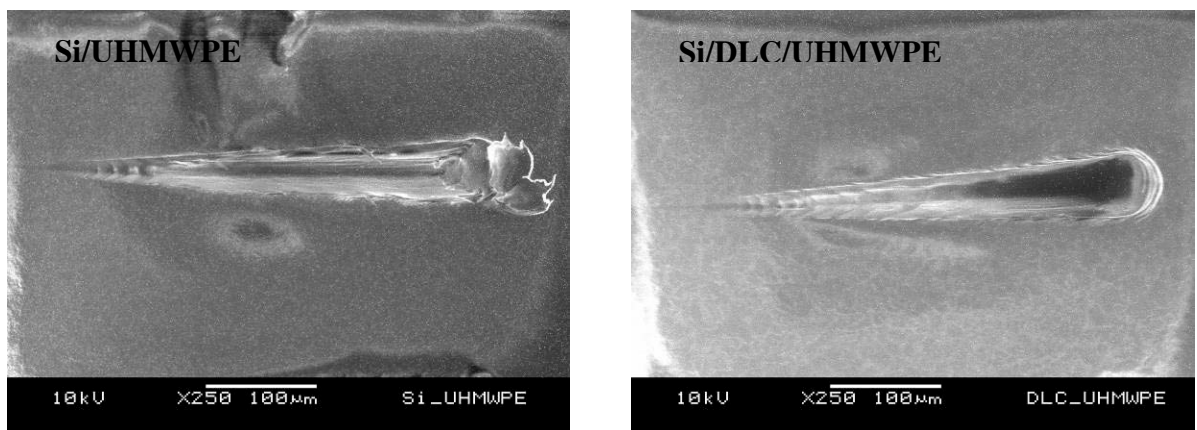
4.3.3 Nanoscratching and nanoindentation analysis

Figure 4.4 (a) shows nanoscratch resistances of Si/UHMWPE and Si/DLC/UHMWPE (28 μm thickness) samples. The scratch tests were conducted using a ramp loading setup from 0 to 250 mN at a constant scratch velocity of 10 $\mu\text{m/s}$ using a 90° conical shaped diamond tip with 5 μm tip radius. There is a clear distinction between the penetration depths for the two films as the load increases. It is noted that the load carrying capacity or the scratch hardness of Si/UHMWPE is much inferior to that of Si/DLC/UHMWPE.

The behaviors of scratch on both films were studied using SEM and images are shown in Figure 4.4 (b). It is seen that Si/UHMWPE film was easier to penetrate and peel off the substrate as can be observed at the end of the scratch. A clear damage of polymer was observed along both sides of the scratch and there was a pile of the polymer at the end of the scratch by a process of plastic deformation and partial delamination [Briscoe *et al.* 1996]. However, there were no clear wear debris, visible detachment or delamination of the film along the scratch for Si/DLC/UHMWPE film and the scratch resembled plastic deformation of the polymer by ploughing.



(a)



(b)

Figure 4.4: (a) Scratch penetration depth as a function of progressively applied normal load and (b) SEM images of the scratch deformation for Si/UHMWPE and Si/DLC/UHMWPE films. The thickness of UHMWPE is 28 µm for both cases. The progressive scratch tests were conducted using a 5 µm-radius 90°-conical shape diamond tip with scratch velocity of 10 µm/s for a scratch distance of 500 µm. Normal load varied from 0 to 250 mN and the scratching direction is from left to right.

The hardness, elastic modulus and penetration depth values for UHMWPE film with different thicknesses using nanoindentation are shown in Table 4.2. It is indicative that the presence of hard DLC layer provides higher hardness and elastic modulus with shallower penetration depth than those of Si/UHMWPE (i.e. without

DLC layer) where UHMWPE thickness is 28 μm . For Si/DLC/UHMWPE film, the hardness and elastic modulus increased and accordingly the penetration depth decreased as the thickness of UHMWPE film was reduced. Comparing with the bulk polymer, the hardness and elastic modulus of the bulk UHMWPE is approximately one order of magnitude lower than those of the 28 μm thickness film which indicates that there is considerable amount of substrate effect. It is also observed that the effect of hard DLC layer became more prominent for UHMWPE films of thickness below 6.2 μm . As a result, the contact area decreases gradually with a significant increase in the contact pressure.

Table 4.2: Mechanical properties and other parameters for different samples.

Sample	Thickness of UHMWPE (μm)	Hardness (GPa)	Elastic Modulus (GPa)	Theoretical contact area (10^{-10}m^2)	Theoretical contact pressure (MPa)	Nanoindentation penetration depth (μm)
Bulk UHMWPE	-	0.038	0.993	80	7.7	7.25
Si/UHMWPE	28	0.06	6.51	23.5	26	5.3
	3.4	11.9	171.87	3.7	165	0.45
Si/DLC/UHMWPE	6.2	0.86	43.74	7.3	85	1.52
	12.3	0.12	18.65	12	51.6	3.81
	28	0.09	8.81	19.4	31.8	4.5

4.3.4 Comparison of UHMWPE film with and without DLC interface for friction and wear

Bare Si without any protective coating gives high friction (0.65) and low wear life within a few sliding cycles. It is easy to generate wear debris after five sliding cycles as shown in Figure 4.5. Clear indications of Si debris are observed at both sides of the track along the sliding. The damage of the counterface ball is also found.

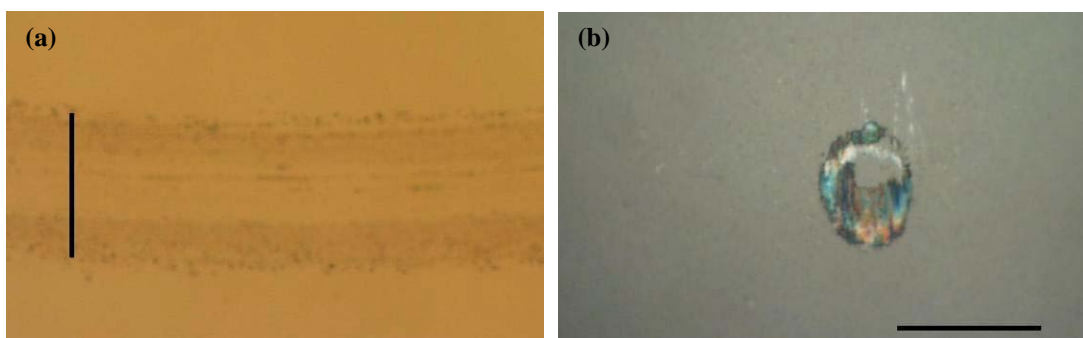


Figure 4.5: Optical images of (a) wear track on bare Si and (b) counterface ball after five cycles. The scale bars are 100 μm .

The friction and wear life data for samples with differently coated layers are provided in Figure 4.6 where UHMWPE film thickness was 28 μm . Bare Si and Si/DLC surfaces show high coefficients of friction of 0.65 and 0.25, respectively. In the presence of UHMWPE film on Si and Si/DLC, the initial coefficient of friction reduces to 0.18 and 0.13, respectively because of the self-lubricating properties of UHMWPE. This softness is able to reduce shear stress in comparison with bare Si or Si/DLC. After applying PFPE layer onto UHMWPE film, the coefficient of friction further reduces to 0.06 and 0.07 for Si/UHMWPE/PFPE and Si/DLC/UHMWPE/PFPE, respectively. PFPE molecules serve as liquid lubricant that can reduce shear stress and as a result friction is very low. The effect of PFPE overcoating onto UHMWPE film in reducing the coefficient of friction is well explained in a previous work [Satyanarayana *et al.* 2006].

It is seen in Figure 4.6 (b) that the hard DLC layer intermediate has provided approximately five times improvement in wear durability in comparison with Si/UHMWPE. This implies that the underlying DLC provides high load carrying capacity to the UHMWPE film, reduces the contact area and thus a better tribological result of Si/DLC/UHMWPE film.

It is obvious that a composite film of hard DLC and soft UHMWPE layers can provide better tribological performances. When PFPE is overcoated, the coefficient of friction reduces even further and the wear life is improved by several times to a few orders of magnitude. In the case of Si/DLC/UHMWPE/PFPE, the composite film did not show any sign of failure when the experiment was stopped due to long test duration. The coefficient of friction remained low for the entire sliding test and no wear debris was observed on the wear track after 300,000 cycles of sliding. In order to detect film failure, EDS test was conducted on the track to check for the intensity of Si peak. EDS result shows no Si peak inside the wear track and it was concluded that the film had not failed even after 300,000 sliding cycles. Figure 4.6 (c) shows the coefficient of friction trace versus sliding cycles for some films.

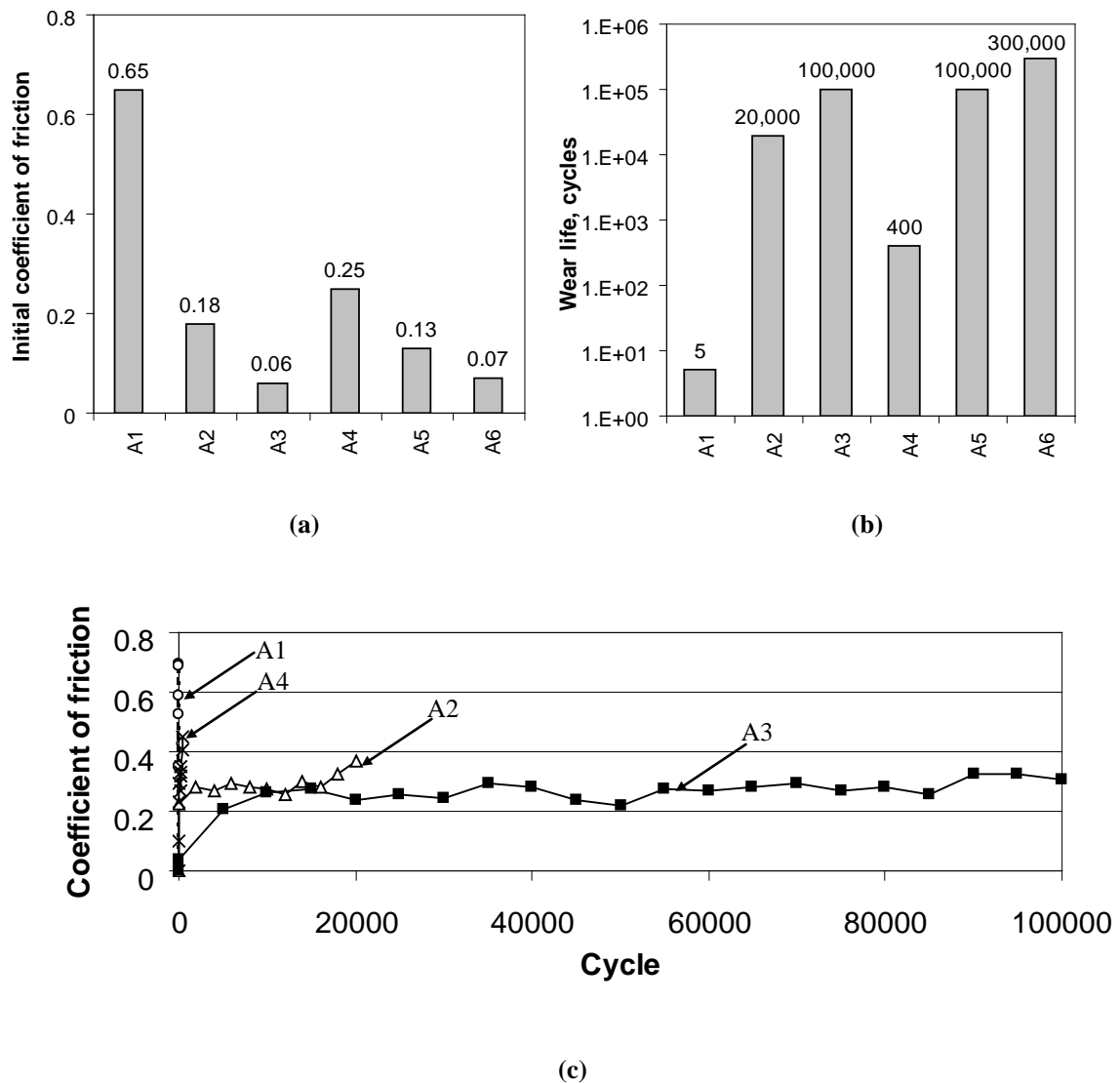


Figure 4.6: (a) Coefficient of friction, (b) wear life (logarithmic scale) of bare Si and Si coated with different single and composite films and (c) coefficient of friction versus sliding cycles of some films at a normal load of 40 mN and at a rotational speed of 500 rpm (linear speed is 5.2 cm/s) where UHMWPE thickness is fixed as 28 μm for all coated samples. (A1 = bare Si, A2 = Si/UHMWPE, A3 = Si/UHMWPE/PFPE, A4 = Si/DLC, A5 = Si/DLC/UHMWPE, A6 = Si/DLC/UHMWPE/PFPE)

The optical images of Si/UHMWPE/PFPE and Si/DLC/UHMWPE/PFPE before and after the sliding tests, and, the counterface balls after the sliding tests, are shown in Figure 4.7. It is obvious from the wear track image of Si/UHMWPE/PFPE

that the film is worn severely after the sliding test (100,000 cycles). It can be seen on the counterface ball that much polymer is transferred from the film to the ball for Si/UHMWPE/PFPE whereas Si/DLC/UHMWPE/PFPE composite film shows very little polymer transfer. The transferred polymer has greatly influenced the coefficient of friction by roughening the interface and by increasing the adhesion between the film and the counterface. Hence, there are many factors that provide the best tribological performances of Si/DLC/UHMWPE/PFPE. Firstly, hard DLC has high load carrying capacity and provides better penetration resistance and reduces the contact area. Secondly, the linear UHMWPE has self-lubricating property that helps reduce shear stress. In other words, although the hard DLC alone has high shear stress, the overcoating of soft UHMWPE layer onto DLC can reduce the shear stress drastically. Thirdly, the water contact angle of Si/DLC/UHMWPE/PFPE is 102° compared with 95° for Si/UHMWPE/PFPE and hence the surface energy of the film is reduced because of DLC interlayer. Surface energy has strong influence on the friction, wear and material transfer, as will be presented in Chapter 8 of this thesis. Fourthly, the higher thermal stability and excellent lubricating properties of PFPE can provide further reduction in the coefficient of friction and increase the resistance to frictional heating. Also, frictional heat dissipation is less when the coefficient of friction is low.

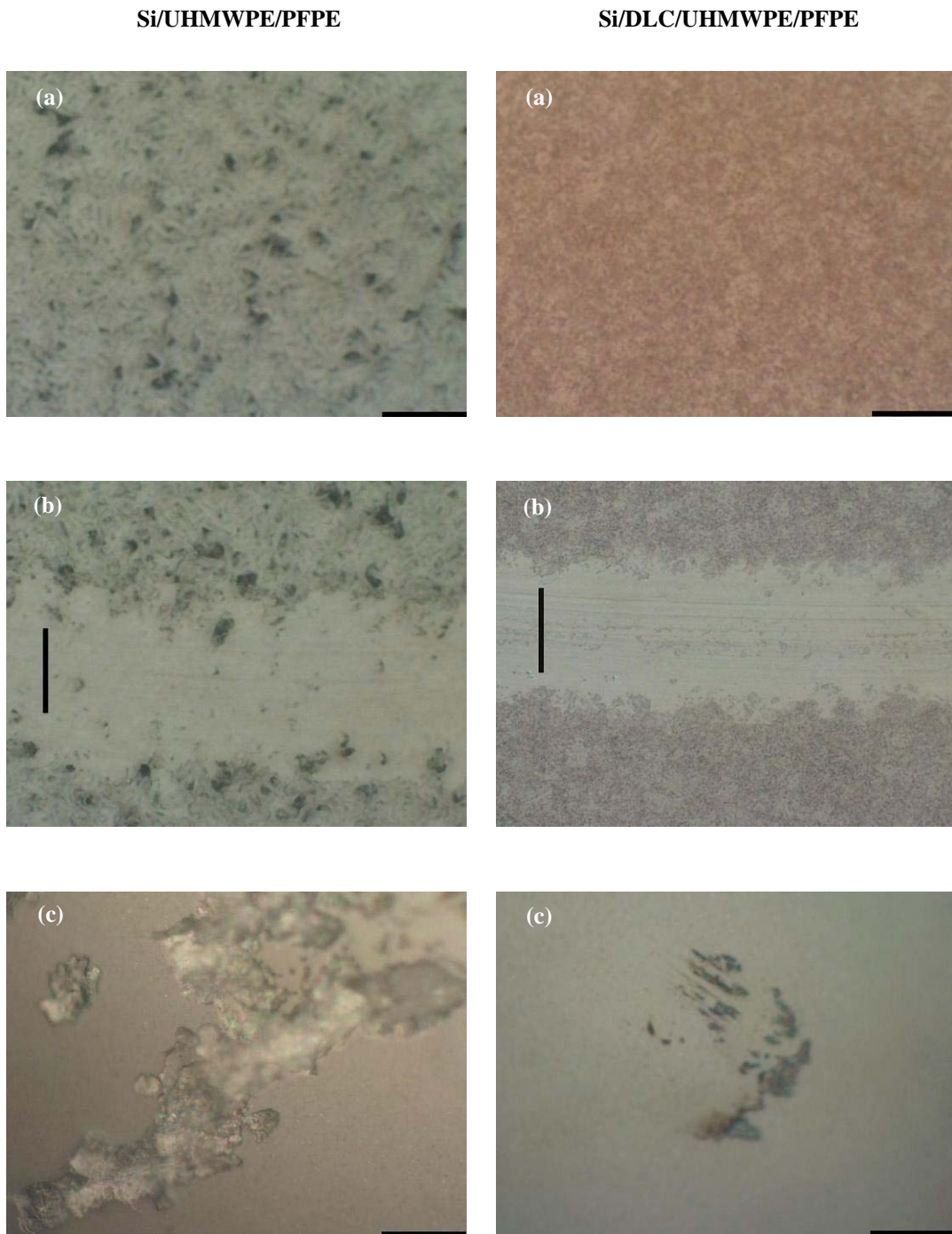
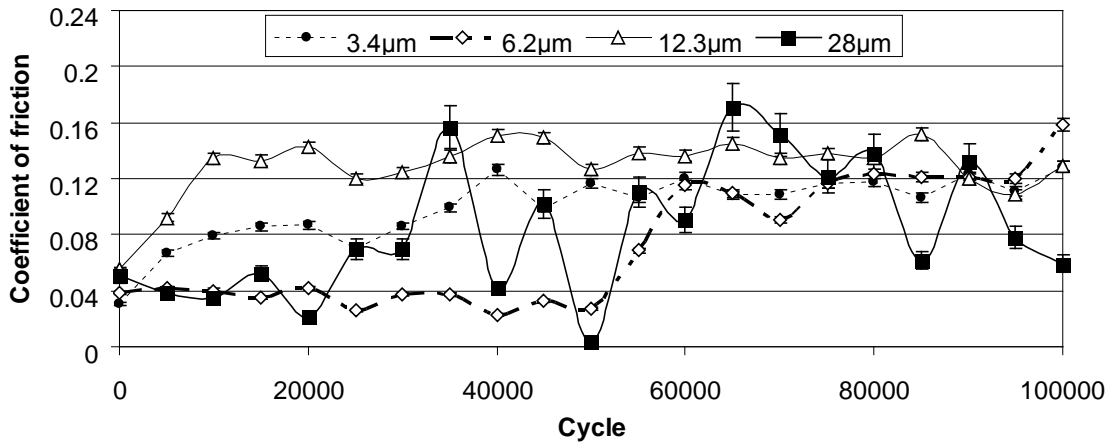


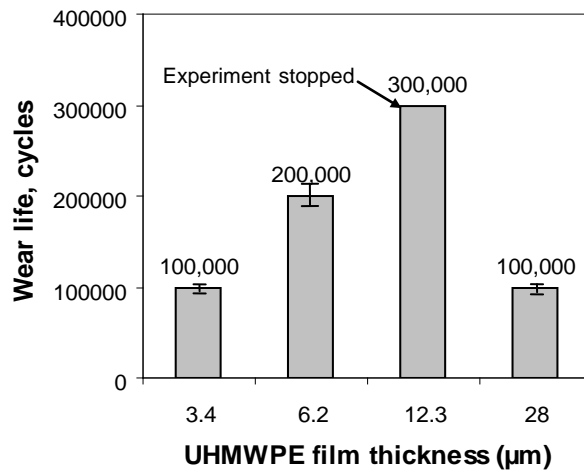
Figure 4.7: Optical images of Si/UHMWPE/PFPE (first column) and Si/DLC/UHMWPE/PFPE (second column) surfaces (a) before the test, (b) after sliding 100,000 cycles and (c) counterface ball after 100,000 cycles. The scale bars are 50 μm .

4.3.5 Effect of UHMWPE thickness on the friction and wear

The effect of UHMWPE thickness on the friction and wear properties of Si/DLC/UHMWPE is shown in Figure 4.8. At the early stage of sliding cycles, the coefficients of friction are the same and variations are within the measurement errors for all thicknesses. However, the effects of thickness are observed on friction and wear as the number of sliding cycles is increased. For a film thickness of 3.4 μm , the coefficient of friction increases with increasing number of cycles and the role of underlying hard DLC is dominant which causes high shear stress or coefficient of friction and the film fails at $\sim 100,000$ cycles. For the 6.2 μm film, the friction shows the same trend as thinner film (3.4 μm), but the shear stress or coefficient of friction on 6.2 μm film is lower in comparison with that on 3.4 μm film and thus the wear life extends to 200,000 cycles. The coefficient of friction for 12.3 μm film is stable at 0.14 ± 0.02 for 300,000 cycles when experiments are stopped. Although the coefficient of friction of 28 μm film is low until 20,000 cycles, the friction starts showing large fluctuations and fails at 100,000 cycles. These large fluctuations are due to the different removal rates of polymer from the sliding track that increases roughness. Detailed explanations on this aspect will be provided in Section 4.3.7.



(a)



(b)

Figure 4.8: (a) Coefficient of friction with respect to sliding cycles in typical runs for different thicknesses of UHMWPE in composites films of Si/DLC/UHMWPE, (b) Wear life for different UHMWPE thicknesses for Si/DLC/UHMWPE. Data are averages of three repeated tests. For 12.3 μm thick film there was no failure at 300,000 cycles of sliding when the experiments were stopped due to long test duration.

4.3.6 Wear mechanisms for different UHMWPE thicknesses

The optical images of the wear tracks for Si/DLC/UHMWPE film of different thicknesses with respect to the number of cycles are shown in Figure 4.9. The widths of the wear tracks increase as the number of sliding cycles increases for all films. The increase in the width of the contact area leads to high friction as the sliding progresses.

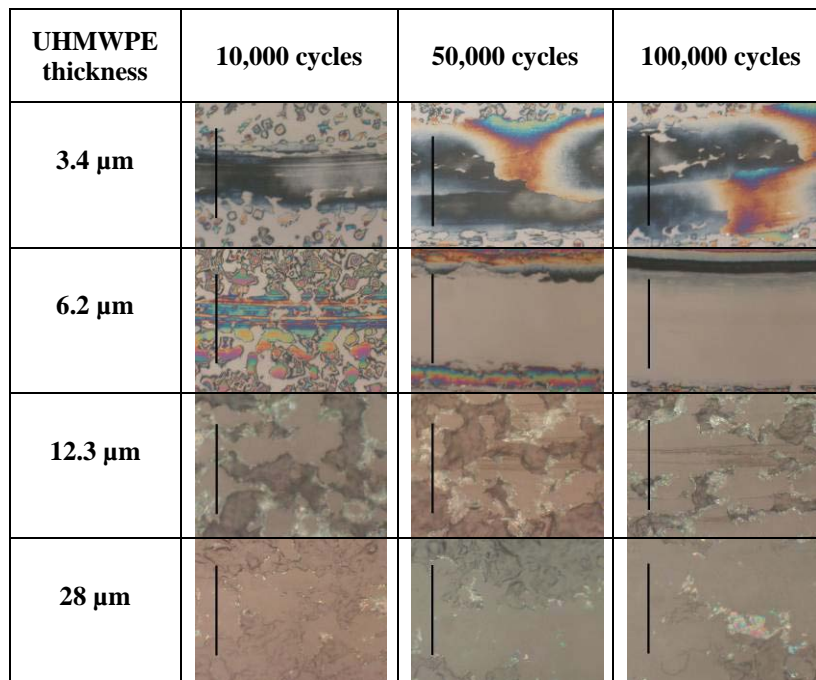


Figure 4.9: Wear track optical images of 3.4 μm , 6.2 μm , 12.3 μm and 28 μm UHMWPE thicknesses for Si/DLC/UHMWPE (at a normal load of 40 mN, at a rotational speed of 5.2 cm/s (500 rpm) and test radius 1 mm) against Si_3N_4 counterface ball after 10,000, 50,000 and 100,000 sliding cycles. The scale bars are 50 μm .

It is clearly seen in the optical images that the contact stress is a major factor contributing to friction and wear of 3.4 μm film thickness. It agrees well with the nanoindentation results (Table 4.2) where the contact pressure of 3.4 μm film is highest and contact area is lowest. As a result, the surface image shows some kind of polymer degradation possibly due to high frictional heat generated within a small

contact area. The optical image of 6.2 μm film thickness after 50,000 cycles shows smooth surface after removing the asperities and the effect of roughness on friction diminishes after 50,000 cycles. It is indicative of a very smooth track that suggests softening of the sliding surface [Tanaka *et al.* 1973]; soft polymer surface can help maintain low coefficient of friction. It is obvious from the optical images of 12.3 μm and 28 μm films that the rates of material removal from the sliding track are not uniform. The surface becomes roughened because of the asperities of the films that are removed non-uniformly at an early stage. Though there is an uneven removal of the polymer for 12.3 μm film thickness, the surface becomes as smooth as 6.2 μm film thickness with increasing cycles and the effect of surface roughness on friction and wear becomes less. On the other hand, 28 μm thick film fails quite easily. The possible reason is that the large amount of polymer being transferred to the ball causes large fluctuations in the coefficient of friction. The optical images of Si_3N_4 balls after sliding against different UHMWPE thicknesses are provided in Figure 4.10. The amount of polymer transferred from the thickest film (Figure 4.10 d) is much greater than that from film of any other thickness.

4.3.7 Discussion

Nanoscratching data shows a large difference in penetration resistance between Si/UHMWPE and Si/DLC/UHMWPE for 28 μm UHMWPE thickness. The slope of load penetration depth of Si/UHMWPE is steeper than that of Si/DLC/UHMWPE, which means the penetration resistance of the latter is greater due to the higher load carrying capacity provided by the hard DLC intermediate layer. In other words, the

contact area of Si/UHMWPE is larger than that of Si/DLC/UHMWPE and as a result the friction of former is higher than that of the latter. The hardness data from nanoindentation (Table 4.2) are consistent with nanoscratching results. At the early stage, the initial penetration depth (5.3 μm for Si/UHMWPE) is shallower than the whole film thickness (28 μm).

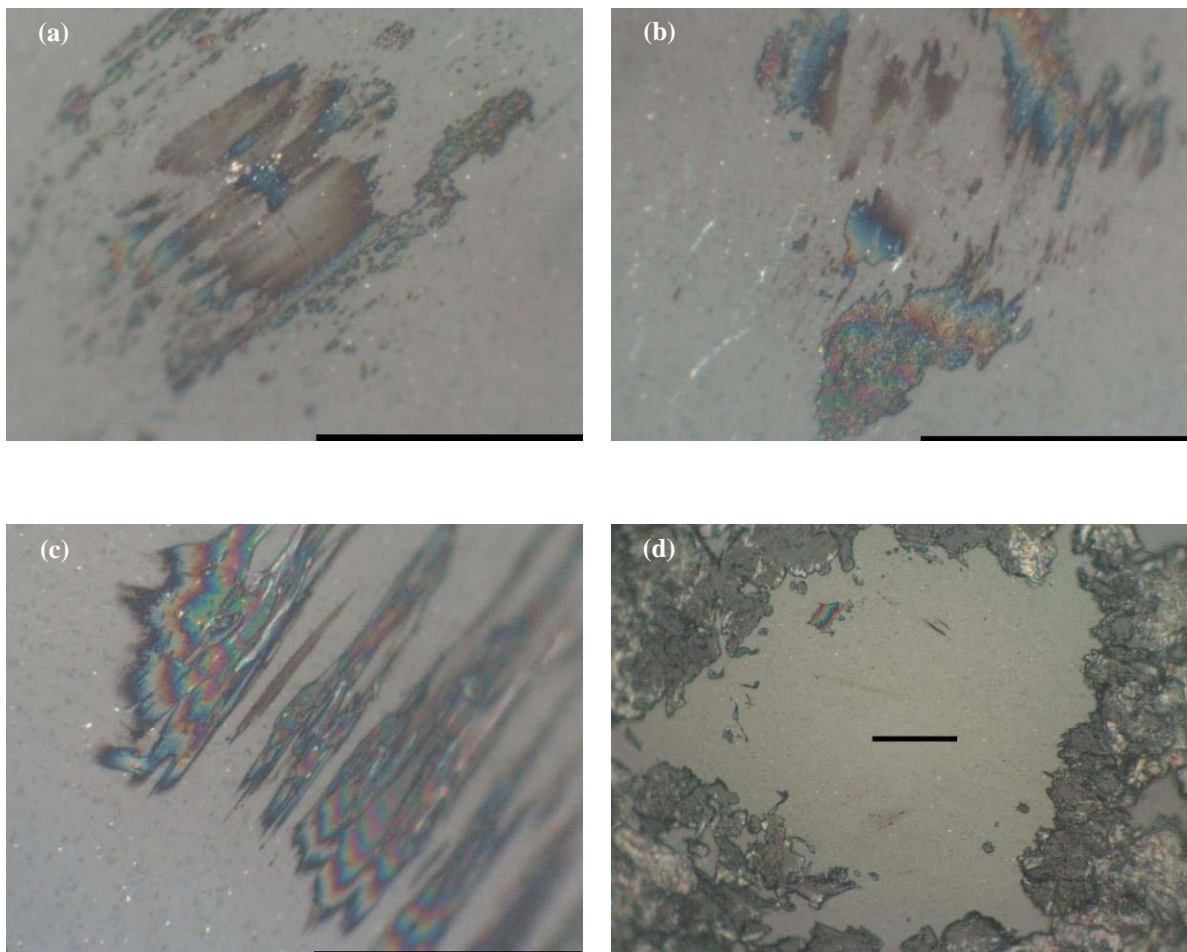


Figure 4.10: Optical images of Si_3N_4 counterface ball against Si/DLC/UHMWPE with different polymer film thicknesses (a) 3.4 μm (b) 6.2 μm (c) 12.3 μm and (d) 28 μm after sliding 100,000 cycles. Figures (a, b and c) are magnified 500 times and Figure (d) is magnified 200 times. The scale bars are 50 μm .

However, as the sliding continues, the transferred film on the ball surface is progressively renewed by wearing out of the polymer from the contact point and the

ball reaches the Si substrate after about 20,000 cycles due to weak penetration (low hardness) resistance and large contact area. For Si/DLC/UHMWPE, no sign of film failure was observed until 100,000 cycles because of strong penetration resistance and small contact area in comparison with Si/UHMWPE.

The elastic modulus of Si/DLC/UHMWPE is also higher than that of Si/UHMWPE. That means Si/DLC/UHMWPE layer has greater relaxation time for any change in the elastic property due to the interfacial temperature or creep. This is because of the lower elastic modulus and the higher mobility of the molecules to flow in viscous manner due to less strong inter-molecular bonding. Hence, the relaxation time for larger contact area decreases with decreasing elastic modulus [Gorokhovskii and Agulov 1966] and thus the film is prone to damage because of thermal effect. As a result, the polymer is easily removed from the sliding track due to thermal and time dependent changes in the modulus of the film and the wear life of Si/UHMWPE is shorter than that of Si/DLC/UHMWPE. Thus, better bonding strength of the UHMWPE molecules with DLC and better mechanical properties of DLC with self-lubricating property of UHMWPE are the main reasons for higher tribological performance of Si/DLC/UHMWPE film.

The hydrophilic nature of bare Si attracts water molecules and the presence of these water molecules effectively weakens the adhesion strength between substrate and UHMWPE [Armstrong and Wright 1993 and Mansfeld 1995]. The investigation of surface wettability on the tribology of UHMWPE film will be discussed in Chapter 6. When DLC is coated onto bare Si, the film surface became hydrophobic and repels water. The adhesion strength between Si/DLC and UHMWPE is stronger than that

between bare Si and UHMWPE. As a consequence, the polymer from Si/UHMWPE is easily removed during contact sliding in comparison with that from Si/DLC/UHMWPE.

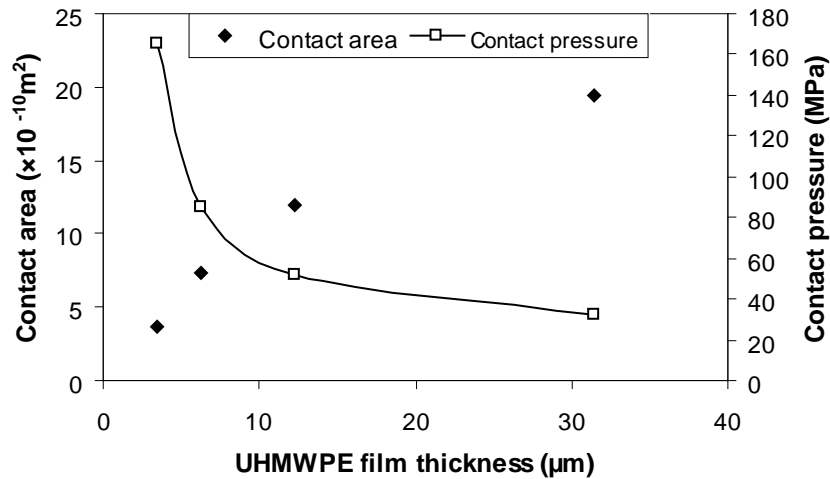


Figure 4.11: Contact area and contact pressure vs. UHMWPE thickness for Si/DLC/UHMWPE where contact area and contact pressure are theoretically calculated using Hertzian equation and nanoindentation data presented in Table 4.2.

In order to further extend the wear life, because of its high lubricity and thermal stability, PFPE was coated onto Si/UHMWPE and Si/DLC/UHMWPE. After PFPE coating, the coefficient of friction was lower than 0.1 for both films, and, wear lives extended to 100,000 cycles for Si/UHMWPE and at least 300,000 cycles for Si/DLC/UHMWPE when the experiments were stopped. The chemical bonding between UHMWPE and PFPE films is ruled out since UHMWPE film does not have any reactive chemical groups. It is assumed that PFPE molecules are trapped in the initial roughness of the UHMWPE films and these molecules may serve as liquid lubricant to reduce shear stress and friction [Satyanarayana *et al.* 2006]. Another

possible reason for better enhancement in the wear durability is the thermal stability of PFPE, which can withstand higher (up to a range of 327-477 °C [Lei *et al.* 2001]) frictional heat generated at the interface without degradation. The lower coefficient of friction in the presence of PFPE also means low frictional energy dissipation and less heating of the interface.

As the UHMWPE film thickness decreases, the load carrying capacity of the film is greatly affected by the underlying hard DLC layer and the effects of shear stress (in the dynamic case) and contact pressure becomes high leading to the high friction and early failure of the film. As shown in Figure 4.11, the relationship between the contact area and UHMWPE film thickness is linear but the contact pressure has two trends: below 6.2 μm it increases significantly and above 6.2 μm it displays a gradual decrease. For the thin film (3.4 μm), though the contact area decreases slightly, its contact pressure increases significantly which means that the shear stress could increase significantly since the ratio of shear stress to contact pressure is assumed to be constant within the experimental range. If the film thickness is too low in comparison with the contact radius, the counterface ball will reach DLC film and detach the DLC particles. The detached particles can serve as third-body abrasive particles at the interface which will increase friction and initiate wear [Arnell 1990]. For the 6.2 μm film, the contact area is high and the shear stress is low and its wear life extends to 200,000 cycles. Under this condition, UHMWPE film helps in lubricating the interface without any failure of the DLC which was seen in the case of 3.4 μm thick film.

When the film thickness increases, the contact area will increase with deeper penetration depth that leads to large friction coefficient (due to large transfer of the

film polymer to the counterface) and low wear life. This result agrees with the work of Aubert *et al.* [1990]. At the early stage of the test, the asperities of the film are removed by microcutting [Sherbiny and Halling 1977] and the removal rates of the polymer film vary in different parts of the sliding tracks (28 μm film in Figure 4.8), which lead to non-uniform contact points.

When the amount of transferred polymer on the ball surface is large and surface becomes rough, the coefficient of friction between non-uniform film and roughened polymer adhered ball is highly fluctuating. As a result, the thicker film (28 μm) fails earlier at about 100,000 cycles. For the 12.3 μm film, though its optical image (Figure 4.9) shows similar non-uniform pattern as that of the 28 μm film, the amount of polymer transferred is relatively low. Furthermore, the surface becomes smoother as the sliding cycles increases. Thus, though the coefficient of friction for 12.3 μm film is slightly high, it shows consistent value at 0.14 ± 0.02 for at least 300,000 cycles when the experiments are stopped. In order to obtain higher wear life for the UHMWPE film, the film thickness should be in an optimum range to avoid factors that increase or fluctuate friction, such as high contact stress, large contact area and greater polymer transfer to the counterface.

According to the present results, the range of optimum thickness to obtain higher wear life for Si/DLC/UHMWPE film is approximately within 6.2 μm -12.3 μm . The advantage of high wear resistant UHMWPE film can be obtained only if the film thickness is optimum so as to avoid the large interface/substrate effect on friction and wear (for low film thickness) or, the substantial polymer transfer to the counterface (for high film thickness).

4.4 Summary

The current Chapter presented the results on the advantages of Si/DLC/UHMWPE composite film (with and without PFPE as the top overcoat) and the role of UHMWPE thickness on the tribological performance. After coating UHMWPE onto Si, the coefficient of friction reduced to 0.18 and wear durability is remarkably increased to 20,000 cycles compared to only few cycles for bare Si surface. The presence of DLC intermediate layer provides higher load carrying capacity (high hardness and elastic modulus) and better adhesion between UHMWPE and DLC coated substrate and as a consequence, the coefficient of friction decreased to 0.13 and wear durability extended to 100,000 cycles for Si/DLC/UHMWPE. This is five times improvement over the film without DLC intermediate layer. Overcoating with PFPE as the top layer gave coefficient of friction as low as 0.06 and wear durability increased to 100,000 cycles and more than 300,000 cycles for Si/UHMWPE/PFPE and Si/DLC/UHMWPE/PFPE, respectively, when thickness of UHMWPE was fixed at 28 μm . For Si/DLC/UHMWPE film, the wear lives of thin film (3.4 μm) and thick film (28 μm) are approximately 100,000 cycles, which are shorter than those of the moderate (optimum) thicknesses (6.2 μm and 12.3 μm). The wear lives of moderate films are 200,000 cycles and more than 300,000 cycles for 6.2 μm and 12.3 μm , respectively. The lower wear durability of 3.4 μm thick film is due to high contact stress that generates high frictional heat at the interface contributing to film failure and that of 28 μm thick film is due to larger contact area owing to soft layer and large fluctuations in the coefficient of friction with occasional high peaks due to polymer transfer to the counterface.

It should also be noted that some other parameters can affect the frictional characteristics of the films. For example, the interfacial strength and the crystallinity of the polymer film are two very important parameters and an investigation on their effects on the frictional characteristics of UHMWPE film will be presented in next Chapters.

Chapter 5

Tribology of UHMWPE Film with Different Hard Intermediate Layers

Detailed studies on the tribological advantages of UHMWPE film on Si in the presence of hard DLC as an intermediate layer were presented in Chapter 4. The effects of UHMWPE thickness on the friction and wear performances were investigated too. Though superior tribological properties of the composite hard and soft films have been well recognized, the exact relationship between the wear life of the composite film and the hardness of the intermediate harder layer is still unclear. In this Chapter, an attempt is made to investigate such a relation with an UHMWPE thickness of 4-5 μm which is in the optimum range of thickness.

Silicon was used as the substrate with its hardness value of 12.4 GPa. Different hard intermediate layers such as CrN, TiN and tetrahedral amorphous carbon, (ta-C or DLC) were deposited onto Si substrate and then followed by a soft UHMWPE film as top layer. Firstly, the tribological properties of different composite films are compared at a fixed applied load of 40 mN. Secondly, scratch tests with different applied normal loads are conducted on the composite films in order to understand the critical scratch load for film failure. A correlation between the critical loads and the wear durability has been discussed using scratch tests. Thirdly, perfluoropolyether (PFPE) is overcoated onto UHMWPE film to further reduce the shear stress and enhance the wear life for the composite films.

5.1 Experimental procedures

5.1.1 Materials

Polished n-type Si (100) wafers (obtained from Engage Electronics (Singapore) Pte Ltd), of about 455-575 μm in thickness and with a hardness of 12.4 GPa, were used as the substrate. Chromium nitride, titanium nitride and tetrahedral amorphous carbon, ta-C (non-hydrogenated DLC) films with different hardness values were deposited onto Si substrate. All the films were deposited by Nanofilm Technologies International Pte Ltd, Singapore using Filtered Cathodic Vacuum Arc technique. The thicknesses of all hard films were fixed in the range of 50 nm. UHMWPE powder (bulk density = $0.33 \pm 0.03 \text{ g/cm}^3$ and average particle size of $20 \pm 5 \mu\text{m}$) was dissolved in decahydronaphthalene (decalin) for the purpose of dip-coating UHMWPE films (Section 3.2). In order to further extend the wear life of the film, a commercial Z-dol 4000 of 0.2 wt% (dissolved into H-Galden ZV60 purchased from Ausimont INC) was overcoated onto UHMWPE film.

5.1.2 Preparation of different layers on Si substrate

The detailed procedures of cleaning substrates and preparing UHMWPE solution have been described in Section 3.2. The cleaned samples were dipped in UHMWPE solution for 30 seconds with a fixed dipping and withdrawal speeds of 2.4 mm/s. The thickness of the UHMWPE film was approximately 4-5 μm and its roughness (R_a) was approximately 0.56 μm (measured by AFM). For some samples, PFPE (0.2 wt.% in H-Galden ZV60) was dip-coated onto UHMWPE film at dipping and withdrawal speeds of 2.4 mm/s with a fixed dipping duration of 30 seconds. The

thickness of PFPE is expected to be a few (3-4 nm) nanometers as measured in an earlier study. After coating, the samples were kept in a clean room for 24 hours before any test was conducted. A schematic diagram and a FESEM image of the coated layers on the Si substrate are provided in Figure 5.1. The image shows cross-section of the sample. The polymer coating is clearly visible whereas the hard intermediate coating is not very precisely identifiable due to very low thickness (~ 50 nm).

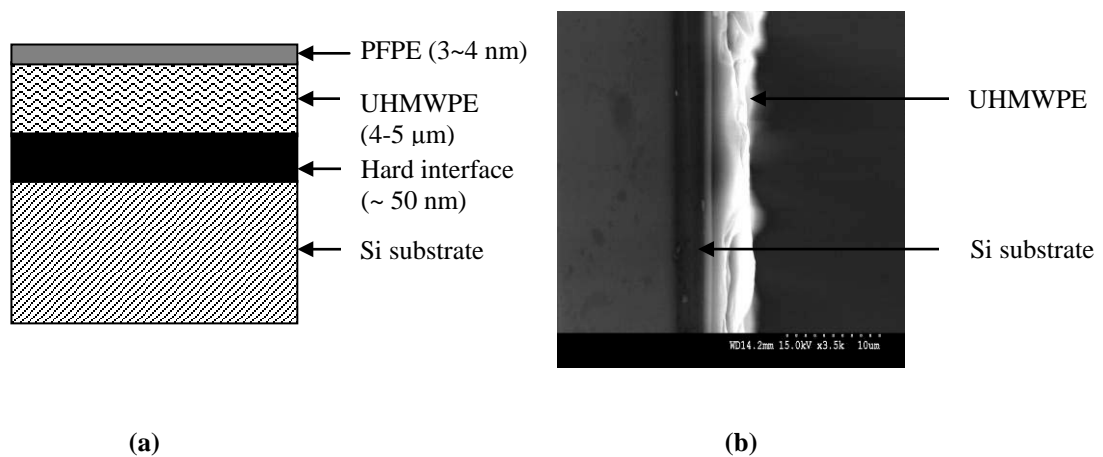


Figure 5.1: (a) Schematic (not to scale) diagram of different layers coated onto Si substrate and (b) FESEM image of the cross-section of UHMWPE (white region) film on Si substrate. The scale bar is $10 \mu\text{m}$. The thickness of the polymer film is in the range of 4-5 μm .

5.1.3 Surface characterizations

The surface wettabilities of different hard interfaces on Si substrate were determined by measuring the water contact angles with a VCA Optima Contact Angle System (AST product, Inc., USA). Distilled water droplets of $0.5 \mu\text{L}$ were used for the measurements. The contact angles are reported as an average of five independent measurements on the samples. The measurement error is within $\pm 3^\circ$.

In order to verify the hardness of different intermediate layers provided by the supplier, nanoindentation tests were conducted on samples using a constant load of

300 μN with a 100 nm radius diamond tip. The nanoindentation system consists of the Nanoscope IIIa controller (Digital Instruments, Santa Barbara, CA, USA) with a triboscope indenter system (Hysitron Inc., MN, USA). The time taken during loading on the sample was 5 seconds with a constant holding time of 10 seconds before unloading. The penetration depth of indentations was less than 5 nm.

In order to understand the load bearing capacity of the composite films, microhardness tests were also carried out on Si/UHMWPE films with different hard intermediated layers using Shimadzu-HMV automatic digital microhardness tester. The microhardness test was performed using a Vickers indenter (manufactured by Gilmore Diamond Tools, Inc) under a test load of 10 gf and a dwell time of 15 seconds.

5.1.4 Friction and wear tests

Friction and wear tests were carried out on a custom-built ball-on-disc type tribometer (Figure 5.2). A 4-mm diameter silicon nitride (Si_3N_4) ball (Vickers hardness = 1500 Hv, from supplier's data) was used as a stationary counterface whereas the sample coated with UHMWPE film acted as the disc. The test radius was ~ 1 mm with a fixed disc rotational speed of 500 rpm (linear relative speed at the sliding contact = 0.052 m/s). During the sliding tests, the vertical and lateral displacements of the force sensing cantilever holding the ball were carefully measured using laser instruments (MTI Instruments Inc., New York, USA). These displacement values were then converted to forces (normal and frictional) using a calibration chart. The sensitivity of the laser instrument is 0.5 μm which is equivalent to a force of 0.125 mN according to

our calibrations. In this study, the wear life of each sample is defined as the number of cycles when the coefficient of friction exceeds 0.3 or large fluctuations of the coefficient of friction occur continuously, whichever happens earlier. Energy dispersive spectroscopy (EDS) (Hitachi S4300 FESEM/EDS system) tests were used to identify the presence of Si peak on the wear tracks in order to confirm the failure of the sample. The tribological tests were conducted in a class-100 clean booth environment at a temperature of $25 \pm 2^\circ\text{C}$ and a relative humidity of $55 \pm 5\%$. The reported friction and wear data are averages of at least three repeated tests.

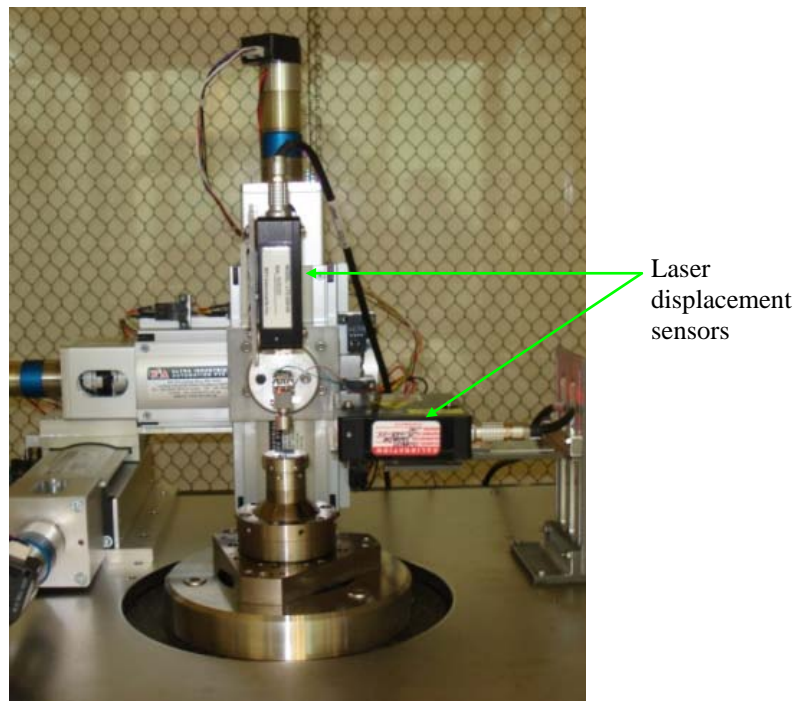


Figure 5.2: A ball on disc tribometer with two laser sensors.

5.1.5 Scratch tests

A $2\ \mu\text{m}$ radius diamond tip was used to conduct scratch tests on every sample in order to compare the adhesion strength and load carrying capacity of the samples. The diamond tip was indented into the UHMWPE film under an increasing applied

load from 10 mN to 100 mN with an increment of 10 mN. The scratching velocity and the linear scratch distance were fixed at 0.1 mm/s and 5 mm, respectively. After the scratch test, the scratches were studied under an FESEM in order to observe the surface failure mechanisms such as the generation of debris particles or delamination of the film. Before taking FESEM images, gold coating was performed on the tested polymer films at 10 mA for 40 seconds (JEOL, JFC-1200 Fine Coater). EDS (energy dispersive spectroscopy) tests were conducted on the scratches on samples with gold coating to record carbon and silicon peaks.

5.2 Results and Discussion

5.2.1 Surface analysis

The surface wettability of the film can be determined by measuring the water contact angle which is an important parameter for better adhesion between the polymer film and the substrate. Greater hydrophilic surface generally can provide better adhesion of the film to the substrate and higher wear durability. However, at the same time, this hydrophilic surface tends to attract more water molecules from atmosphere. The presence of water molecules can, on the other hand, reduce the adhesion strength [O'Brien *et al.* 2006] of the film to the substrate. The relationship between surface wettability and wear durability will be discussed in next Chapter in detail. In addition to surface wettability, the hardness of the substrate is also an important factor in determining the tribological properties of composite films as it can provide better load carrying capacity.

The water contact angle and nanoindentation hardness values of different hard intermediate layers are provided in Table 5.1. The water contact angle of bare Si shows 21° that indicates very hydrophilic nature. The contact angles of all the rest coatings are in the range of 68 - 81°. Within this range, the effect of contact angle (surface wettability) on the adhesion strength between UHMWPE film and the substrate is assumed to be comparable. In the presence of UHMWPE as top layer, all composite films show a contact angle of 91°. The water contact angle for the Si₃N₄ ball was measured as 70°.

Table 5.1: Water contact angles and nanohardness for different intermediate hard layers.

Interface	Contact angle (°)	Nanohardness (GPa)
Bare Si	21	12.4
Si/CrN	80	13.5
Si/DLC15	79	15
Si/TiN	68	24
Si/DLC57	81	57
Si/DLC70	80	70

Bare Si and Si/CrN have the lowest hardness values of 12.4 GPa and 13.5 GPa respectively. Increasing hardness values were observed for DLC15, TiN, DLC57 and DLC70 films as 15 GPa, 24 GPa, 57 GPa and 70 GPa respectively. The suffix mentioned in various DLCs represented their respective hardness values. The nanoindentation hardness of the UHMWPE film was measured as 35 MPa for all samples regardless of the intermediate layers and the variation was within the measurement errors where the indentation depth was approximately 400 nm. This

shows that in nanoindentation test there is no substrate effect in the measurement of nano-mechanical properties of several micron thick polymer films.

The microhardness of the composite data in Table 5.2 also confirms that the film with harder intermediate layer provides higher overall hardness and hence better load carrying capacity. Consistent with the nanoindentation hardness of the intermediate layers, there is considerable increase in the microhardness of the composite films with the DLC57 and DLC70 intermediate layers. Obviously, this increase in microhardness is arising from the substrate effect as the depth of indentation in microhardness is large [Buckle 1973, Ross *et al.* 1987, Lebovier *et al.* 1989, and Manika and Maniks 1992].

Table 5.2: The microhardness, critical loads in scratching and wear lives of 4~5 μm thick UHMWPE films with different intermediate hard layers. The applied load used for wear life determination is 40 mN.

Interface	Microhardness (HV)	Critical load (mN)	Wear durability (cycles)
Bare Si/UHMWPE	11.2 ± 1	20	1,000
Si/CrN/UHMWPE	11.4 ± 1	20	2,000
Si/DLC15/UHMWPE	12.5 ± 0.8	30	35,000
Si/TiN/UHMWPE	15.4 ± 1.7	60	>300,000
Si/DLC57/UHMWPE	23 ± 1.7	60	>300,000
Si/DLC70/UHMWPE	30.7 ± 1.9	80	>300,000

5.2.2 Friction and wear results on hard intermediate layers

In order to understand their individual performances, the friction and wear tests were conducted on all hard layers used before depositing UHMWPE film onto them. Figure 5.3 shows the typical graphs of the coefficient of friction versus the number of sliding cycles in the sliding tests with an applied load of 40 mN. Data show that except for DLC70, the friction of all other hard films increased above 0.3 within 50-400 number of sliding cycles which was considered as film failure by the current definition. Si/CrN and Si/DLC15 layers have shown higher coefficients of friction and failed within 50 cycles and 200 cycles, respectively, whereas Si/TiN and Si/DLC57 have a wear durability of nearly 400 cycles. In all cases, the wear of the silicon nitride ball was observed and a clear wear track was seen on the film indicating wear of the film as well. DLC70 film gave very low coefficient of friction and also the wear life was much longer than for other hard films. However, even for this film, the maximum life was only ~ 11,000 after which there were large fluctuations in the coefficient of friction reaching as high as 0.25. The silicon nitride ball and the film showed wear even in this case. The initial coefficient of friction and wear durability are also summarized in Table 5.3.

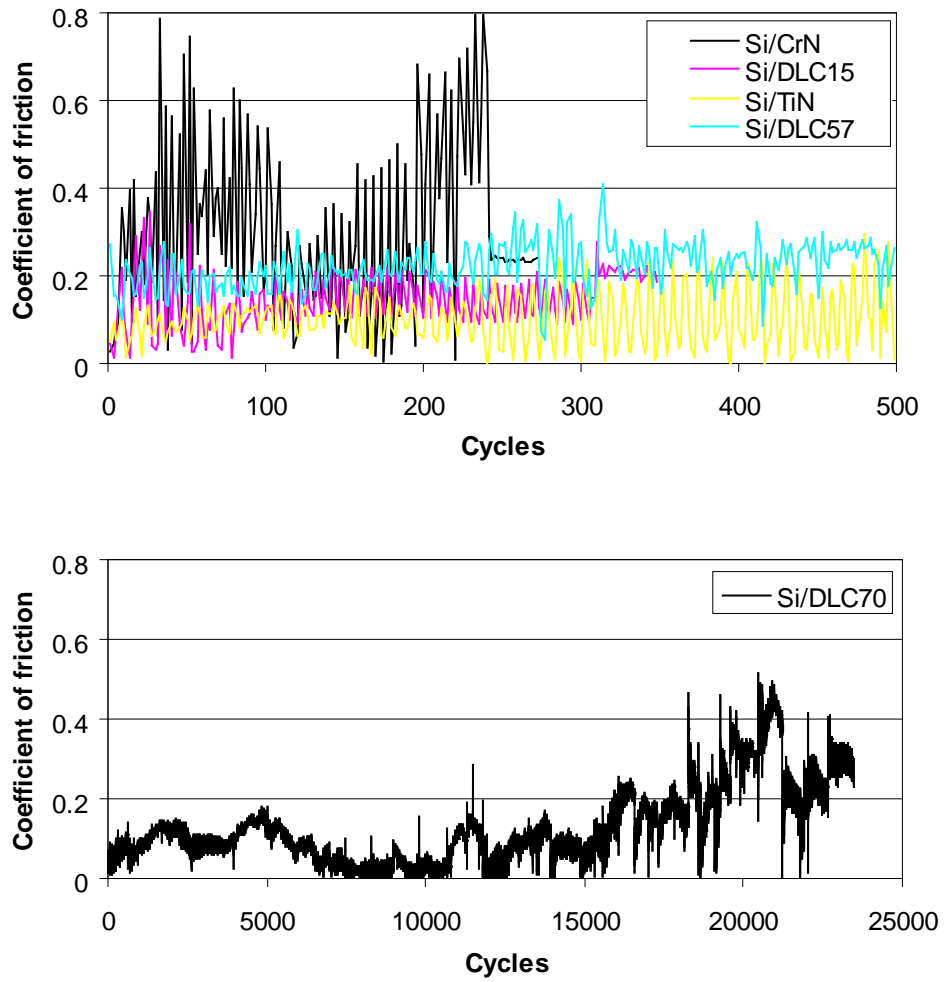


Figure 5.3: *The variation of coefficient of friction with respect to the number of sliding cycles for Si/CrN, Si/DLC15, Si/TiN, Si/DLC57 and Si/DLC70.*

Table 5.3: The initial coefficient of friction and wear durability of different intermediate layers. The ball and the film are worn at failure in all cases.

Sliding pair	Initial coefficient of friction	Wear durability (Cycles)	Remark at failure
CrN film – Si ₃ N ₄ ball	0.25 ± 0.15	50	CoF is above 0.3
DLC15 film – Si ₃ N ₄ ball	0.14 ± 0.11	200	CoF is above 0.3
TiN film – Si ₃ N ₄ ball	0.13 ± 0.05	400	CoF is above 0.3
DLC57 film – Si ₃ N ₄ ball	0.18 ± 0.05	400	CoF is above 0.3
DLC70 film – Si ₃ N ₄ ball	0.05 ± 0.018	11,000	Occurrence of large fluctuations between 0.03 and 0.25

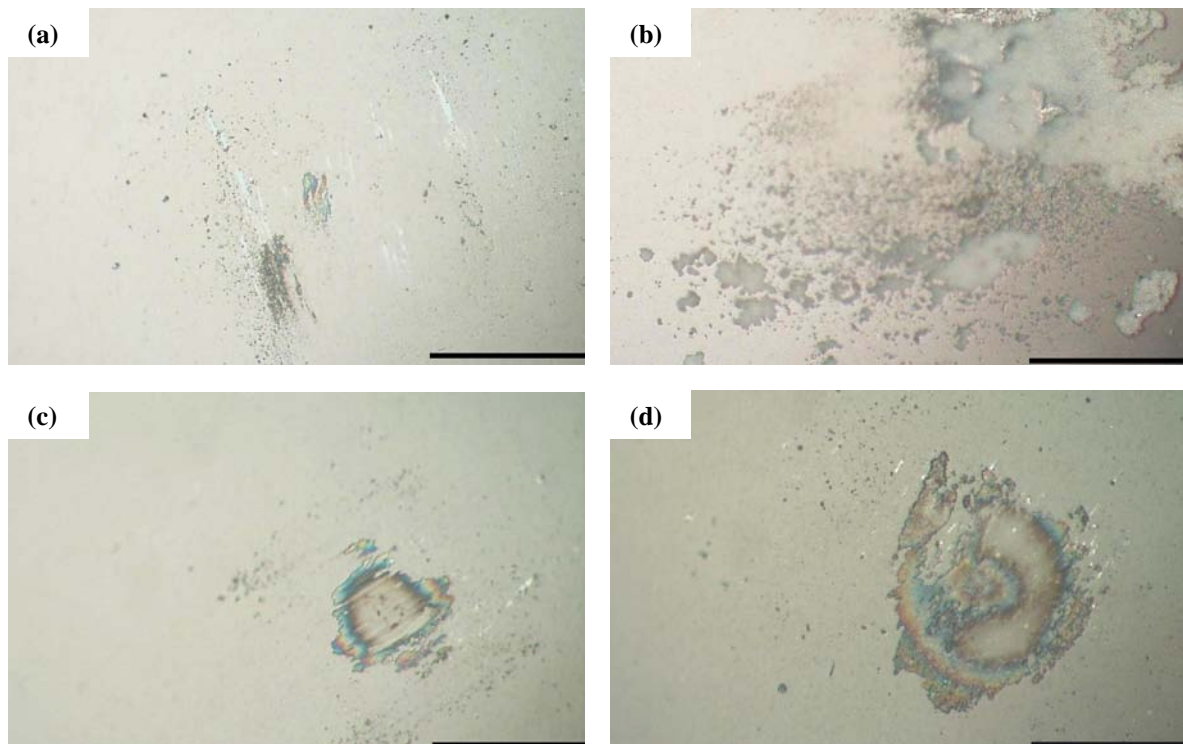
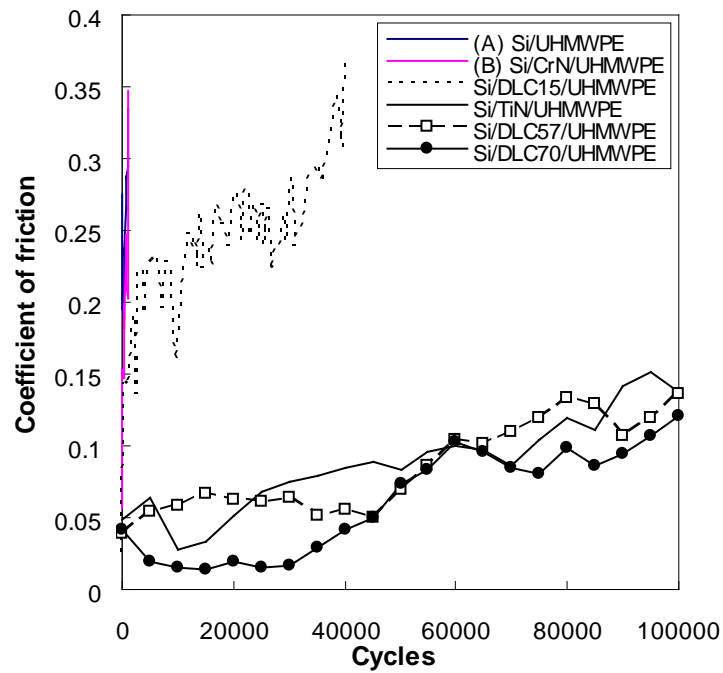


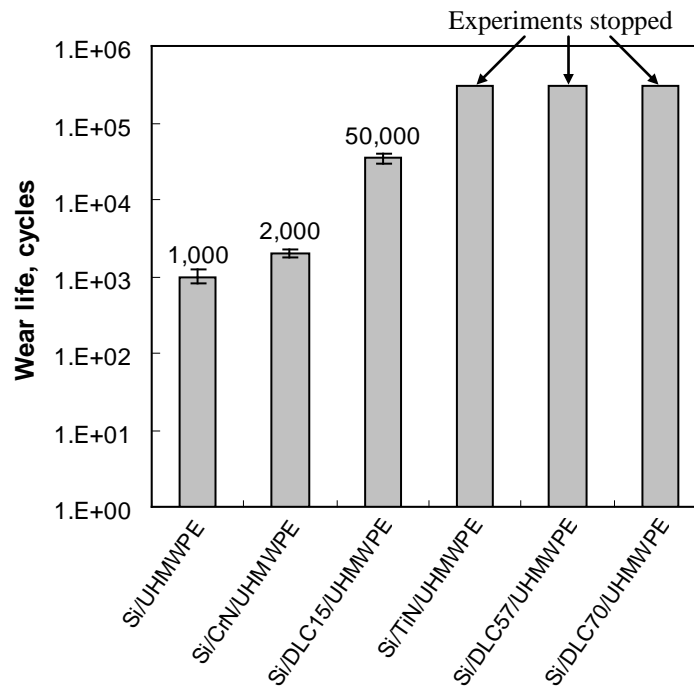
Figure 5.4: The optical images of Si₃N₄ balls after sliding against (a) CrN, (b) TiN, (c) DLC57 and (d) DLC70 films with respective number of cycles mentioned in Table 5.3. The scale bars are 100 μm.

5.2.3 Friction and wear results of UHMWPE film with different hard intermediate layers

The tribological properties of the UHMWPE films coated onto different hard layers are shown in Figure 5.5. At the start of the sliding, the initial coefficient of friction is mostly related to the shear strength of the UHMWPE film and is in the range of 0.08~0.13 for all the composite films. During the test, the coefficients of friction of Si/UHMWPE and Si/CrN/UHMWPE are above 0.3 when the sliding reaches 1,000 cycles and 2,000 cycles, respectively. This early failure could be related to the hardness of the intermediate layer. Though UHMWPE has self-lubricating property and can reduce the coefficient of friction, it is easy to be penetrated in its coated form owing to its softness. The easy penetration of the counterface ball increases the real area of contact and the amount of polymer peeled out from the polymer film increases as well. The results suggest that the substrates with lower hardness limit the wear life of the composite film. When UHMWPE is coated onto a harder layer (e.g. Si/DLC15/UHMWPE), the wear life extends to 50,000 cycles. With further increase in the hardness of the intermediate layer as in Si/TiN/UHMWPE, Si/DLC57/UHMWPE and Si/DLC70/UHMWPE, the composite films did not show any sign of failure till 300,000 cycles of sliding when the experiments were stopped. The results confirm that higher hardness of the intermediate layers provides better penetration resistance to the softer UHMWPE film and reduces the contact area of the ball and promotes wear durability [Minn and Sinha 2008 a].



(a)



(b)

Figure 5.5: (a) Coefficients of friction and (b) wear lives of Si substrate coated with different composite films. The applied load was 40 mN and the rotational speed was 500 rpm (linear speed = 0.052 m/s).

5.2.4 Polymer transfer mechanism

The polymer transfer mechanism during sliding between the ball and the polymer film is an important phenomenon as the transfer film can greatly influence the friction and wear characteristics. When a hard ball is slid against a soft UHMWPE film, the transfer film will eventually be formed on the ball. At this stage, the sliding is between the polymer film and the transfer film on the ball. Thus, because of the self-lubricating property of UHMWPE, in the beginning of the transfer process, the shear stress will reduce further and so will the coefficient of friction [Makinson and Tabor 1964, Briscoe 1981, Bahadur and Tabor 1984, Blanchet *et al.* 1993 and Bahadur 2000].

As the sliding continues, the polymer will deform plastically and more polymer debris will accumulate on the ball (counterface) which in turn widens the wear track and increases the friction gradually. The material transfer process is studied under an optical microscope and the optical images of the balls and the wear tracks for Si/TiN/UHMWPE, Si/DLC57/UHMWPE and Si/DLC70/UHMWPE films are shown in Figure 5.6. The sliding test conditions were fixed as 40 mN applied load, 500 rpm sliding speed and 300,000 sliding cycles. The transferred polymer consists of lumps that seem to be from the asperities and the top layer of the film which were sheared by the ball. The lumps from Si/TiN/UHMWPE (which has lower hardness than the other two composite films) are larger and thicker. The amount of polymer transferred is directly related to the track width as the polymer has been pulled out from the track. It is obvious that, because of its lower hardness, TiN layer provides lower penetration resistance to the UHMWPE film in comparison to DLC57 and DLC70 layers. As a

consequence, the contact area or track width on Si/TiN/UHMWPE film becomes larger with greater polymer transfer.

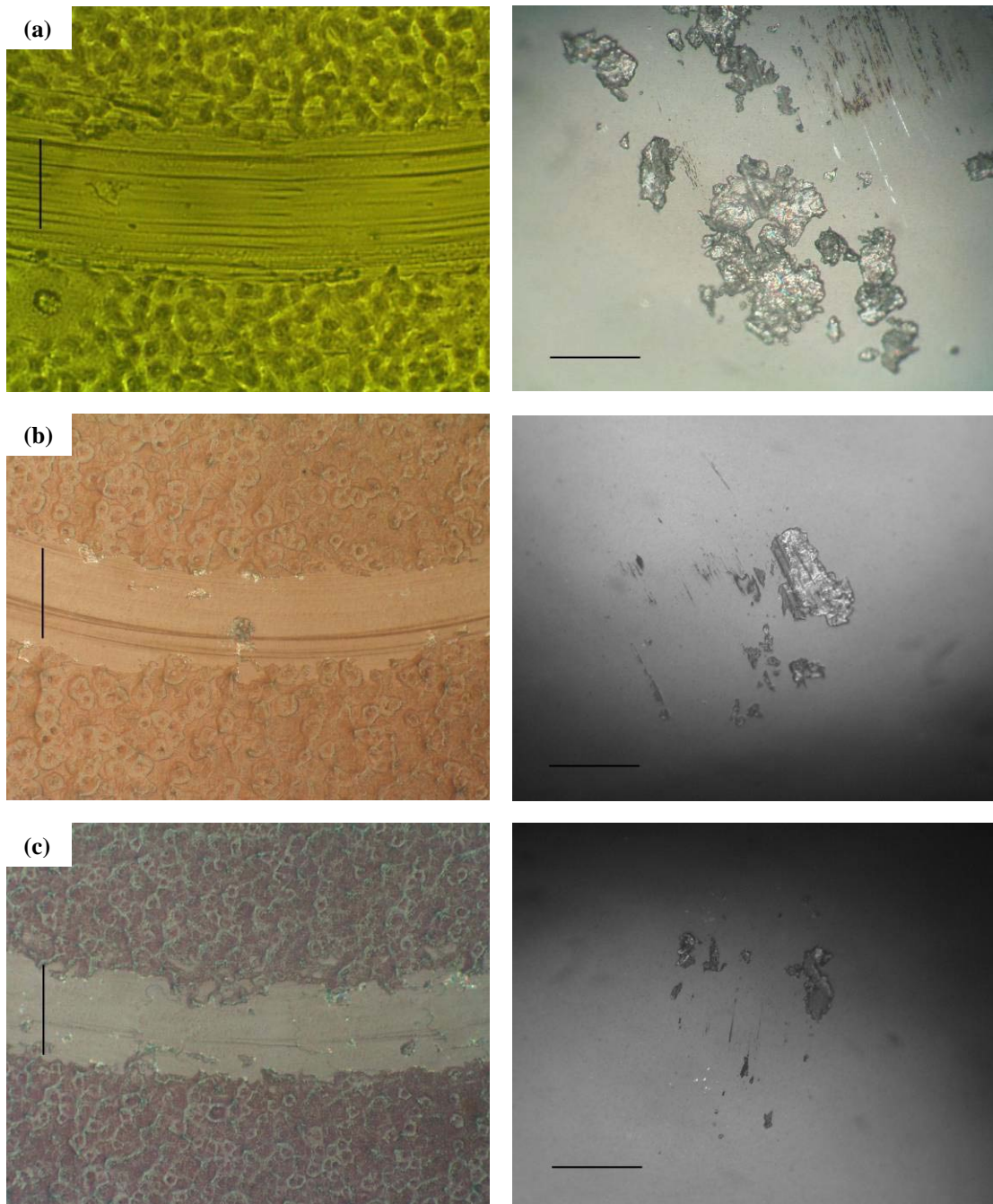


Figure 5.6: Optical microscopy images of (a) Si/TiN/UHMWPE, (b) Si/DLC57/UHMWPE and (c) Si/DLC70/UHMWPE films (first column) after sliding against respective Si_3N_4 balls (second column) for 300,000 cycles where the normal load is 40 mN and the linear sliding speed is 0.052 m/s. The vertical or horizontal scales correspond to 100 μm.

However, harder intermediate layers (such as Si/DLC57/UHMWPE and Si/DLC70/UHMWPE) have better ability to provide penetration resistance and reduce the contact area. Hence, the amount of polymer transfer is less with smaller contact area. It can be seen that the lumps of polymer transfer is less and thin (Figures 5.6 b and c).

5.2.5 Critical load in scratch tests and film adhesion

For a better understanding of the supportive role of different hard intermediate layers on the tribological properties of top UHMWPE film, scratch test was conducted using a 2 μm diamond tip at a fixed scratching velocity of 0.1 mm/s and a scratching distance of 5 mm. The applied load was varied from 10 mN to 100 mN with an increment of 10 mN as the critical loads required to peel the top UHMWPE film can vary with different hard intermediate layers. In this study, the critical load is defined as the applied normal load when the film fails during scratching exposing the intermediate layer and the substrate.

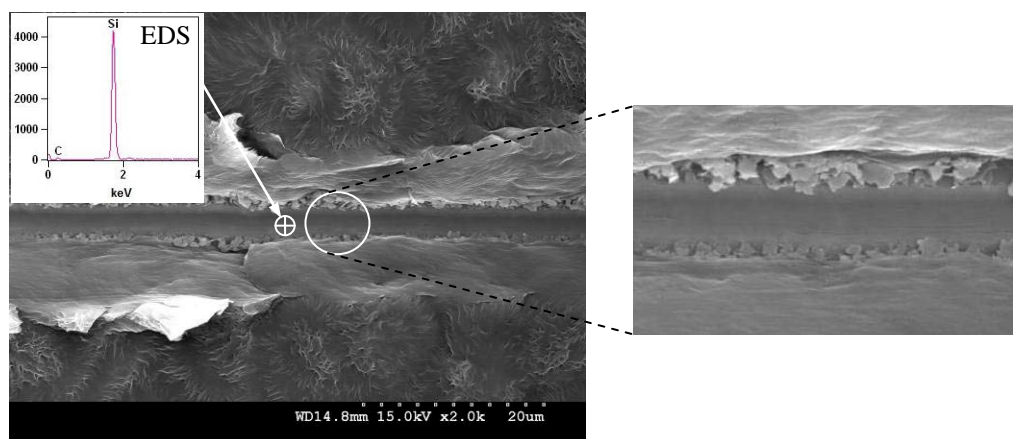


Figure 5.7: The FESEM image of a scratch on Si/DLC70/UHMWPE where the normal load was 80 mN and the scratching velocity was 0.1 mm/s. The Si peak seen in the EDS indicates film failure due to scratching.

The failure of the film is confirmed by observing the debris shape originating from the film and by measuring the Si peak inside the scratches using EDS. Because of the lower thickness of the intermediate layers used in this study (50 nm), it is difficult to measure the peaks of the elements such as Cr, N and Ti when the film fails. And hence, Si peak is used as a reference peak to identify polymer film failure from the substrate. A summary of the critical loads of UHMWPE films with different hard intermediate layers is provided in Table 5.2. It is found that the critical loads of Si/UHMWPE and Si/CrN/UHMWPE are the lowest at 20 mN. The critical load of Si/DLC15/UHMWPE increased to 30 mN. Higher critical loads were found for Si/TiN/UHMWPE and Si/DLC57/UHMWPE as 50 mN and 60 mN respectively. For Si/DLC70/UHMWPE film, the high intensity of Si peak was observed when the applied load was 80 mN; a 4 times increase over bare Si as the substrate. An FESEM image of Si/DLC70/UHMWPE film where the applied load was 80 mN is shown in Figure 5.7. Clear signs of severe plastic deformation with brittle debris were produced at both edges of the scratch and the debris at the centre of the scratch were Si fragments, as confirmed by EDS (see Figure 5.7 inset). This brittle Si debris release was observed for all samples when the films failed by scratching.

The critical loads of the films are consistent with their respective wear lives as presented in Table 5.2. The critical loads of Si/UHMWPE and Si/CrN/UHMWPE are the lowest and their wear lives are 1,000 cycles and 2,000 cycles respectively. The critical load of Si/DLC15/UHMWPE is 30 mN and its wear life extends to 35,000 cycles. The critical loads of the rest three films are 60 mN (for Si/TiN/UHMWPE and

Si/DLC57/UHMWPE) and 80 mN (for Si/DLC70/UHMWPE) and they did not fail till 300,000 cycles when the experiments were stopped.

5.2.6 Friction and wear results of Si/TiN/UHMWPE, Si/DLC57/UHMWPE and Si/DLC70/UHMWPE films at higher normal load

To facilitate a better understanding of the tribological performances of the best three films, the applied load was increased to 70 mN. The friction and wear data of these three films are shown in Figure 5.8. A sharp increase in the coefficients of friction for Si/TiN/UHMWPE and Si/DLC57/UHMWPE films is observed in early cycles and their wear lives are 8,000 cycles and 22,000 cycles respectively. Large amount of lumpy polymers pulled out from the film is found around the contact point of the ball in both cases. The coefficient of friction of Si/DLC70/UHMWPE film gradually increases with the number of sliding cycles and reaches above 0.3 after 120,000 cycles. The hardest intermediate layer (Si/DLC70) still provides maximum wear life. When the applied load is increased to 70 mN, the contact radius becomes larger and then the shear stress force is largely determined by the shear property of the composite film [Arnell 1990]. As a result, the coefficient of friction increases and the wear durability of all composite films are shortened, as would be expected.

5.2.7 Effects of PFPE overcoat on composite films

In order to increase the wear lives of the composite films by further reducing the shear stress, PFPE was applied as a top lubricant on UHMWPE film. PFPE with its presence of fluorine is a very effective nano-lubricant which can reduce friction and

increase wear life of a polymer film [Satyanarayana and Sinha 2005]. Friction tests were conducted on Si/Ti/UHMWPE/PFPE, Si/DLC57/UHMWPE/PFPE and Si/DLC70/UHMWPE/PFPE samples with an applied normal load of 70 mN and at a rotational speed of 500 rpm.

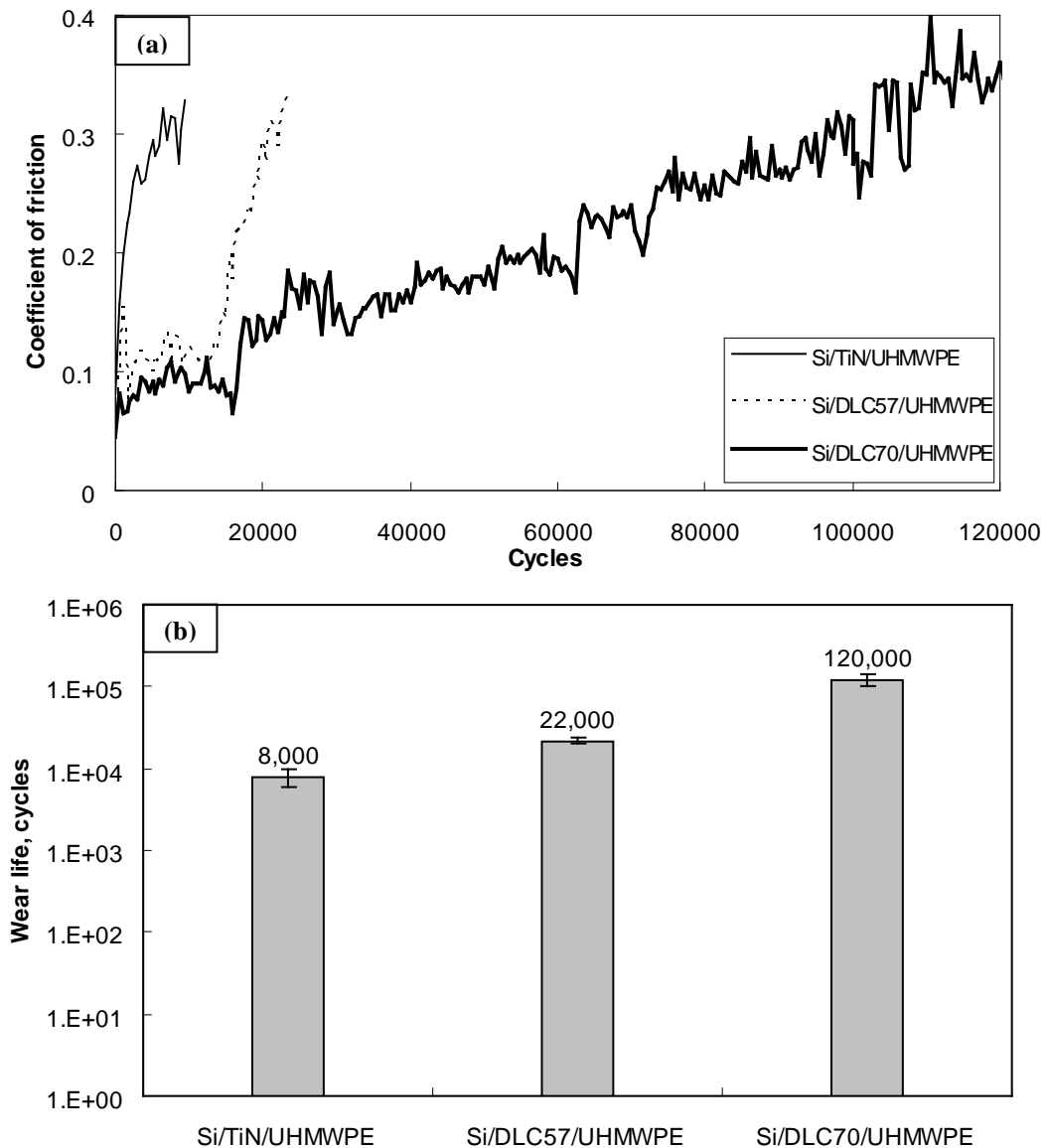


Figure 5.8: (a) Coefficient of friction and (b) wear life of Si substrate coated with different composite layers (as mentioned in the figures). The applied load was 70 mN at a rotational speed of 500 rpm (linear speed = 0.052 m/s).

With PFPE overcoat, none of the three films failed till one million cycles when the experiments were stopped. UHMWPE film used in this study has no reactive chemical group and it is not expected to form any chemical bonding between UHMWPE and PFPE. It is assumed that PFPE molecules are trapped in the valleys of the UHMWPE film [Satyanarayana *et al.* 2006]. PFPE over-coated layer provides more hydrophobic property with a water contact angle of 102°. High contact angle means lower surface energy which in turn reduces the adhesion between the ball and the film (thus, no polymer transfer to the silicon nitride ball counterface).

The optical images of the balls and the films after friction tests are shown in Figure 5.9. The images of the ball surfaces do not show any significant amount of polymer transfer. During the sliding, some PFPE molecules can transfer to the ball and provide lubrication. Another advantage of PFPE is its thermal stability and it can withstand high frictional heat generated at the interface without being degraded. In fact, the presence of PFPE molecules at the interface results in less frictional heating because of the overall low coefficient of friction (~ 0.07). The low friction and wear resistance characteristics of PFPE coated films are seen even after one million sliding cycles at the highest applied normal load used.

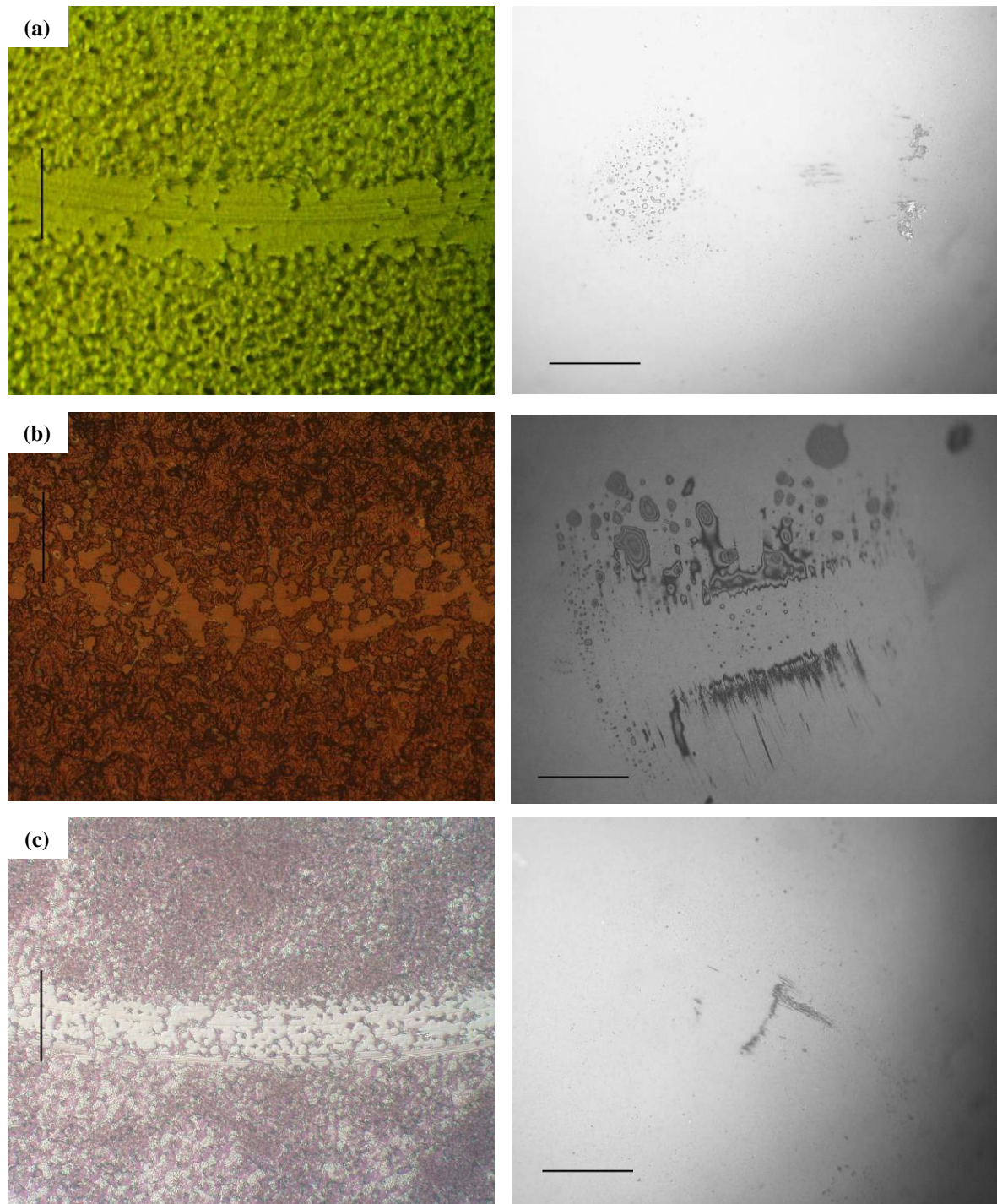


Figure 5.9: Optical microscopy images of (a) Si/TiN/UHMWPE/PFPE, (b) Si/DLC57/UHMWPE/PFPE and (c) Si/DLC70/UHMWPE/PFPE films (first column) after sliding against respective Si_3N_4 balls (second column) for one million sliding cycles. The ball surfaces show transfer of PFPE molecules but very little of UHMWPE. The applied load was 70 mN and the linear sliding speed was 0.052 m/s. The vertical and horizontal scales correspond to 100 μm .

5.3 Summary

The tribological properties of UHMWPE film (thickness of 4~5 μm) coated onto five different hard intermediate layers (CrN, DLC15, TiN, DLC57 and DLC70) with Si as the substrate are studied using a ball-on-disc method. The top UHMWPE film reduces the shear stress and the coefficient of friction because of its self-lubricating property while the hard intermediate layers provide higher load carrying capacity that can increase the wear durability by several folds to orders of magnitude. The wear life of UHMWPE composite film is directly related to the hardness of the intermediate layer as higher hardness provides higher wear life. The lowest hardness layer, bare Si/UHMWPE, has a wear life of 1,000 cycles whereas the higher hardness layers, Si/TiN/UHMWPE, Si/DLC57/UHMWPE and Si/DLC70/UHMWPE have shown the wear lives of more than 300,000 cycles at an applied normal load of 40 mN and a sliding speed of 0.052 m/s. The critical loads from scratch tests are also consistent with the tribological test results, as Si/UHMWPE failed at 20 mN whereas Si/DLC70/UHMWPE, with the hardest intermediate layer, at 80 mN. Based on the critical load data, the friction and wear tests are conducted on the best three composite films at a higher applied load of 70 mN. The influence of hard intermediate layer on the wear life is still observed as the wear lives of Si/TiN/UHMWPE, Si/DLC57/UHMWPE and Si/DLC70/UHMWPE are obtained as 8,000 cycles, 22,000 cycles and 120,000 cycles, respectively. Over-coating with few nanometers thickness of PFPE as a top layer on these three films further reduces the coefficient of friction (~ 0.07) and extends the wear lives to more than one million cycles under an applied normal load of 70 mN and a sliding speed of 0.052 m/s.

The present composite films will find applications in many tribological components such as bearing and gears where extremely high wear life is desirable with low and stable coefficient of friction.

Chapter 6

Effects of Interfacial Surface Energy on the Tribology of UHMWPE Film on Si

Despite the wider use of polymers as protective coating film in industrial applications, the wear durability is relatively low compared to the desired product lifespan. One of the main properties that affect the wear durability is the adhesion strength between the polymer film and the substrate. It is very difficult to obtain strong adhesion between UHMWPE and many substrates since, like most of the polymers, UHMWPE has no functional groups unless it has been chemically functionalized. The poor adhesion strength can lead to rapid detachment of the polymer film from the substrates. It is necessary to give a pre-treatment to the substrate in order to enhance adhesion [Ryntz 1994]. The surface wettability of the substrate is an important parameter to determine the adhesion of a polymer film. The presence of moisture contents on a substrate can also change the surface energy of the substrate that strongly affects the adhesion strength of a coating [O'Brien *et al.* 2006]. Moy and Karasz [1980], Lee and Peppas [1993] and Nogueira *et al.* [2001] have shown that the moisture content on the substrate lowers the glass transition temperature of the coatings that deteriorates the mechanical properties of the films. Wong and Broutman [1985] and Xu and Ashbee [1991] have proved that the presence of moisture on a substrate can create cracks or voids in the coatings. As a consequence, the adhesion loss between the coatings and the substrate is inevitable [Armstrong and Wright 1993]

and Mansfeld *et al.* 1998]. Yoon *et al.* [1997] have studied the adhesion force between a glass sphere and a silica plate by varying the surface hydrophobic nature with OTS (octadecyltrichlorosilane). Their results show that the adhesion force increased with increasing hydrophobicity of the substrate. It is obvious from the literature that the surface wettability is an important factor in determining the adhesion strength of a polymer film to a substrate.

In this Chapter, friction and wear durability of ultra-high molecular weight polyethylene (UHMWPE) is studied with a variation in the surface energy or surface wettability of the Si substrate. Different interfaces (different surface wettabilities) were first prepared as the first layer on the Si substrate followed by the coating of the UHMWPE (6 μm thickness) film as the second layer. The friction and wear tests were conducted on every sample with different interfaces including on one control sample without any interface modification (i.e. bare Si coated with UHMWPE). The adhesion strengths at the polymer/substrate interfaces were determined by scratch tests on all samples with various applied normal loads.

6.1 Experimental procedures

6.1.1 Materials

3-aminopropyltrimethoxysilane (APTMS) and Octadecyltrichlorosilane (OTS), obtained from Aldrich Inc., were used without further purification. The chemical formulae of APTMS and OTS are $\text{H}_2\text{N}(\text{CH}_2)_3\text{Si}(\text{OCH}_3)_3$ and $\text{CH}_3(\text{CH}_2)_{17}\text{SiCl}_3$, respectively. Toluene (99.5% anhydrous) was used as the solvent for the preparation of

APTMS and OTS solutions. Decahydronaphthalin (decalin) was used as the solvent to dissolve UHMWPE powder for dip-coating purpose.

6.1.2 Preparation of different interfaces on Si substrate

The detailed cleaning procedure of Si substrate is mentioned before. The cleaned Si substrates were heated in an oven for 1 hour at 100 °C in order to remove water content and are referred as heated Si in this study. The hydrogen terminated silicon (Si-H) substrates were obtained by immersing cleaned Si substrates into a dilute aqueous solution of hydrofluoric acid (2 vol%) for 30 seconds. After that, Si-H substrates were rinsed with distilled water for 1 minute and dried with nitrogen gas.

In this study, two well known self-assembled monolayers (APTMS and OTS) have been chosen as surface modifiers for the purpose of changing the surface wettability of the Si substrates. APTMS and OTS SAMs were formed on the Si substrates by immersing the cleaned Si substrates into 3 mM and 5 mM concentrations of APTMS and OTS solutions, respectively, for 5 hours each. After that, the SAMs coated substrates were ultrasonically washed for 7 minutes each with toluene and methanol to remove any physisorbed SAM molecules (that could remain on Si sample) and finally, the samples were dried with nitrogen gas.

The thickness of the UHMWPE film after heat treatment was confirmed as 6 ± 2 μm . A schematic diagram of UHMWPE coating on the Si substrates with different interfaces is shown in Figure 6.1.



Figure 6.1: A schematic diagram of the Si/UHMWPE sample with different interfaces. Interfacial conditions used were bare Si (i.e. no interface modification), heated Si, APTMS, hydrogen-terminated Si and OTS.

6.1.3 Surface characterizations

The surface wettabilities of different interfaces on Si substrate were determined by measuring the contact angles with a VCA Optima Contact Angle System (AST product, Inc., USA). The contact angles are reported as an average of five independent measurements on the samples using a distilled water droplet of 0.5 μL . The data scatter is within $\pm 3^\circ$. The nanoindentation and XPS tests were conducted according to the procedures mentioned in Sections 3.3.3 and 3.3.4.

6.1.4 Friction and wear tests

The friction and wear tests were conducted on a ball-on-disc tribometer (detailed description are available in Section 3.3.7). A 4 mm diameter silicon nitride (Si_3N_4) ball was used as a stationary counterface whereas the coated Si substrate acted as rotating disc. The normal load and the rotational speed were 40 mN and 500 rpm, respectively. The test radius was 2 mm giving a linear sliding speed of 0.1 m/s. The initial coefficient of friction is taken as an average of the first 4 seconds of sliding. The wear life of each sample is defined as the respective number of cycles when the coefficient of friction exceeds 0.3. The friction and wear data are reported as an

average of three repeated tests. After the friction tests, an optical microscope is used to study the transfer films and the wear track morphology.

6.1.5 Scratch tests

As a comparison of adhesion strength, a 2 μm tip radius (diamond tip) was used to conduct a scratch test on every sample. The scratching velocity and the linear scratch distance were fixed at 0.1 mm/s and 1 cm, respectively. The applied normal load was varied from 10 mN to 70 mN with an increment of 10 mN. The surface topography of the scratches was observed under field emission scanning electron microscopy (FESEM) as described in Section 3.3.5.3.

6.2 Results and discussion

6.2.1 Surface characterizations (nanoindentation and XPS peaks)

Nanoindentation tests were performed on the coated films for obtaining the hardness and the elastic moduli of the polymer films. The measured hardness and elastic modulus were 35 MPa and 1 GPa, respectively, for all samples regardless of the interface and the variation was within the measurement errors. The penetration depth was approximately 400 nm.

The wide scan spectrum of XPS results of bare Si, heated Si, Si/APTMS, Si-H and Si/OTS samples before UHMWPE coating are provided in Figure 6.2. As can be seen, the C1s peaks on bare Si, heated Si and Si-H is due to the organic contaminants which could not be removed during the piranha treatment or were adsorbed from the atmosphere before the XPS tests. The highest O1s peak for bare Si indicates the

presence of oxide and moisture on the surface. The O1s peak for heated Si is lower than that in bare Si. The possible reason is that the moisture, which can increase the O1s peak, is removed during the heat treatment of Si. The hydrogen termination on Si can prevent the formation of oxide and as a result the O1s peak is the lowest for the Si-H specimen. Because of the amine terminal group, the N1s peak can be seen in the Si/APTMS surface. The C1s concentration is the highest in Si/OTS due to its long hydrocarbon chain. The XPS results confirm the successful formation of different layers onto the Si substrate. Any chemical bonding between the modified Si substrates and the polymer films in a dip-coating method is not expected as the UHMWPE used in present tests was non-functionalized. For additional confirmation, XPS tests were conducted to study the chemical bonding for all samples.

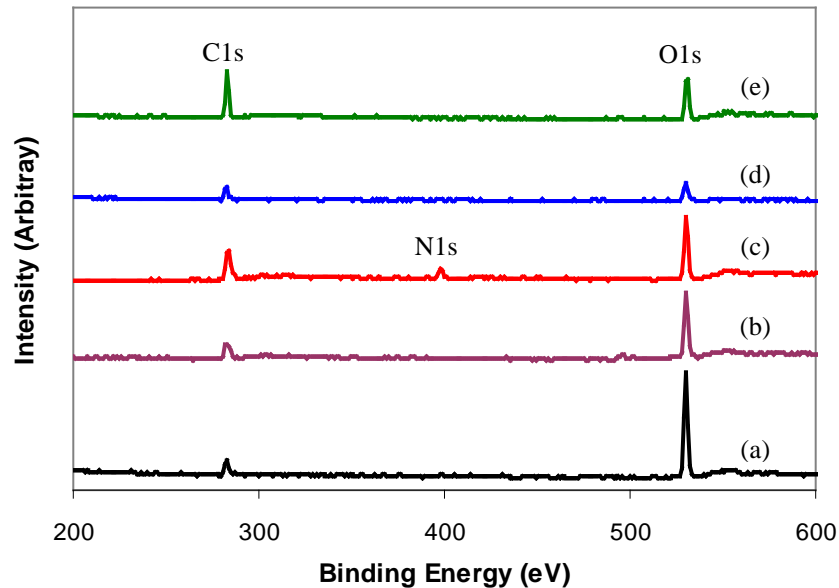


Figure 6.2: XPS wide spectrum for (a) bare Si, (b) heated Si, (c) Si/APTMS, (d) Si-H and (e) Si/OTS surfaces.

In order to remove chemically-unbonded UHMWPE coating, the UHMWPE coated samples were dipped into the decalin solvent and heated in an oven at 250° C

for 15 minutes and ultrasonically cleaned in acetone for 15 minutes. The EDS tests were conducted on the cleaned samples and the original bare Si in order to compare the Si peak and the results showed that the intensities of the Si peak were nearly the same for both the surfaces.

The XPS tests were conducted on the cleaned samples and there was no additional or extra peak of any chemical bonding except Si and UHMWPE peaks. The presence of the Si peak is due to the uncovered Si substrate and the UHMWPE peak is due to residual polymer. These tests have proved that UHMWPE molecules do not chemically bond with the Si substrate in the dip-coating process as followed in this study. Hence, all interactions between UHMWPE and the Si substrate are physical or mechanical in nature.

Thus, it is confirmed that the different interfacial layers have no effect on the hardness and the elastic modulus of the top surface of UHMWPE film and there is no chemical bonding between different interfacial layers and the UHMWPE film.

6.2.2 Friction and wear results

The tribological properties of the UHMWPE film with different interfaces on Si substrate are shown in Figures 6.3 (a) and (b). The initial coefficients of friction for all samples are nearly the same at 0.17, since the uppermost layers for all the samples are UHMWPE films. As the top layer is the same, the wear life of each sample is determined entirely by the properties of the interfaces. Three types of interfaces based on surface wettability: very hydrophilic (Si), very hydrophobic (Si/OTS) and an

intermediate wettability between these two extremes were selected to compare the wear durability.

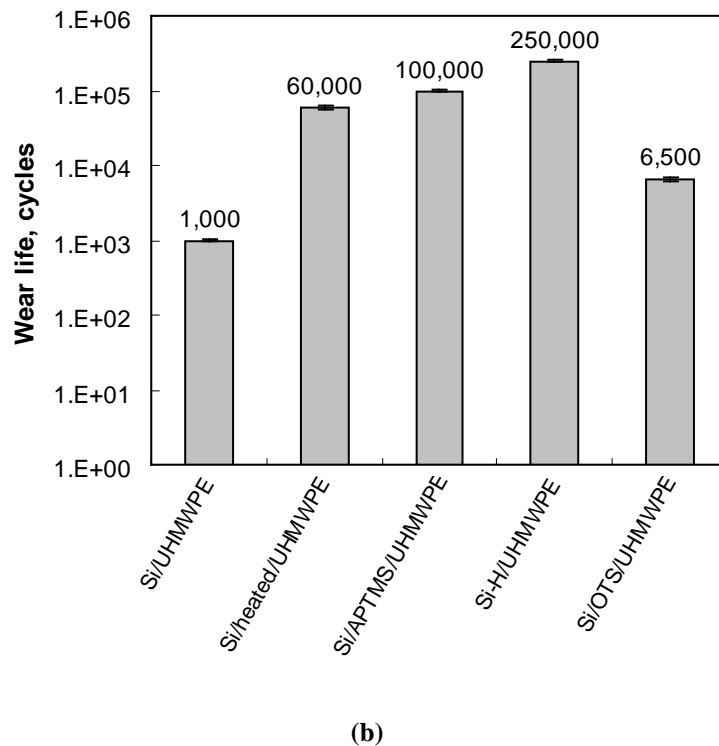
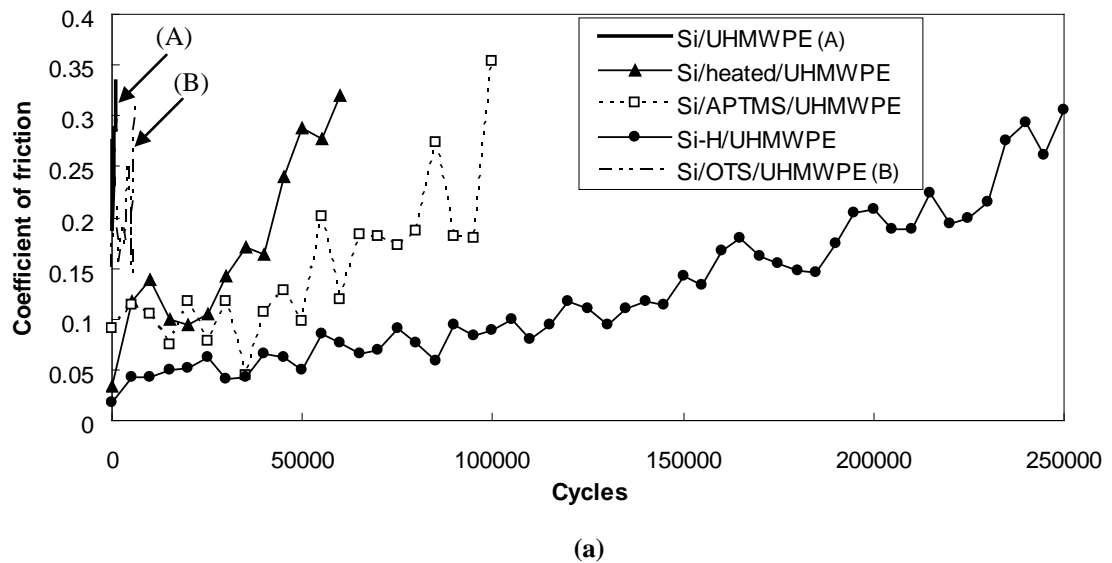


Figure 6.3: Friction and wear properties of UHMWPE film with different interfaces where the normal load is 40 mN and sliding speed is 500 rpm (0.1 m/s). (a) Typical friction traces as a function of the number of sliding cycles for all samples. (b) Consolidated wear life data for all samples.

The coefficients of friction of Si/UHMWPE and Si/OTS/UHMWPE did not increase slowly but abruptly. The sudden change in the coefficient of friction indicates that within a small number of sliding cycles, a large amount of polymer is pulled out from the substrate and gets transferred to the ball surface leading to the early failure of the film. As a result, when the sliding continues, first, the polymer from the ball may get transferred back to the substrate that increases the roughness and, second, the lumps of polymer in the ball make the wear track very uneven.

The coefficient of friction increases sharply within a few sliding cycles and wear initiates due to the presence of exposed Si surface. The wear lives of the films with the most hydrophilic (Si), and the most hydrophobic (Si/OTS), substrate/interfaces are 1,000 cycles and 6,500 cycles, respectively. Due to the presence of moisture on hydrophilic Si substrate, it is seen that the UHMWPE film does not strongly adhere to bare Si. The possibility of the presence of condensed moisture on a surface decreases with increasing water contact angle [O'Brien *et al.* 2006]. Though the highly hydrophobic Si/OTS substrate has less moisture content, the UHMWPE solution is difficult to coat onto Si/OTS due to non-wettability of the substrate. It is hard to obtain a uniform coating and some patches of polymer are clearly seen on the Si/OTS/UHMWPE. This indicates that very low and very high surface energies (water contact angles) of Si cannot provide sufficient adhesion to UHMWPE in order to enhance the wear durability. In contrast to bare Si and Si/OTS substrates, the coefficients of friction of the heated Si/UHMWPE, Si/APTMS/UHMWPE and Si-H/UHMWPE samples increased rather slowly with the number of cycles of disc revolution. Heated Si/UHMWPE has a wear life of

approximately 60,000 cycles. Since the water contact angle of heated Si is higher than that of bare Si, heated Si has less attraction for water molecules and as a result the adhesive strength and the wear resistance of the film increase significantly. After increasing the surface wettability further, the Si/APTMS/UHMWPE (water contact angle of 52°) and Si-H/UHMWPE (water contact angle of 71°) films have wear durability of 100,000 cycles and 250,000 cycles, respectively. The wear durability increases with increasing water contact angle of the substrates up to an optimum value of the water contact angle. Beyond that value, the wear durability decreases again as observed in the case of Si/OTS/UHMWPE film. The optimum wear life is found when the surface wettability is approximately 71° (Si-H).

The investigation of the adhesive strength between UHMWPE and different interfaces is studied and explained in Section 6.2.6 using scratch tests.

6.2.3 Study of the wear track morphology

The interfaces with different surface energies can be grouped into two. One group has either very hydrophilic or very hydrophobic, and, the other with interfaces in between these two extremes. In this section and the following section, the results of one sample from these two groups will be compared. The wear tracks on the Si/UHMWPE and Si-H/UHMWPE films after 1000 cycles are shown in Figures 6.4 (a) and (b). The tests were conducted under a normal load of 40 mN with 500 rpm (0.1 m/s). The wear track on Si/UHMWPE (Figure 6.4 a) shows a clear wear groove and some small debris particles. The small particles either remain on the wear track or get transferred to the ball surface. Continuous sliding over the same track induces further

wear of the substrate and high friction [Fusaro 1982]. If the adhesion strength between the polymer and the interface is strong enough, the probability of the polymer getting pulled out from the substrate is less.

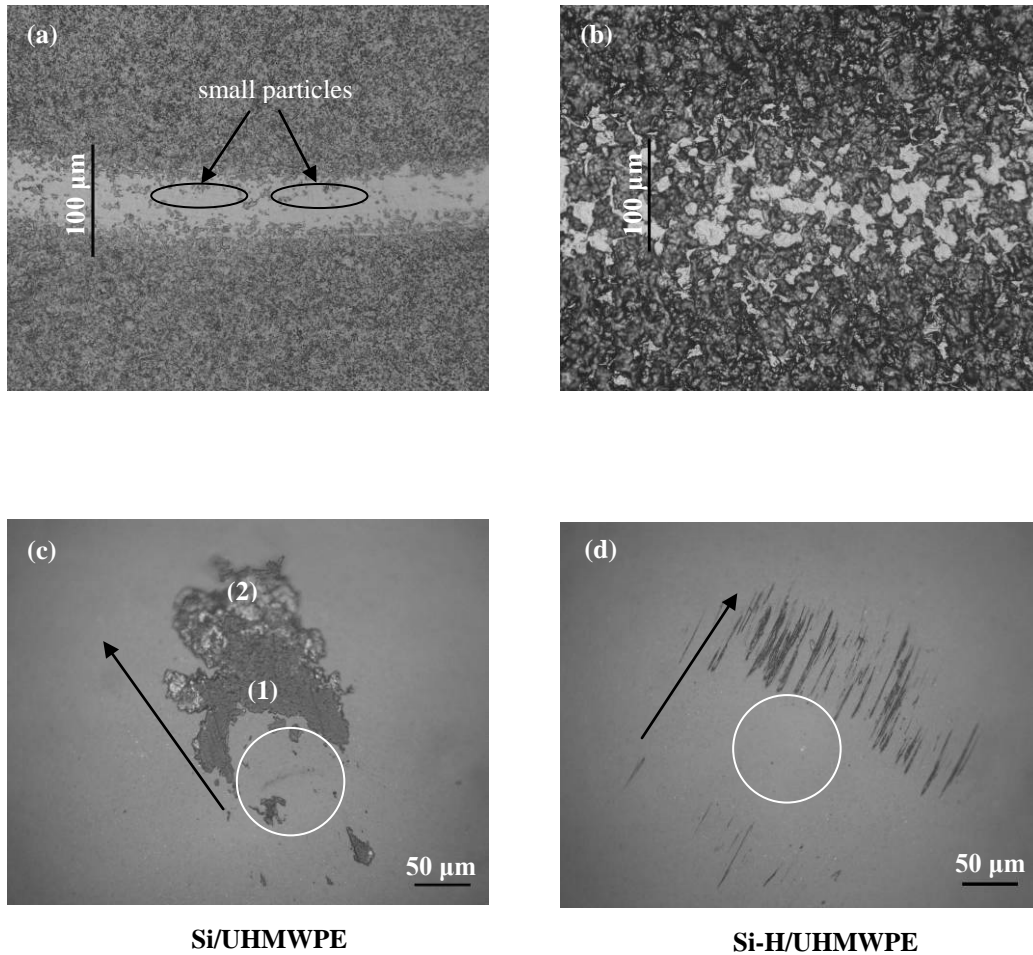


Figure 6.4: Optical microscopy images of (a) Si/UHMWPE film and (b) Si-H/UHMWPE film after sliding against Si_3N_4 ball for 1,000 cycles where the normal load is 40 mN and the sliding speed is 500 rpm (0.1 m/s). (c) is the image of the ball after sliding against (a), and, (d) is image of the ball after sliding against (b). Solid arrows indicate the direction of sliding; white circles indicate the point of contacts.

The interfacial strength is influenced by the surface condition of Si before coating the polymer film. Thus for Si-H/UHMWPE, the film strongly adhered to the

substrate giving higher wear life to the polymer film. In fact this interface-film combination did not show any removal of the polymer but only sliding mark (due to ironing or flattening of the asperities of the polymer film) on the wear track (Figure 6.4 b). Similarly, the ball surface for Si-H/UHMWPE is clear without the transfer of any wear debris.

Figure 6.5 (a) shows the optical image of the wear track on the Si-H/UHMWPE film after 250,000 cycles of sliding, which is the wear life of this film as defined in this study. The coefficient of friction at this point was 0.3. A clear wear track can be seen but there is no accumulation of loose wear debris or material pile-up along it. The central dark colored scratch mark on the track indicates deeper grooves. This type of wear track formation without wear is typical of the UHMWPE film, which indicates extensive plastic deformation in the very top thin layer of the film. The bulk of the film remains firmly attached to the substrate through the interface.

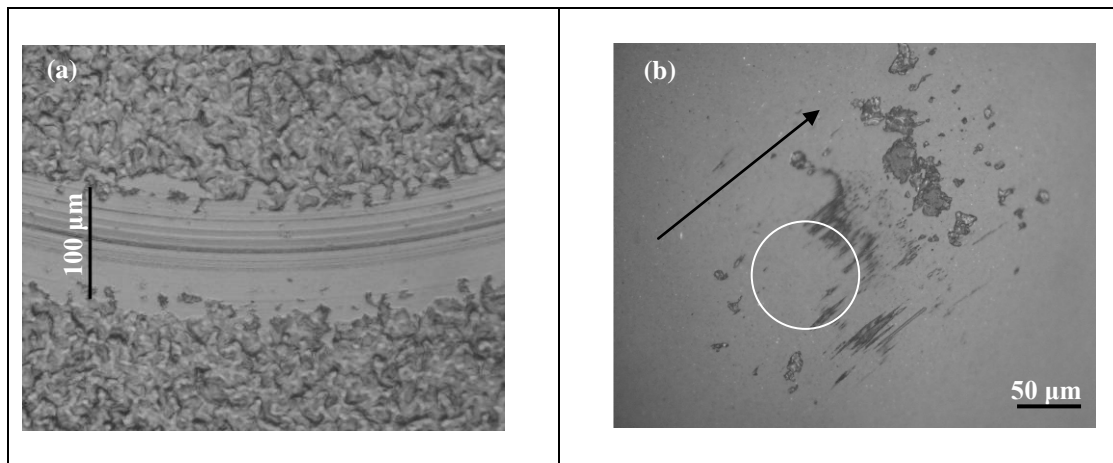


Figure 6.5: Optical microscopy images of (a) Si-H/UHMWPE film after sliding against Si₃N₄ ball for 250,000 cycles where the normal load is 40 mN and the sliding speed is 500 rpm (0.1 m/s). (b) is the image of the ball after sliding against the film shown in (a). Solid arrow indicates the direction of sliding. The white circle indicates the point of contact.

6.2.4 Optical microscopy: study of the transfer films

Polymer transfer to the ball was studied with an optical microscope. Figures 6.4 (c) and (d) show the polymer transfer to the balls that were slid against Si/UHMWPE and Si-H/UHMWPE after 1,000 cycles of sliding. It is obvious that extensive polymer transfer had taken place on the ball slid against the Si/UHMWPE film. The lumpy transfer films increase the roughness and the sliding becomes uneven in the contact zone causing further wear to take place [Weightman and Light 1986]. The thickness of the transfer polymer near the contact zone (1) is thinner than that away from the contact zone (2). The transfer films seem to be pushed away from the contact zone in the direction of the sliding. The thicker transfer film can block or impose resistance against the sliding, and at that stage the coefficient of friction sharply increases and the film fails. For a coated specimen, lumpy removal of materials from the substrate exposes the substrate (Si) to wear against silicon nitride ball at a very fast rate.

The transfer films formed against the heated Si/UHMWPE, Si/APTMS/UHMWPE and Si-H/UHMWPE films are different from those formed against the Si/UHMWPE and Si/OTS/UHMWPE films. The transfer films of the former group showed elongated fibrous structures. These structures were formed by the asperities of the film while the bulk of the film was firmly attached to the substrate. There was no gross transfer of the film from Si to the silicon nitride ball.

Figure 6.5 (b) shows the optical image of the counterface ball that was slid against the Si-H/UHMWPE film after 250,000 cycles, i.e. at the point of failure as defined by the coefficient of friction. The transfer polymer on the ball consists of some

fibrous structure and detached wear debris. No evidence of extensive polymer transfer film means that the counterface did not change throughout the test. Continuous sliding causes plastic deformation and accumulates more polymer debris, which in turn widens the wear track and increases the friction gradually.

6.2.5 Effect of interfacial energy

Five different interfaces (water contact angles) as substrates for the UHMWPE polymer coating were used in this study. Figure 6.6 shows a sketch of the interaction between the polymer molecules and the surfaces with hydrophilic, moderate surface energy and hydrophobic conditions. Since the presence of moisture is independent of the polymer coating [Vogt *et al.* 2004], its presence is mainly dependent upon the surface energy of the substrate prior to film deposition. Highly hydrophilic surface attracts a large number of water molecules that leads to low adhesion [O'Brien *et al.* 2006] of the polymer molecules to the substrate. The samples with water contact angle and wear life are shown in Table 6.1.

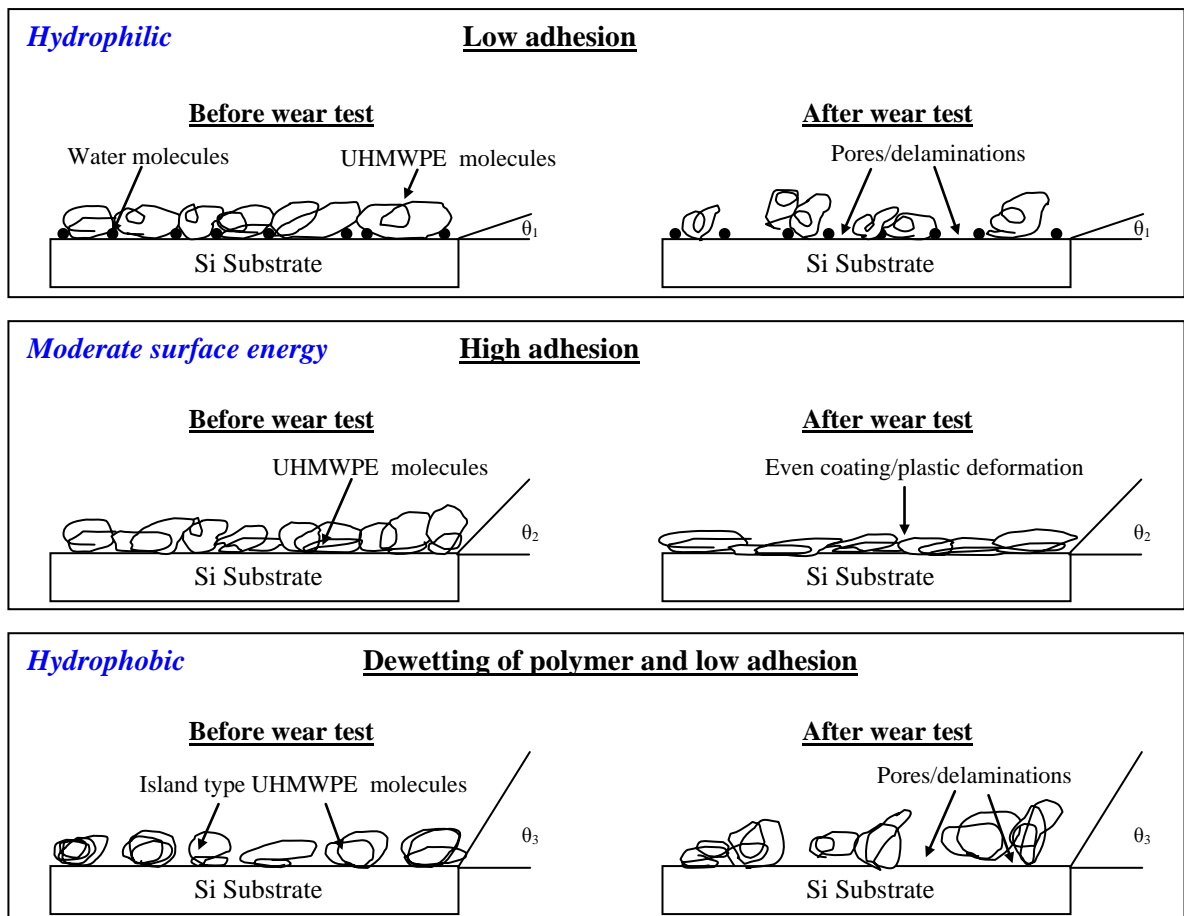


Figure 6.6: A diagrammatic model showing the interactions between the polymer molecules and the Si surface with different wettabilities as measured by water contact angle. θ_1 , θ_2 and θ_3 represent relative water contact angles of the interfaces before polymer coating where $\theta_1 < \theta_2 < \theta_3$.

Table 6.1: Water contact angles and wear lives for different interfacial modifications on Si.

Interface	Bare Si	heated Si	Si/APTMS	Si-H	Si/OTS
Contact angle (°)	21	46	52	71	104
Wear life (cycles)	1,000	60,000	100,000	250,000	3,000

The water contact angles of bare Si, heated Si, Si/APTMS, Si-H and Si/OTS interfaces are 21°, 46°, 52°, 71° and 104°, respectively. Increasing the water contact

angle of the interface provides a strong adhesion between the substrate and the polymer film. As a consequence, the wear life increases with increasing water contact angle of the interfacial layer. However, when the surface is very hydrophobic ($>100^\circ$), the surface becomes difficult to wet and behavior of dewetting happens as soon as the sample is brought out of the UHMWPE solution. Some patchy or island type deposition is clearly seen on Si/OTS/UHMWPE. UHMWPE molecules cannot properly hold onto the substrate. As a result, there is lumpy transfer of the polymer to the counterface and the wear life of Si/OTS/UHMWPE is drastically reduced.

6.2.6 Study of interfacial adhesive strength using scratch tests

The adhesion strengths of UHMWPE films on different interfacial conditions were compared by scratch tests using a 2 μm diamond tip with different applied loads. The critical loads of the film were determined by measuring the Si peak inside the scratches using EDS. The scratch length was 1 cm and the scratching velocity was 0.1 mm/s.

Table 6.2: The critical load as a function of different interfaces; the scratch length is 1 cm and the scratching velocity is 0.1 mm/s.

Interface	Bare Si	heated Si	Si/APTMS	Si-H	Si/OTS
Critical load (mN)	20	40	40	70	20

Table 6.2 provides the critical loads of samples where critical load refers to the applied normal load when the film fails during scratching. It is seen that the critical loads of Si/UHMWPE and Si/OTS/UHMWPE are the same at 20 mN. The FESEM

images of the scratches on the Si/UHMWPE and Si/OTS/UHMWPE films under the applied load of 20 mN are shown in Figure 6.7.

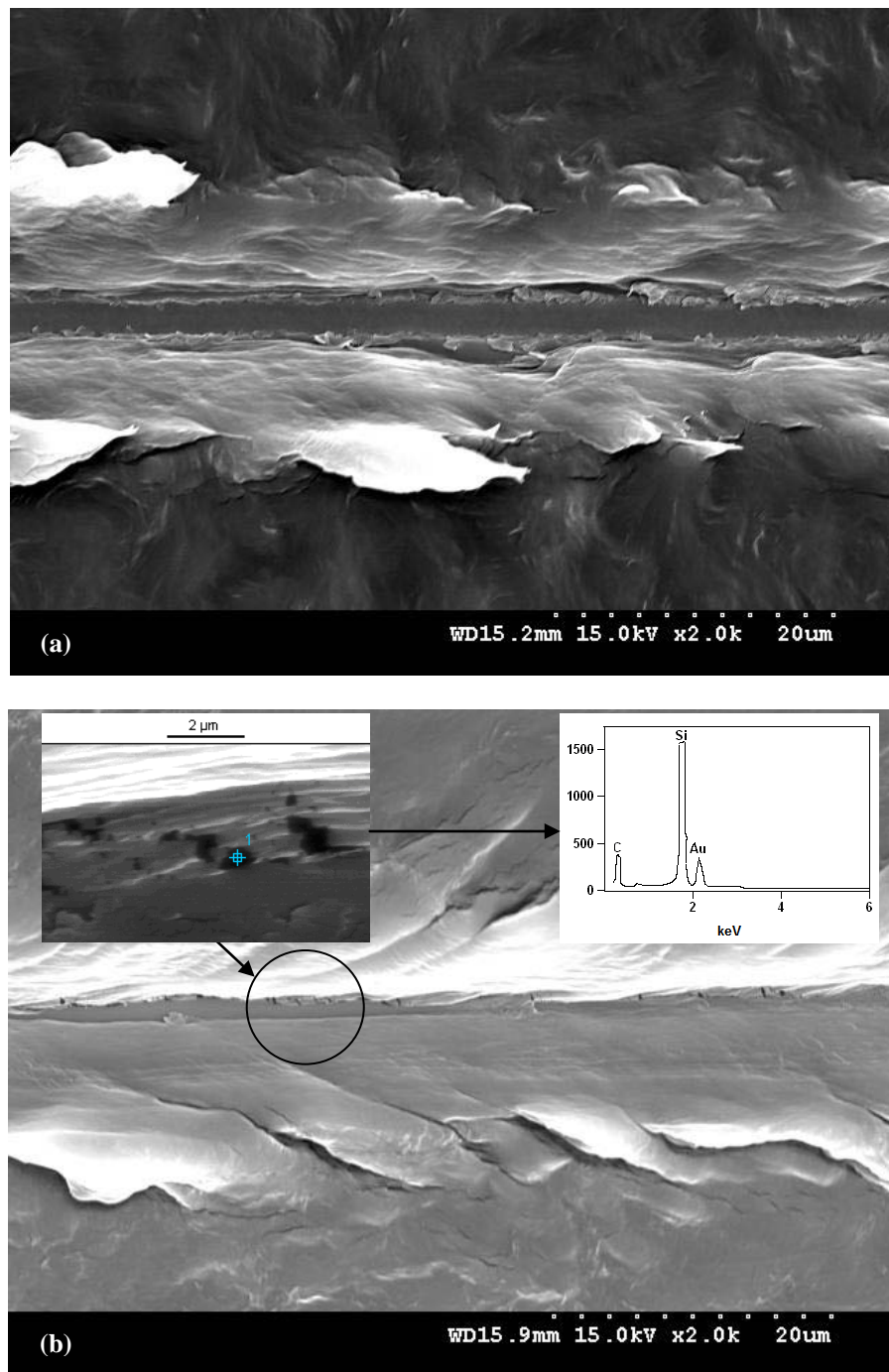


Figure 6.7: The FESEM images of the scratches on (a) Si/UHMWPE and (b) Si/OTS/UHMWPE where the normal load is 20 mN and the scratching velocity is 0.1 mm/s.

The scratch on Si/UHMWPE (Figure 6.7 a) shows severe plastic deformation with polymer debris (breakage) at both edges of the scratch. There is a clear sign of debris particles coming from the Si substrate as they are fragments owing to brittle fracture. The EDS result, in fact, confirms that those brittle particles are Si debris. In the Si/OTS/UHMWPE film (Figure 6.7 b), pores or cracks are clearly visible which are formed by the delamination of the polymer from the surface during scratching. The high intensity of Si peak of EDS test on the pores (see inset) confirms that the UHMWPE film has failed along the centre line of the wear track. The Si substrate was also scratched by the sharp end of the diamond tip.

The scratches on the heated Si/UHMWPE and Si/APTMS/UHMWPE films showed a similar trend. Their critical loads were higher. Neither pores nor cracks were seen on the scratches until the applied load reached 40 mN. Higher critical load means that the scratching resistance or the adhesion strength of UHMWPE film on the heated Si and Si/APTMS substrates, is higher than those on bare Si and Si/OTS. Although the critical load increases, some pores are clearly seen when the film has failed. The presence of pores is indicative of the detachment of the polymer from the substrate, which could be the main reason for film failure.

For the Si-H/UHMWPE film, the high intensity of Si peak was observed when the applied load was 70 mN. However, no pores were found at the interface even at the critical load of 70 mN. This shows that the polymer film is still strongly attached to the Si-H interface and the adhesion strength is very strong compared with all other interfaces tested. Figure 6.8 shows the FESEM images of Si-H/UHMWPE where the applied loads were 20 mN, 40 mN and 70 mN.

The scratch, under the applied load of 20 mN (Figure 6.8 a), shows that the polymer film is very ductile and no wear debris particles are observed along the scratch. The scratch width increases with increasing applied load. Severe plastic deformation was obvious under higher loads. At 70 mN, some occasional brittle debris particles (Si, as confirmed with EDS) were observed on the track. After careful investigation along the scratch, no pores were found. That means, UHMWPE film was not pulled out or torn from the substrate. Therefore, the adhesion strength at the interface is much stronger than those shown for other interfaces.

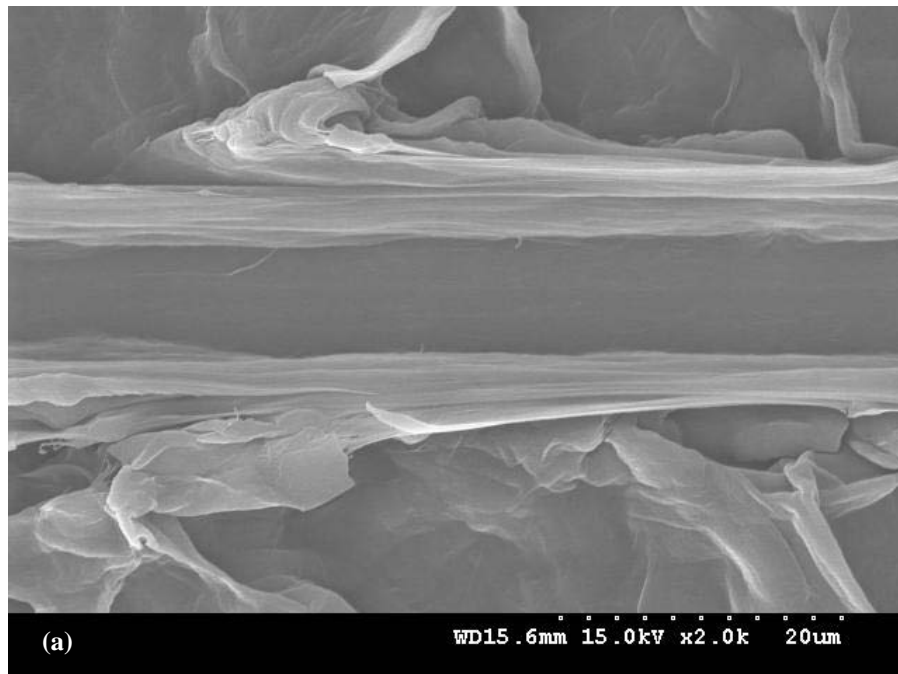


Figure 6.8 Continued to the next page...

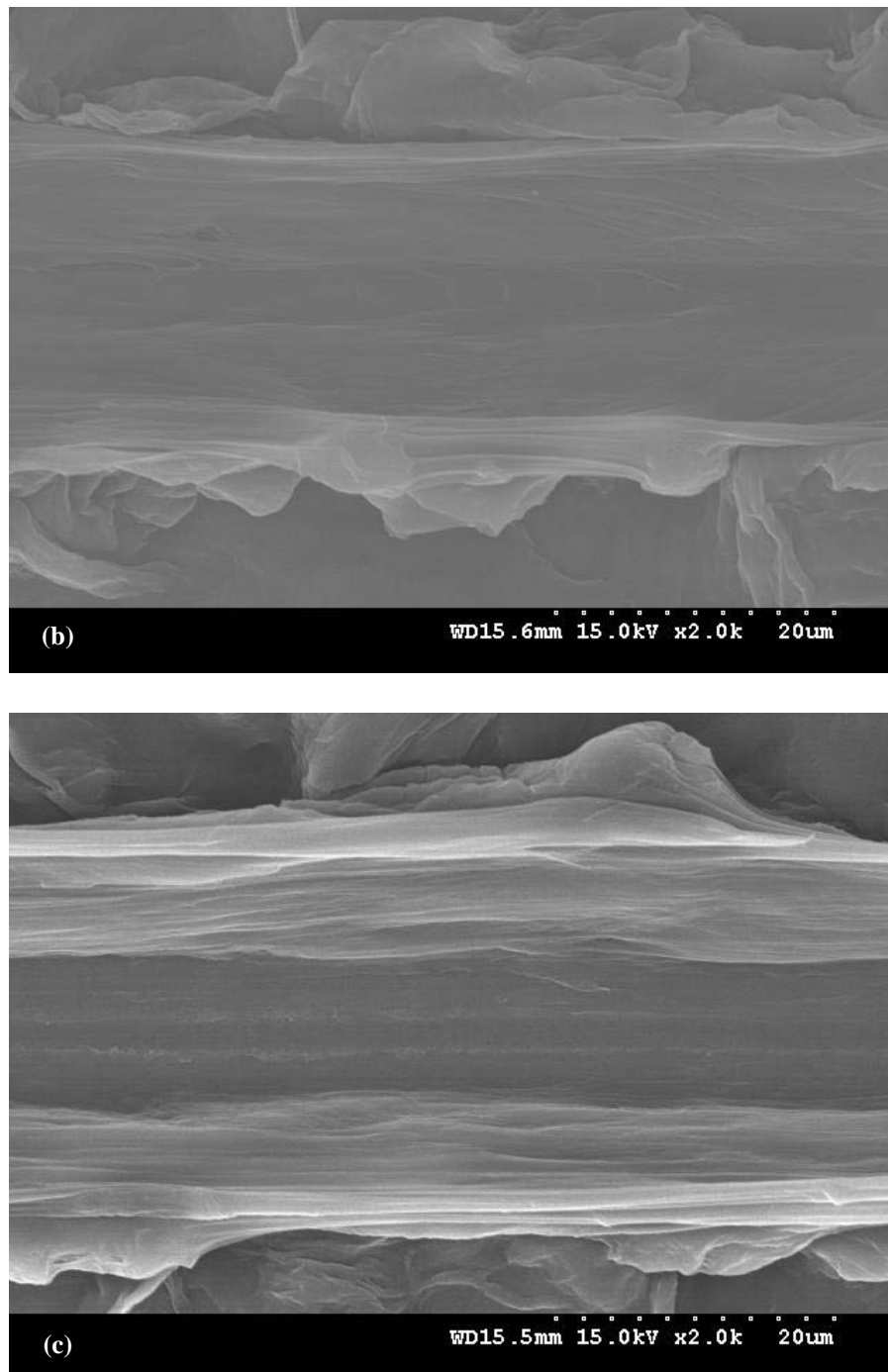


Figure 6.8: The FESEM images of the scratches on Si-H/UHMWPE films where the normal loads are (a) 20 mN, (b) 40 mN and (c) 70 mN, and the scratching velocity is 0.1 mm/s.

The scratch resistances of the films are well consistent with the friction and wear results presented in Section 6.2.2. Namely, the critical load of Si/UHMWPE and

Si/OTS/UHMWPE is the lowest (20 mN) and their wear lives are also the shortest. The critical load and wear lives of heated Si/UHMWPE and Si/APTMS/UHMWPE are moderate. The critical load of Si-H/UHMWPE is the highest (70 mN) and as a result, its wear life is the longest. It is interesting to note that strong adhesion of UHMWPE molecules on hydrogen terminated Si (Si-H) does not change the property of the polymer in any way. For example, the extensive plastic deformation in the very top layer of the polymer helps in providing low shear stress (low coefficient of friction) and no generation of debris particles. Thus, a combination of strong adhesion of UHMWPE and Si-H substrate and extensive plasticity in the top layer of the polymer film is responsible for very high wear life.

6.3 Summary

The friction and wear properties of UHMWPE film on Si with different interfacial energies were determined using a ball-on-disc method. Though the initial coefficients of friction are the same, approximately 0.17, the wear life is strongly related to the surface wettabilities of the interfaces. The most hydrophilic interface, Si/UHMWPE, has a wear life of 1,000 cycles whereas the most hydrophobic interface, Si/OTS/UHMWPE, has a wear life of 6,500 cycles. Between these extremes, heated Si/UHMWPE, Si/APTMS/UHMWPE and Si-H/UHMWPE have shown wear lives of 60,000 cycles, 100,000 cycles and 250,000 cycles, respectively. The adhesion results studied by a scratch test were consistent with the friction and wear data. The critical loads for Si/UHMWPE and Si/OTS/UHMWPE are the same at 20 mN. The critical loads for heated Si/UHMWPE and Si/APTMS/UHMWPE are also the same at 40 mN,

whereas that of Si-H/UHMWPE is the highest at 70 mN. Except for the Si-H interface, the rest have shown some pores inside the scratches which clearly indicate inferior adhesion strengths of the polymer coatings. The final conclusion is that by simply modifying the surface wettability in an optimum range, the tribological performance of UHMWPE film can be increased by several orders of magnitude. Hydrogen termination of Si substrate currently works well with UHMWPE film for high wear durability.

Chapter 7

Molecular Orientation, Crystallinity, and Topographical Changes in Sliding and their Frictional Effects for UHMWPE Film

In the previous Chapters, different modification techniques of enhancing the tribological properties, especially the wear durability, of UHMWPE thin film on Si were presented. In fact, when the polymer film is applied in actual working environment, in addition to the interfacial bond strength there are many other factors that affect the friction property of the polymer film. For example, the sliding or rolling on polymer film is not always in uni-direction but bi-directional. The changes in the sliding direction can have great influence on the frictional properties. As UHMWPE film is semicrystalline, the molecular orientation and crystallinity can vary with the number of sliding cycles, especially in dry sliding. Not only from the application point of view but also from the scientific perspective, the understanding of these molecular and crystallinity changes with the number of sliding cycles and the effect of those changes on friction are very important to explore. In the present Chapter, these effects on friction behavior of UHMWPE film will be studied.

Bulk UHMWPE has been widely used as a bearing material in total knee and hip joint replacement [Kurtz *et al.* 1999] and as a solid lubricant film [Satyanarayana *et al.* 2006 and Minn and Sinha 2008 a]. Though it has been extensively used, the

tribological and mechanical properties of this polymer still limit the lifespan of such load bearing applications. Many researchers have tried to improve the wear resistance of UHMWPE by means of different approaches. Among them, cross-link density is one of the ways to enhance the wear resistance of UHMWPE [Muratoglu *et al.* 1999]. Cross-link density promotes the resistance to plastic flow and lamellae alignment [Wang *et al.* 1997 and Edidin *et al.* 1999]. Providing treatments such as radiation [Muratoglu *et al.* 1999 and 2001] and ion-implantation [Shi *et al.* 2001 and Ge *et al.* 2003] can increase the degree of cross-linking of the polymer. Simis *et al.* [2006] established the link between the mechanical properties and the microstructure in terms of crystalline mass fraction, lamellae size, and distribution. Sperling [2006] has also proved that the wear resistance of a polymer is affected by its mechanical properties which are related to the crystallinity of the polymer. These studies show that the crystallinity is one of the most important factors in determining the friction and wear properties of UHMWPE.

However, it is also to be noted that when UHMWPE is used as a film, its crystallinity can be changed during the course of sliding process which in turn affects the friction and wear properties, especially in continuous sliding tests. Another factor that affects friction is the molecular orientation of the polymer film. The molecular orientation of bulk PTFE has been extensively studied by Tabor's and Tanaka's groups [Pooley and Tabor 1972, Tanaka and Miyata 1977] in the 1970's in which they showed that the polymer molecules were oriented along the sliding direction during the course of sliding process. They also showed that when the sliding direction was perpendicular to the highly oriented polymer, the friction was remarkably increased.

However, they did not study how the friction would behave for example when the sliding direction was reversed. This Chapter will explore a deeper study of the friction of UHMWPE films in terms of changes in the crystallinity, molecular orientation, and micro-topography due to the sliding cycles and directions.

7.1 Experimental procedures

7.1.1 Materials

Tetrahedral amorphous carbon, ta-C (non-hydrogenated DLC) was deposited on Si (100) wafers. The thickness of the DLC film is in the range of 50 nm and hardness is 57 GPa. UHMWPE film was coated onto a cleaned Si/DLC substrate by simple dip-coating. The cleaning and coating procedures have been explained in Section 3.2. The thickness of the UHMWPE film used was approximately 12.3 μm .

7.1.2 Friction measurements

The friction measurements were conducted on a custom built tribometer. The setup has been described in Section 3.3.7. A silicon nitride ball of 4 mm diameter with a surface roughness of 5 nm was used as the stationary counterface. The normal load of 40 mN was applied which gave a normal contact pressure in the range of 51.6 MPa calculated using Hertzian contact model. The test track radius and rotational speed were fixed at 1 mm and 500 rpm (0.052 m/s), respectively. In order to study the effects of the number of initial sliding cycles and the sliding directions on the frictional behavior of the polymer film, 10,000, 30,000, 50,000, and 100,000 sliding cycles were selected as different initial test cycles. After running different cycles, the experiments were stopped and the counter ball was replaced with a new one in order to diminish the

effects of the transfer film deposited on the ball during the initial sliding cycles. Then, the new friction tests were continued precisely on the same track in the same direction as the initial sliding in forward direction (denoted as FD) or in the reverse direction (denoted as RD). All experiments were carried out in a clean booth environment at a temperature of 25 ± 2 °C and a relative humidity of $55 \pm 5\%$. The optical microscopy was used to examine the surface morphologies of the samples and the balls before and after the tests. All experiments were repeated at least three times and the averages of the data are reported.

7.1.3 Nanoscratching and nanoindentation

Nanoscratching and nanoindentation tests were carried out using a MTS Nano Indenter XP machine. The indenter for nanoscratching was a conical shape diamond tip with 90° cone angle and a tip radius of 5 μm. The applied load, the scratch velocity, and the scratch distance were 5 mN, 10 μm/s, and 50 μm, respectively. The scratching was conducted on the wear track after having done the sliding tests in both forward (FD) and reverse directions (RD). The main purpose of conducting nanoscratching is to examine localized frictional behavior in micrometer range and then to compare it with the ball-on-disc test data.

A constant load of 40 mN with a standard Berkovich diamond tip was used for nanoindentation. For each indentation, loading time duration of 100 seconds followed by 10 seconds of holding time at the final depth of indentation and unloading (retracting of the tip) was set. Fifteen independent indentations were conducted and averages of their hardness were reported. The nanoindentation results provided

information on any changes in the mechanical properties of the film as a result of different sliding cycles.

7.1.4 Measurement of molecular crystallinity of UHMWPE on the sliding track

The percent crystallinity of UHMWPE on the wear tracks was measured using Fourier Transform Infrared Spectroscopy (FTIR, Spectrum 1000, Perkin Elmer Life and Analytical Sciences, Boston, MA, USA). The spectra were obtained with an accumulation of 16 scans on transmission mode with a spot size of 100 μm diameter. The crystalline peaks were observed at 729 cm^{-1} [Cole *et al.* 2000] and 719 cm^{-1} [Elliot 1969 and Alves *et al.* 2005], respectively. The relative percentage crystallinity was calculated as the total area under the crystalline peaks (A and B) divided by the overall area (A, B, and C) [Davey *et al.* 2004], as shown in Figure 7.1. Five independent measurements were conducted on the track for each sample and the average values are reported in this paper.

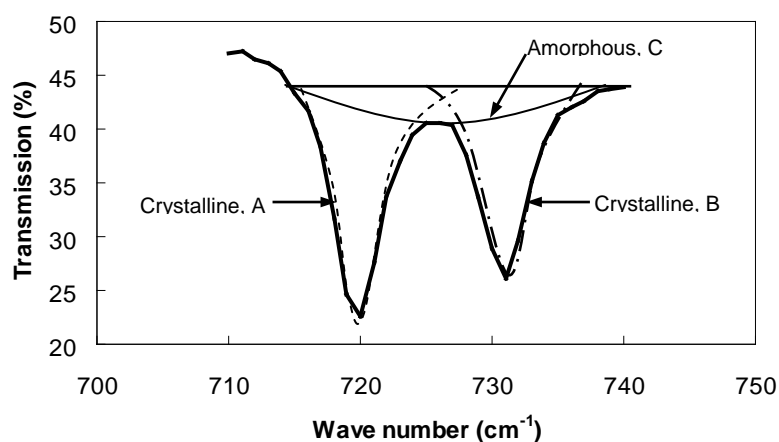


Figure 7.1: UHMWPE curve with amorphous and crystalline peaks using FTIR.

7.1.5 Wear track profilometry

Surface roughness was measured by Tencor P-10 alpha step profiler using a diamond tip (2 μm radius) with a load of 2 μN . The scanning speed was 5 $\mu\text{m/s}$ and the sampling rate was 100 Hz. The RMS roughness (rms) reported in this paper was taken from a scan length of 50 μm along the sliding track.

7.2 Results

A prior friction test was performed on the new UHMWPE film for the purpose of comparing the coefficients of friction before and after slidings. After sliding for different numbers of cycles, the counterface was replaced with a new ball in order to prevent the effects of the transfer films on the friction. During replacing the ball, the old ball was carefully replaced without moving the test location in order to obtain the friction precisely on the same track. As an additional confirmation of the exact location, the tracks were examined under an optical microscope after every test. There were no additional track confirming that all the friction data reported were recorded on the same track for different initial sliding cycles and in different sliding directions.

7.2.1 Friction of UHMWPE film as a function of sliding cycles in the forward direction

The coefficients of friction of UHMWPE film as a function of sliding cycles in the forward direction are shown in Figure 7.2. The initial coefficient of friction (FD) on new film was generally observed as less than 0.05. The coefficients of friction of 10,000 cycles and 30,000 initial sliding cycles in the forward direction were

approximately in the range of 0.07-0.08. However, if a new counterface ball was slid against the surface of higher initial number of cycles such as 50,000 cycles and 100,000 cycles, it is seen that the coefficient of friction drops to 0.05 or less.

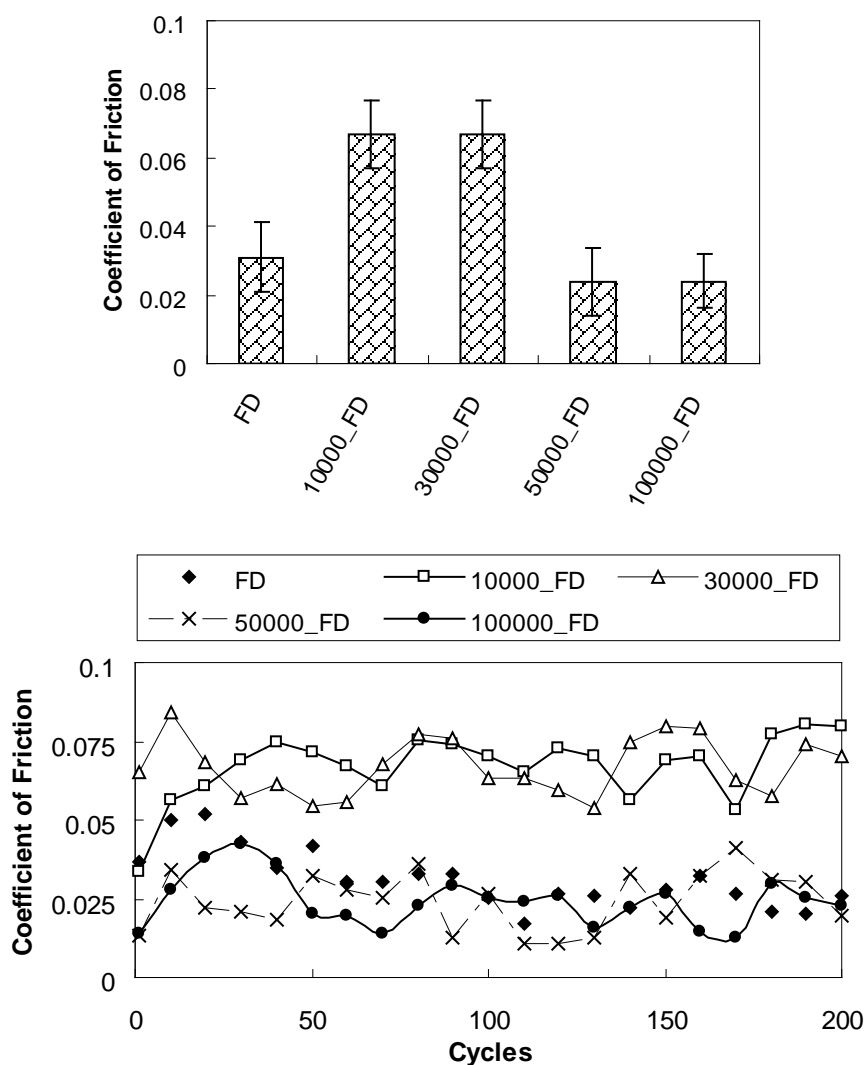


Figure 7.2: Coefficient of friction of UHMWPE film plotted against cycles in forward direction. FD refers forward direction. 10000_FD means after sliding 10,000 cycles in forward direction, the counterface has been replaced with a new ball and continued on the same track in forward direction.

7.2.2 Friction of UHMWPE film as a function of sliding cycles in the reverse direction

The coefficients of friction of UHMWPE film as a function of cycles in the reverse direction after different numbers of initial sliding cycles are shown in Figure 7.3. The coefficient of friction on new film in the forward direction (FD) is provided for the purpose of comparison. When the sliding direction is reversed, the most significant observation is that all the friction data in the reverse direction are higher than that of the original (new) film as well as that in the forward direction for the same number of sliding cycles (measured by a new silicon nitride ball).

Changing the sliding direction to reverse remarkably affected the friction for all number of initial cycles. The friction in the reverse direction generally increases as the number of initial sliding cycles increases. It is seen that up to 30,000 cycles, the friction in the reverse direction increases gradually to 0.15. However, beyond that number of sliding cycles the friction is observed to fall again. This behavior suggests that the frictional property of UHMWPE film is influenced by the number of initial sliding cycles which probably changes some features of the polymer film such as crystallinity, molecular orientation and topography. Those changes are major factors on friction when the sliding direction is reversed after different number of initial sliding cycles. Therefore, it is important to understand the frictional behavior of UHMWPE film with two sliding directions for different numbers of initial sliding cycles. The changes in friction in the reverse direction are re-examined by conducting nanoscratching test on the track.

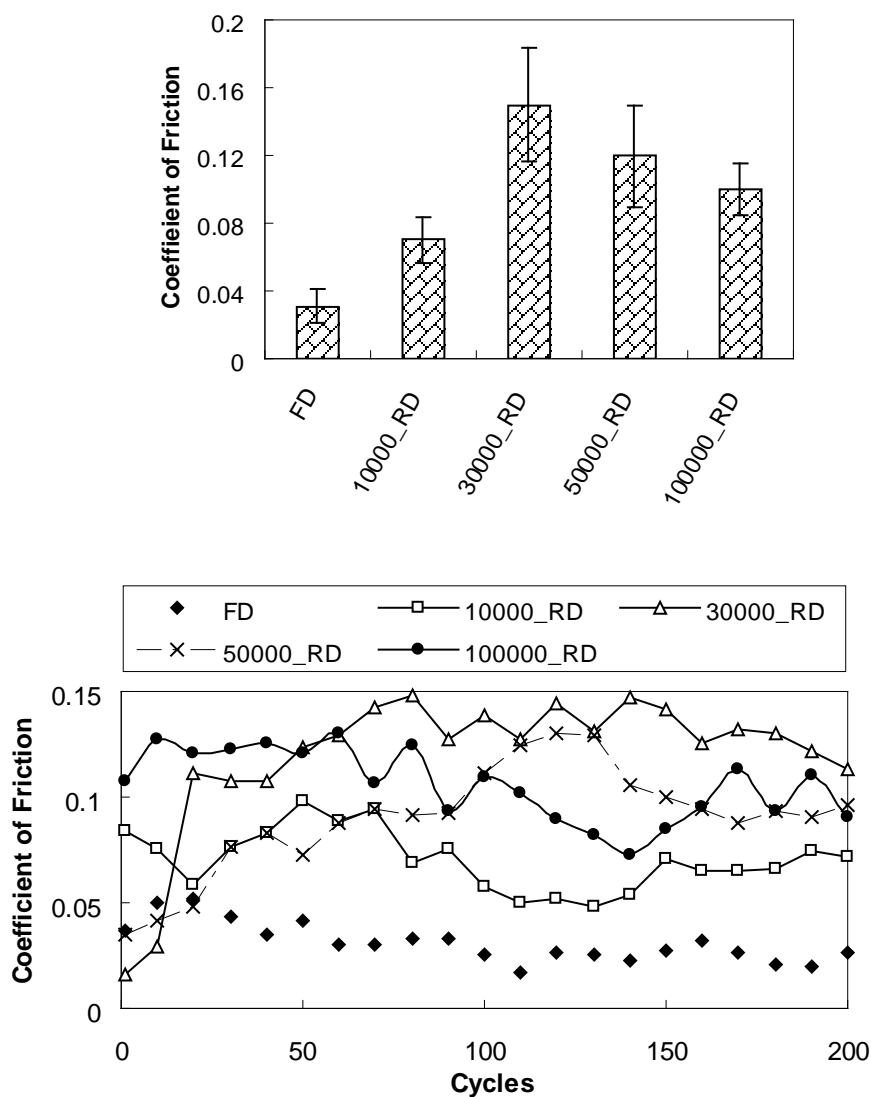


Figure 7.3: Coefficient of friction of UHMWPE film plotted against cycles in reverse direction. RD refers reverse direction. 10000_RD means after sliding 10,000 cycles in forward direction, the counterface has been replaced with a new ball and continued on the same track in reverse direction.

7.2.3 Friction of UHMWPE film as a function of scratch distance in nanoscratching

The coefficients of friction of UHMWPE film from the nanoscratching tests are shown in Figure 7.4. The initial friction is below 0.05 up to 20 μm scratching distance and then increases to approximately 0.08. The sudden change in friction is because of

the polymer debris that adhered to the tip by abrading the asperities in scratching. Except for this sudden change, both the initial frictions from ball-on-disc and nanoscratch tests were the same (less than 0.05). The coefficients of friction with different number of cycles using nanoscratching in forward direction have shown similar results as for ball-on-disc.

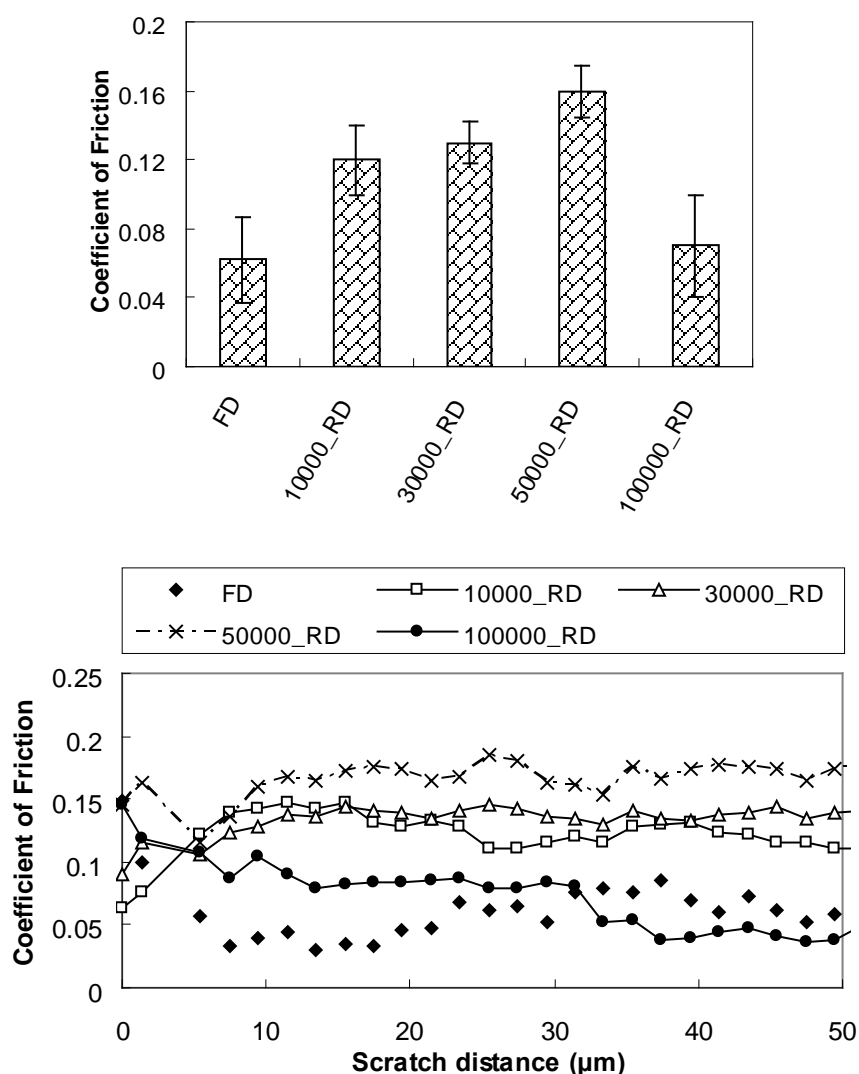


Figure 7.4: Coefficient of friction of UHMWPE film plotted against scratch distance in reverse direction. RD refers reverse direction. 10000_RD means after sliding 10,000 cycles in forward direction, the nanoscratching has been done on the same track in reverse direction.

However, when the sliding direction is reversed after different number of sliding cycles, it is observed that the coefficient of friction increases with increasing number of initial sliding cycles. The nanoscratching data are well consistent with the ball-on-disc sliding test data. The coefficient of friction drops when the number of initial sliding cycles is high enough (see data for 100,000 RD in Figure 7.4). The FESEM images of the nanoscratches, for example with initial sliding of 10,000 cycles and 100,000 cycles, are shown in Figure 7.5. The wear track width for 10,000 cycles is approximately 22 μm and that for 100,000 cycles is in the range of 50 μm .

The debris and the curled marks were observed in the image of 10,000 cycles (Figure 7.5 a) but there was no mark in the image of 100,000 cycles (Figure 7.5 b). It is found that there is not much amount of debris on the scratch conducted on 100,000 cycles. In nanoscratching, the role of the debris which comes out from the polymer film has been taken into account. The sizes of the debris pulled out from the film were comparatively small for 4 mm diameter Si_3N_4 ball and their effects could be neglected in ball-on-disc test. However, their sizes could not be negligible in nanoscratching as they can block and resist the scratching. That is why the coefficients of friction increased in nanoscratching. Except this small deviation, it is confirmed that the coefficient of friction is strongly affected by the number of initial sliding cycles and sliding directions.

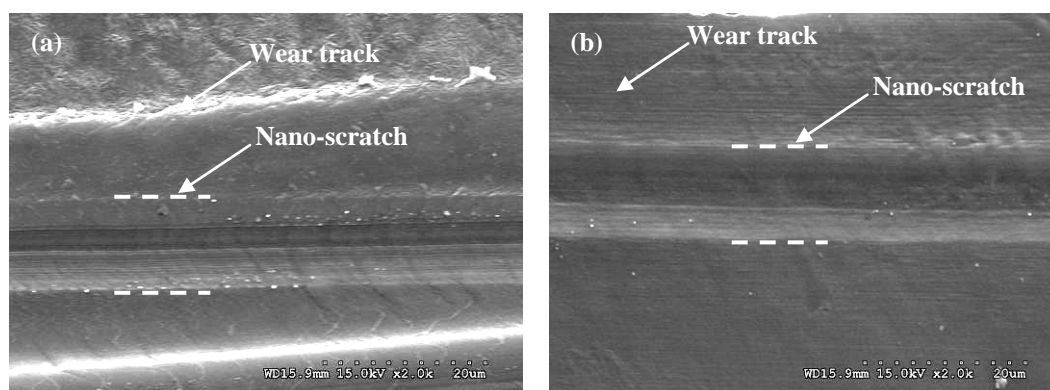


Figure 7.5: The FESEM images of nano-scratches which were done on wear tracks after sliding (a) 10,000 cycles and (b) 100,000 cycles. The scratches were conducted from right to left that was opposite to the initial sliding direction.

7.3 Discussion

The transfer mechanism of UHMWPE film on the counterface ball was studied under an optical microscope. The images of the balls after sliding 10,000 cycles and 100,000 cycles against the films are shown in Figure 7.6. Both images have lumpy polymers near the contact point and sharp-edged polymers are pulled out in the sliding direction. Lumps indicate that polymer first adheres to the ball as soon as the sliding starts. As the sliding continues, more polymer debris are attached near the contact zone and become thick. Sharp-edged polymer debris indicates that the morphology of the polymer on the track has been changed. The roughness of the film can increase with the changes in the surface morphology. Those changes are critically dependent on the number of sliding cycles. As the sliding cycles increase, a steady-state is achieved when all asperities are compressed and there is very little further transfer of the polymer to the ball. At the steady-state, the surface roughness can decrease as the sliding cycles increased.

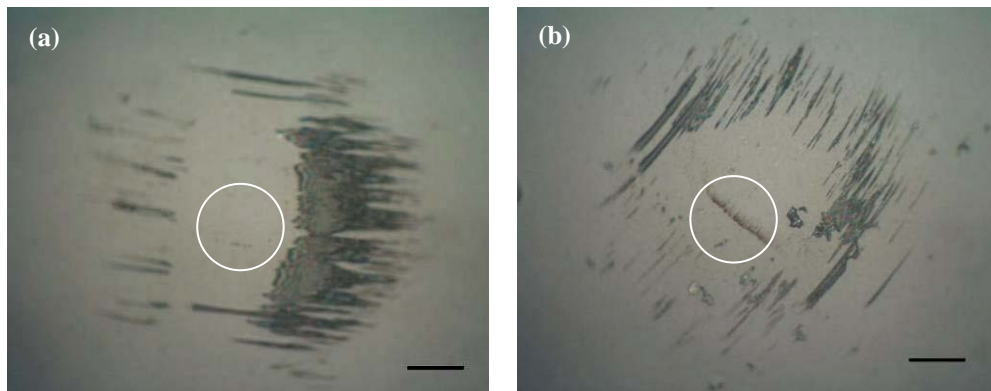


Figure 7.6: *Optical images of Si_3N_4 ball surface after sliding (a) 10,000 cycles and (b) 100,000 cycles against UHMWPE film in forward direction. White circles show the contact points. The scale bars are $50\ \mu\text{m}$.*

After different initial sliding cycles, nanoindentation tests were conducted in the track in order to examine the changes in the hardness of the film and the results are summarized in Table 7.1. The hardness of new UHMWPE film was 0.12 GPa and there was no significant variation until 30,000 cycles. It is obvious that all the frictional changes occurring in this range are not affected by the hardness of the substrate but by the surface morphology changes of the track. This was proved by recording the surface profiles of the wear track at different points. All measurements showed wear track depth of $0.3 \pm 0.1\ \mu\text{m}$ for all sliding cycles which was closer to the initial roughness of the film and much lower than the thickness of the film. Thus, within the given experimental conditions, there is no change in the film thickness due to sliding and only topographical changes take place due to the plastic deformation of the asperities. Hence, high hardness for the film after sliding 50,000 and 100,000 cycles is attributed to the changes in the physical state of the film rather than due to the substrate effect. At the early stage of sliding, the material removal rate from the film by detachment of the asperities was not uniform and the film surface became

roughened. This was confirmed by recording surface roughness profile on the wear tracks (Table 7.1). As the sliding continued with a new ball on the same track in the forward direction (Figure 7.2), the coefficient of friction for 10,000 cycles and 30,000 cycles increased because of the increased roughness of the film. When the sliding cycles were above 30,000 cycles, the surface became smooth again because of the plastic deformation in the top layer and molecular orientation and as a result the hardness has slightly increased. The high hardness of the film provides higher resistance to penetration which in turn reduces the contact area and the coefficient of friction. During the initial sliding process the molecules on the top layer of the film get plastically deformed and oriented in the direction of sliding. Such orientation of the molecules has effect on increasing the relative crystallinity and the strengthening of the film [Gorokhovskii and Agulov 1966]. Moreover, as the number of sliding cycles increases, the density will be high with longer pressing time that can also reduce the friction [Gracias and Somorjai (1998)].

Table 7.1: The hardness and roughness of UHMWPE film with different number of sliding cycles [Minn and Sinha 2009].

Sliding cycles	Hardness (GPa)	Roughness, R_{rms} (nm)
0	0.12 ± 0.008	118.8 ± 2.5
10,000	0.12 ± 0.008	123.8 ± 2.5
30,000	0.12 ± 0.009	135.8 ± 3.0
50,000	0.122 ± 0.023	43.0 ± 1.0
100,000	0.138 ± 0.022	32.0 ± 1.0

However, as can be seen in Figure 7.3, the coefficients of friction of different cycles are higher in the reverse direction than that in the forward direction. It proves that rather than the effects of the surface roughness and hardness, there are other factors such as the relative crystallinity and the molecular orientation that have influenced this change in the coefficient of friction.

The relation between the relative crystallinity on the track and the coefficient of friction in the reverse direction as a function of initial sliding cycles is shown in Figure 7.7. The results suggest that the crystallinity of the film varies with the number of the initial sliding cycles. The film before the test had a relative crystallinity of 76%. The degree of relative crystallinity increased to 79% after 10,000 cycles of sliding. A higher degree of relative crystallinity is because of the molecular arrangement in the amorphous regions due to sliding. The degree of alignment or relative crystallinity increases with sliding cycles but beyond 10,000 cycles the relative crystallinity fell and reached the lowest value of 66% after 50,000 cycles. One possible reason is that as sliding continued, the elevated asperities of the film were flattened and plastically deformed. The plastically deformed top layer must have partially covered the original crystalline region and hence reduced the overall relative crystallinity. The interesting fact is that the degree of relative crystallinity increased again beyond 50,000 cycles and it showed a high value of 87% after 100,000 sliding cycles. This increase in the relative crystallinity beyond 50,000 sliding cycles could be an indication of the molecular alignment in the direction of sliding after the asperities have been flattened in the beginning of the sliding process. This alignment also has a greater strengthening effect as seen in the nanoindentation data for the film after 100,000 sliding cycles

(Table 7.1). The results in Figure 7.7 show that the coefficient of friction in the reverse direction increased with increasing number of cycles up to a point and then decreased with higher number of cycles. The friction was inversely proportional to the crystallinity of the film. The presence of the amorphous region in lower relative crystallinity region is high which can extend and align during the sliding that can increase friction. In contrast, high relative crystallinity somewhat hardens the polymer film and reduces the coefficient of friction. Furthermore, the asperities of the polymer film are unevenly deformed and the remaining roughness features are inclined in the direction of sliding. This change in the surface morphology is coupled with the initial increase in the film roughness when measured along the wear track. When the sliding direction is reversed, the oriented polymers are now against the new sliding direction. This is another important reason for the increase in the friction upon changing the sliding direction. Complete molecular orientation of the polymer takes many initial sliding cycles. However, Pooley and Tabor [1972] also showed on PTFE film that if the molecules were highly oriented in the sliding direction, the coefficients of friction were not very different in both directions (i.e. forward or reverse of the initial sliding directions). When the initial sliding cycles were 100,000, the coefficient of friction in the reverse direction decreased because of:

- (a) nearly complete orientation of the molecules by plastic deformation,
- (b) higher relative crystallinity that increased the hardness, the load carrying capacity and reduced the contact area of the film, and
- (c) general smoothness of the film (i.e. no more asperities deformed in the direction of initial sliding)

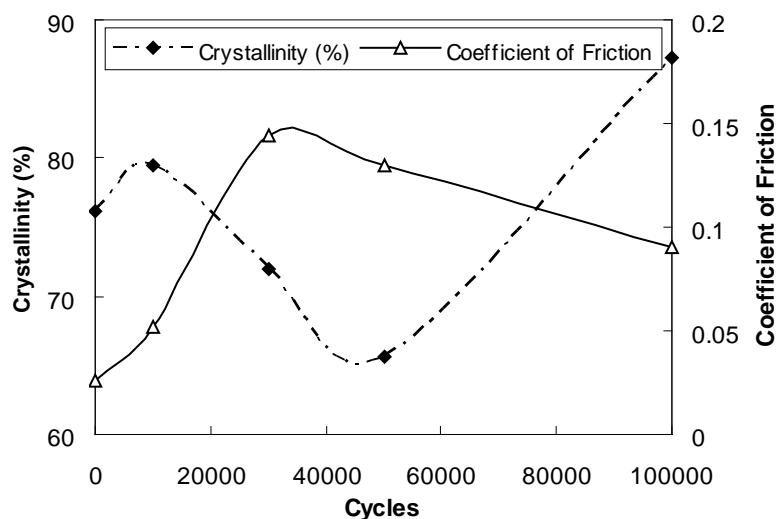


Figure 7.7: The relation between crystallinity and coefficient of friction (in reverse direction) as a function of sliding cycles.

A better understanding of the relative crystallinity and surface morphology on the track is studied by FESEM. Their topography images are shown in Figure 7.8. A distinct type of lamellae structure that is a sign of crystalline region [Turell and Bellare 2004] is clearly seen in Figure 7.8 (a) (before sliding). The images of the tracks after sliding 10,000 cycles and 50,000 cycles (Figures 7.8 b and c) consist of covered and uncovered areas.

The covered areas are due to the plastically deformed layers which were formed by flattening the taller asperities of the crystalline zone. As the sliding cycles increased, the coverage by the deformed polymers on the track appears more and as a result the relative crystallinity of the original film surface drops. It is also found that there are sharp corners with steps at the leading edges of the covered layers that increase with the number of cycles (Figures 7.8 b and c). In the case of the reverse

direction sliding, these steps and corners could obstruct the sliding and increase the friction.

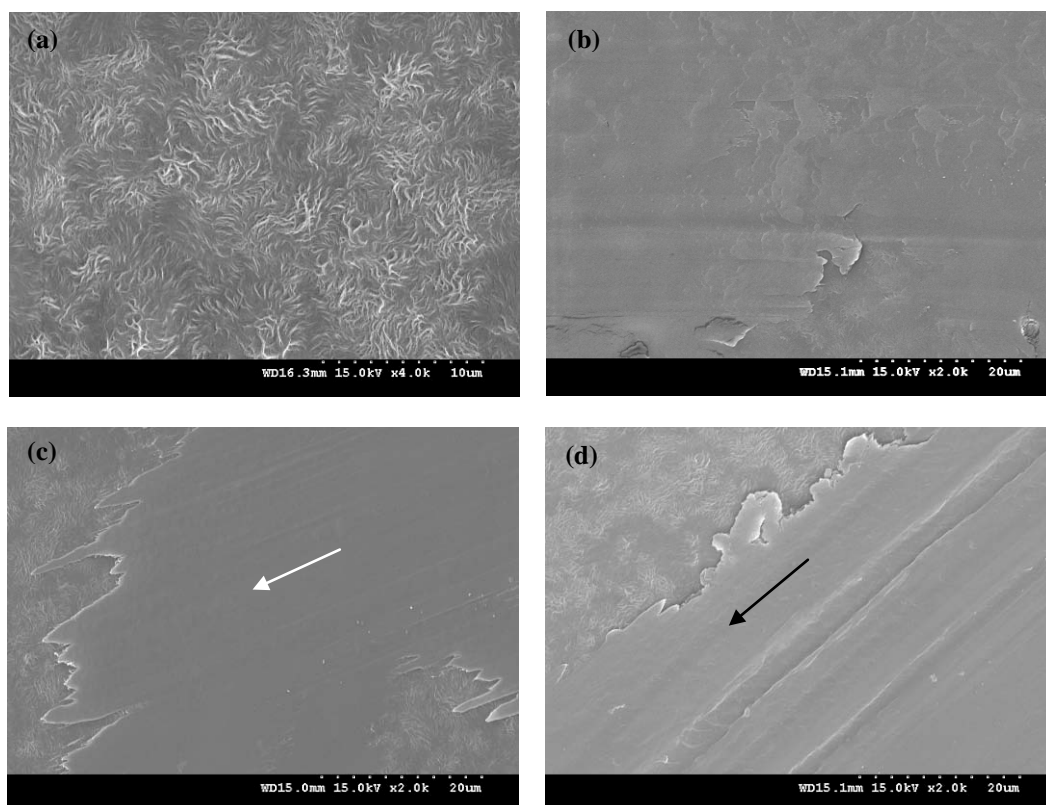


Figure 7.8: *The FESEM images of UHMWPE film (a) before sliding and after sliding (b) 10,000 cycles, (c) 30,000 cycles and (d) 100,000 cycles. Image (a) is taken with 4000 times and the rest are taken with 2000 times magnifications. Solid arrows show the sliding directions.*

It can be seen in Figure 7.8 (d) that the coverage by deformed and oriented molecules is near complete with probably majority of the polymer molecules oriented in the initial sliding direction. Thus, for very high number of initial sliding cycles, the early roughness effect in the reverse direction is lessened and the molecular orientation is increased. It is also possible that the relative crystallinity of the layers below the top plastically deformed layer can increase for the long sliding period [Albrecht and Strobl 1995]. The high crystallinity due to molecular orientation and smoothness of the wear

track for 100,000 initial sliding cycle case, therefore, reduced the frictional resistance in the reverse direction.

7.4 Summary

This Chapter has presented the changes in the relative crystallinity and molecular orientation of UHMWPE film for different numbers of initial sliding cycles. It is seen that the coefficient of friction is different in the forward or reverse directions. During the initial sliding the roughness can increase before the surface becomes very smooth at approximately 50,000 cycles or more. There is slight increase in the hardness of the film because of changing molecular orientation and relative crystallinity effects. The coefficient of friction remains on the higher side until the top film surface is completely modified because of the sliding phenomenon. In the reverse direction, the relative crystallinity, molecular orientation and changes in topography influence the coefficient of friction. As the sliding starts, the asperities of the top layer are plastically deformed that cover the original crystalline region of the film. Initial plastic deformation of the film leads to a decrease in the relative crystallinity in the middle range of sliding cycles (30,000-50,000 cycles) due to the change in the molecular orientation. As the molecules are further aligned along the sliding direction, the sharp corners and steps appear that can provide obstacles to the slider if it were to slide in the reverse direction. The appearance of these patterns is much more in the middle range of the initial sliding cycles. Because of the lower crystallinity and higher number of sharp edges, the coefficients of friction in the reverse direction after 30,000 cycles and 50,000 cycles of sliding are higher than the lower and the higher number of

initial sliding cycles. For the lower number of initial sliding cycle case, the relative crystallinity of the film is still high (original film relative crystallinity) and the topography of the film is not much changed. For very high number of initial sliding cycle case, the film has been totally covered with highly oriented polymer molecules and the surface is also very smooth.

This study has shown that the friction coefficient of a polymer film is highly dependent on the molecular orientation and relative crystallinity and hence these parameters should be considered while making highly lubricious polymer films on a substrate. Also, the process of the continuous sliding in one direction can change the above parameters of the film bringing a clear change in the film frictional behavior.

Chapter 8

The Frictional Behaviors of UHMWPE Film with Different Surface Energies at Low Normal Loads

The enhancement of the tribological properties of UHMWPE film is studied using different methods of modification and its results are reported from Chapter 4 to Chapter 6. The changes in molecular crystallinity, orientation and surface topography of UHMWPE film with different number of sliding cycles and their effects on friction with respect to different sliding directions are reported in Chapter 7. In the present Chapter, the roles of the surface energy of UHMWPE film and the applied normal load on the initial friction of UHMWPE film are studied.

The Amonton's Laws states that friction is only controlled by the geometry of the asperities of surfaces and the friction force needed to slide against an applied load is decided by the apex angles of the asperities. Bowden and Tabor later proposed the two-term model of friction where friction force is separated into the interfacial and cohesive components. The interfacial friction relates to the shear taking place at the very top layer of the surfaces and the cohesive friction is the force required in deforming the materials if there are asperity-asperity interactions. More recently, it has been found that if two surfaces adhere to each other at rest, there is a finite value of friction upon sliding even at no external applied load [Dowson 1998]. It means, friction is decided by not only the geometry of the asperities and two-term model, but also the adhesion energy (surface energy) of the surfaces. JKR [Johnson *et al.* 1971]

and DMT [Derjaguin *et al.* 1975] models have shown that the contact radius was different from the calculated one using the Hertzian model in static contact when surface energy is taken into account. Israelachvili and Tabor [1972] experimentally measured the contact radius with adhesion effect which is directly proportional to the surface energy. Both theoretical and experimental results proved that the role of surface energy on friction is not negligible especially when the applied load is very small. The role of surface energy is still a critical factor in the study of dynamic friction.

Yoshizawa *et al.* [1993] studied the correlation between friction and adhesion by means of adhesion hysteresis and energy dissipation. Recently, Corwin and de Boer [2004] also studied the effect of adhesion on friction in micromachining. In order to reduce the adhesion, monolayer thickness lubricants (usually polymers) are applied on surfaces of the devices [Maeda *et al.* 2002]. The frictional behavior of polymers in terms of adhesion is well studied [Lee 1974, Briscoe and Tabor 1978 a and b, and Briscoe 1978]. For thin liquid films, the surface energy changes with the thickness of the liquid film. Above a critical thickness, the surface energy normally decreases [Tyndall and Leezenberg 1998] but the initial friction increases sharply [Tian and Matsudaira 1993] because of the presence of liquid meniscus between the contacting surfaces. In this study, a fixed film thickness is used for all samples to eliminate the effect of film thickness on the surface energy and initial friction. Effects of surface energy and applied load on the frictional behaviors of UHMWPE film are studied. The initial coefficient of friction and surface energy are correlated using a model and compared with experimental results.

The surface energy is associated with surfaces or interfaces and has a unit of energy per unit area ($\text{ergs/cm}^2 = \text{mJ/m}^2$). The simplest way to measure the surface energy of a solid is to measure the contact angle using water (or any liquid) droplet on it. If the molecules of water (or any liquid) have stronger attraction to each other than to the molecules of the solid (cohesive force is stronger than adhesive force), the droplet will show a spherical shape and does not wet the solid. If the molecules of the water (or any liquid) have stronger attraction to the solid than to each other (cohesive force is weaker than adhesive force), the droplet will spread and wet the solid.

8.1 Experimental procedures

8.1.1 Materials and sample preparations

UHMWPE film was coated onto Si wafer with a thickness of 12 μm . The detailed preparation procedure of UHMWPE film was mentioned in Section 3.2. Silicon nitride (Si_3N_4) ball with 4 mm diameter was used as the counterface material against UHMWPE film in ball-on-disc sliding tests. In order to change the surface energy of the Si_3N_4 ball and the UHMWPE film, some surface treatments were given to them. For changing the surface energy of Si_3N_4 ball, air-plasma treatment with 10 minutes exposure time was given and as another treatment, 3-4 nm thick PFPE film was overcoated onto it. The air-plasma treatment could provide hydrophilic nature whereas PFPE layer could make the surface hydrophobic. It is difficult to enhance the surface hydrophobicity of Si_3N_4 ball only by a physical treatment. This is the reason why PFPE overcoating was chosen as a treatment for hydrophobicity by slightly changing the surface chemistry without affecting the surface roughness.

Perfluoropolyether (PFPE) Z-dol 4000 of 0.2 wt% was dissolved into H-Galden ZV60 solvent. Chemical formulae of PFPE and H-Galden ZV60 are $\text{HOCH}_2\text{CF}_2\text{O}-(\text{CF}_2\text{CF}_2\text{O})_p-(\text{CF}_2\text{O})_q-\text{CF}_2\text{CH}_2\text{OH}$ and $\text{HCF}_2\text{O}-(\text{CF}_2\text{O})_p-(\text{CF}_2\text{CF}_2\text{O})_q-\text{CF}_2\text{H}$, respectively, where the ratio p/q is $2/3$. The dipping and withdrawal speeds were fixed as 2.4 mm/s.

For the UHMWPE film, since it has hydrophobic property, we did not attempt to increase its surface hydrophobic property. In this case, UHMWPE film was given the air-plasma treatment with different exposure times (30 seconds, 5 minutes and 10 minutes) in order to change the surface energy by making the surface hydrophilic.

Harrick Plasma Cleaner/Steriliser was used for air-plasma treatment with the different exposure times and a RF power of 30W under vacuum.

8.1.2 Contact angle measurements and surface energy analysis

After giving different treatments to the samples, their surface energies were determined by the contact angle measurement. The relationship between the contact angle and the surface free energy was first demonstrated by Young with a single droplet on the surface [Young 1855]. The Young equation is written in the form,

$$\gamma_{SV} = \gamma_{SL} + \gamma_{LV} \cos \theta \quad (8.1)$$

where θ is the contact angle, γ is the surface energy and the subscripts SV , SL and LV represent surface-vapor, surface-liquid and liquid-vapor interfaces, respectively. In determining the surface energy from the contact angle measurement, we used acid-base method [van Oss 1994 a] in which at least three test liquids are required. In three liquids, at least two have known acid and base fractions larger than zero and at least

one must be equal basic and polar parts usually water. In the contact angle measurements in this study, four different liquids: distilled water, ethylene glycol, methanol and hexadecane were used with VCA Optima Contact Angle System (AST product, Inc., USA). The surface tension components and the parameter of the liquids used in this study are provided in Table 8.1 [van Oss 1994 b].

Table 8.1: Surface tension component and parameters of distilled water, ethylene glycol, methanol and hexadecane in mJ/m^2 .

Liquid	γ_L^{LW}	γ_L^{AB}	γ_L^+	γ_L^-	Total surface energy, γ_L
Distilled water	21.8	51	25.5	25.5	72.8
Ethylene glycol	29	19	1.92	47	48
Methanol	18.2	4.3	0.06	77	22.5
Hexadecane	27.47	0	0	0	27.47

Droplets of 0.5 μl and 0.05 μl were used for the contact angle measurements of the surfaces (UHMWPE film and Si) and Si_3N_4 ball, respectively. The droplet size for the measurements on Si_3N_4 balls was reduced because of the curvature of the spherical ball. As an additional confirmation of the effect of droplet size (from 0.05 μl to 5 μl), water contact angles were measured on a flat surface with different droplet sizes and the results did not show any droplet size effect within the given size range. A total of five independent measurements were conducted randomly on three samples and an average value was taken for each sample. The measurement error was within $\pm 3^\circ$. After measuring the contact angle with different liquids, the surface energies were calculated using the software installed in the same contact angle equipment. In order to confirm the accuracy of the technique used to determine the surface energy of the

samples, PFPE was overcoated on flat Si and UHMWPE film, and then the measured surface energy values were compared with the reported value [Solvay Solexis 2009].

The friction between two solid bodies depends not only on the surface energies but also on the surface roughness [Tabor 1977]. Therefore, the roughness of the ball and UHMWPE film were measured before and after surface treatments using dynamic MEMS optical profilers (Veeco Wyko NT1100) (a non-contact profiling device). The scanning area for the measurement was 124 μm x 93 μm on VSI (vertical scan interferometry) mode.

8.1.3 Surface energy and attractive force between surfaces

It is known that when two surfaces (e. g. ball and a flat surface) come into contact, there is finite force acting between them called attractive or pull-off force, F_o . This force, which depends upon the surface energies of the solids, was first derived by Bradley [1932] and is given as,

$$F_o = 2\pi R(\gamma_1 + \gamma_2 - \gamma_{12}) \quad (8.2)$$

where γ_1 and γ_2 are surface energies of the two surfaces and $\gamma_{12} = (\sqrt{\gamma_1} - \sqrt{\gamma_2})^2$.

The attractive or pull-off force, F_o between two different surface energies of the ball and UHMWPE film was calculated using Equation 8.2. A detailed calculation procedure of F_o can be found in references [Bradley 1932 and Tabor 1977].

8.1.4 Friction tests

Friction tests were carefully conducted using a custom-built ball-on-disc tribometer (Figure 8.1) where normal and lateral displacements (converted to normal

load and friction force respectively) of the cantilever were simultaneously measured with laser displacement sensors (MTI Instruments Inc., New York, USA). The equipment is a further modification of the ball-on-disc tribometer (mentioned in Section 3.3.7) in which we used four-bridge strain gauge in order to measure the lateral displacement. In the modified equipment, we replaced the strain gauge sensor with a laser sensor. The sensitivity of the laser sensor was 0.5 μm which was equivalent to 0.125 mN force according to our calibrations. UHMWPE film was used as a rotating disc and silicon nitride balls with modified surface energies were used as the stationary counterface. The sliding track radius was 1 mm with a fixed disc rotational speed of 2 rpm (linear relative speed at the contact was in the range of 0.21 mm/s). The sampling rate used in recording data was 10 Hz. In order to eliminate the effect of loading time on friction, the tests were conducted immediately after applying the normal load. The initial coefficient of friction was taken as the maximum friction value as soon as the sliding test started. Three repeats of sliding tests on at least three samples were conducted and averages were reported as the final values. The temperature and the relative humidity were fixed at 25 °C and 65 %, respectively.

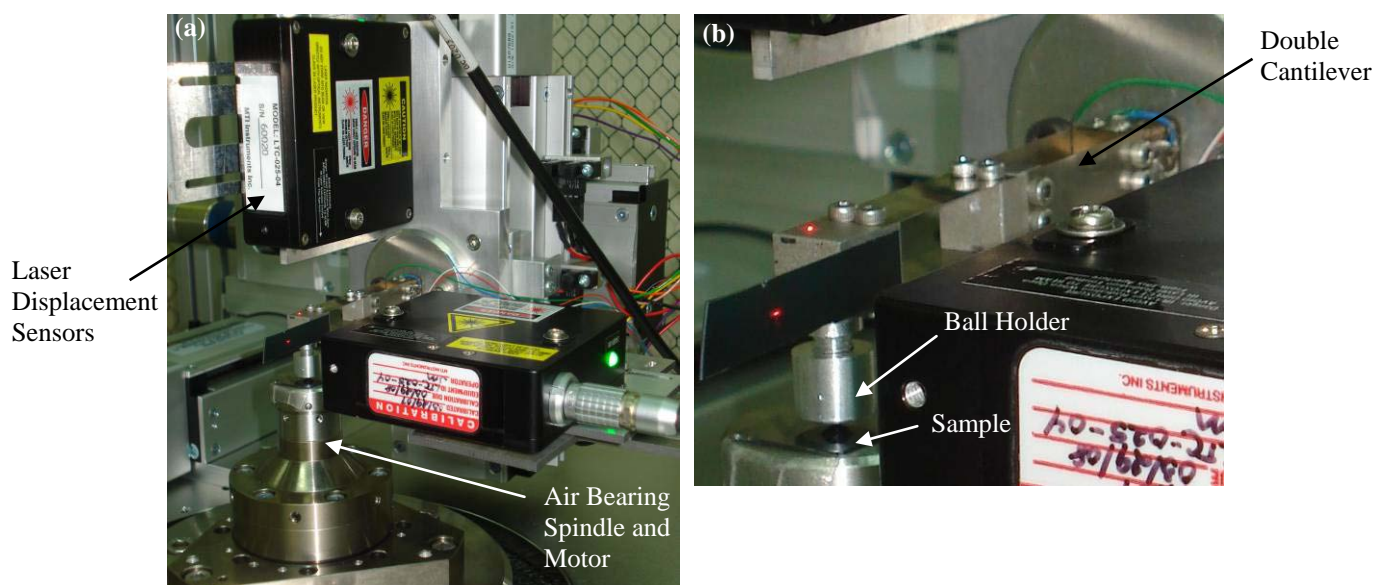


Figure 8.1: (a) The modified ball-on-disc tribometer, (b) larger view of the cantilever and the sample holder.

8.2 Results and discussion

8.2.1 Surface energy and roughness

The surface treatments, surface energies and roughness of the ball and the surfaces used are summarized in Table 8.2. The surface energy of PFPE reported in the literature is in the range of 22~24 mJ/m² depending upon the concentration and molecular weight [Solvay Solexis 2009]. The currently measured values of PFPE layers on Si₃N₄ ball, Si surface and UHMWPE film are 17.9 mJ/m², 24.13 mJ/m² and 23.7 mJ/m² respectively. A slight change in the surface energy of Si₃N₄ ball may be because of the different measurement conditions between flat surfaces (Si and UHMWPE film) and spherical surface (Si₃N₄ ball). Except this small deviation, our measured values and the data provided by the supplier in reference [Solvay Solexis 2009] are close. It shows that our method of surface energy measurement is reliable.

Table 8.2: A summary of surface roughness, treatments and surface energy of silicon nitride ball, UHMWPE film and Si surface. PFPE refers perfluoropolyether (Z-dol 4000) which was coated as 3-4 nm film on the solids mentioned.

Sample	Roughness	Treatment	Surface Energy (mJ/m ²)			
			Dispersive	Acid	Base	Total
Si ₃ N ₄ ball (γ_1)	5 nm	PFPE coated	10.5	2.4	5.7	17.9
		No treatment	21	-	24.9	21
		Air Plasma (10 mins)	24.7	0.1	62.5	29.7
UHMWPE coated Si (γ_2)	0.6 μ m	PFPE coated	23.5	0.1	0.1	23.7
		No treatment	26.9	-	2.6	26.9
		Air Plasma (30s)	27.4	2.5	30.7	44.92
		Air Plasma (5 mins)	27.4	2.9	29.6	45.93
Bare Si (γ_2)	0.41 nm	Air Plasma (10 mins)	27.3	2.4	38.5	46.52
		PFPE coated	13.6	1.9	14.6	24.13

Though the surface energy of most ceramic materials is very high, the surface energy of silicon nitride ball used in this study is low as evident from the contact angle measurements. Before giving any surface treatment, its contact angle was 83.4°. By giving plasma treatment for 10 minutes, the contact angle dropped to 38° but it was still measurable. After PFPE overcoating, the contact angle rose to 95.3° in the hydrophobic range. The water contact angle measurement images on Si₃N₄ balls with different treatments are shown in Figure 8.2.

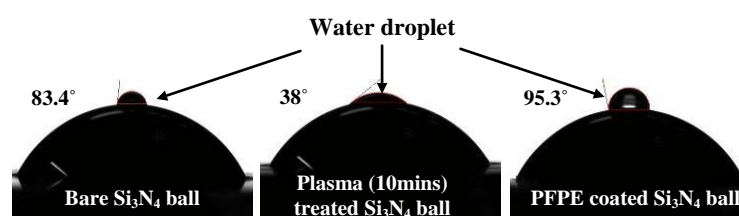


Figure 8.2: The water contact angle measurement on Si₃N₄ balls with different treatments.

The surface energy of UHMWPE without plasma treatment was 26.9 mJ/m².

An increase in the surface energy of UHMWPE was observed by the air-plasma

treatment. After 30 seconds of air-plasma exposure time, the surface energy rose to 44.92 mJ/m^2 . This value did not change further in any significant way with increasing exposure time to 5 minutes and 10 minutes.

The measured roughness value on Si_3N_4 ball and UHMWPE film were 5 nm and $0.6 \text{ }\mu\text{m}$ (Figure 8.3), respectively. Negligible differences in the surface roughness were observed in the cases of Si_3N_4 ball and UHMWPE film after air-plasma or PFPE treatments. Therefore, the effect of surface roughness on the measured surface energies was neglected. Also, the surface roughness did not vary within one single friction test. The effect of interfacial temperature was also neglected as the friction tests were conducted at very low sliding speeds in a temperature controlled environment.

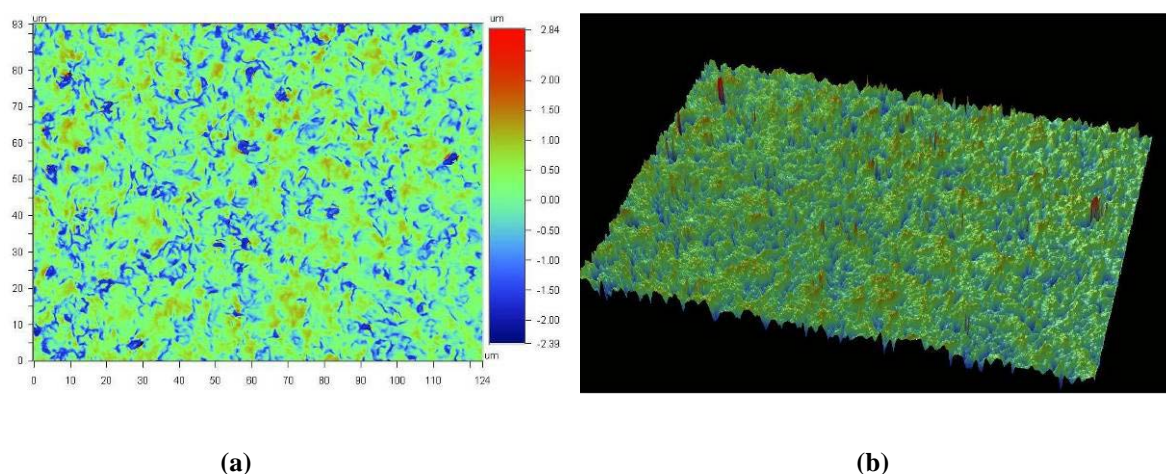


Figure 8.3: The roughness measurement on UHMWPE film using DMEMS. (a) 2D and (b) 3D images where the scan size is $124 \text{ }\mu\text{m} \times 93 \text{ }\mu\text{m}$.

Based on the surface energy of Si_3N_4 ball and UHMWPE film with different treatments, the attractive force, F_0 was calculated using Equation (8.2). The calculated attractive forces between different surface pairs are shown in Table 8.3.

Table 8.3: The attractive force, F_o between Si_3N_4 ball and UHMWPE film with different surface energies.

Si_3N_4 Ball (γ_1)		UHMWPE film (γ_2)		F_o (mJ/m ²)
Treatment	Surface Energy (mJ/m ²)	Treatment	Surface Energy (mJ/m ²)	
PFPE coated	17.9	No treatment	26.9	0.55
No treatment	21	Air Plasma (10 mins)	46.52	0.79
Air Plasma (10 mins)	29.7	No treatment	26.9	0.71
PFPE coated	17.9	Air Plasma (10 mins)	46.52	0.72
No treatment	21	No treatment	26.9	0.6
Air Plasma (10 mins)	29.7	Air Plasma (10 mins)	46.52	0.93

8.2.2 The relationship between the initial shear stress and the surface energy of UHMWPE film

The friction tests were conducted using the different pairs of Si_3N_4 ball and UHMWPE film mentioned in Table 8.3, and the shear stress, τ was calculated by dividing the measured friction force with the contact area [Bowden and Tabor 1986]. In order to obtain the contact area between the ball and the UHMWPE film, JKR model (Equation 8.3) was applied in which the effect of surface energy is taken into account.

$$a^3 = \frac{R}{K} \left(L + 3\pi R + \sqrt{6\pi RL + \left(\frac{3}{2}\pi R \right)^2} \right) \quad (8.3)$$

where a is the contact radius, R is the sphere radius, K depends upon the Poisson's ratio and the elastic modulus of the materials, L is the applied load and γ is the surface energy. The Poisson's ratios and elastic moduli of the materials used are provided in Table 8.4. The contact pressure, P was calculated by dividing the applied normal loads with the contact area, πa^2 . By varying the applied normal load from 15 mN to 75 mN,

the calculated contact pressure is varied from 59 MPa to 117 MPa for the mentioned contacting surfaces.

Table 8.4: The Poisson's ratio and elastic modulus for silicon nitride ball and UHMWPE film.

Material	Poisson's ratio	Elastic modulus (GPa)
Silicon nitride ball	0.22	310
UHMWPE film	0.46	1

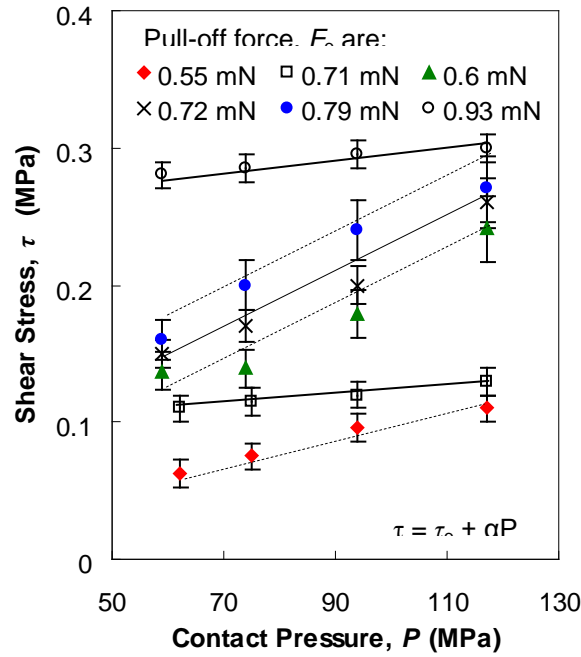


Figure 8.4: Shear stress versus contact pressure on UHMWPE film. For all F_0 , there is a linear relation between the shear stress and the contact pressure.

After obtaining the shear stress, τ and the contact pressure, P for different F_0 (varying from 0.55-0.93 mN) between the ball and the UHMWPE film, we plotted them as shown in Figure 8.4. It is seen that τ increases linearly with increasing P although the magnitude of τ is strongly influenced by the attractive force, F_0 (that is

the adhesive interactions between the surfaces). It is well noted that higher F_o provides higher τ . The data also confirms the linear relation $\tau = \tau_o + \alpha P$ as proposed by Bowden and Tabor [Bowden and Tabor 1986] where the pressure coefficient, $\alpha = 0.0013$, is same for all F_o . However, the normal pressure-independent initial shear stress, τ_o increases as F_o is increased within the range of the presently applied loads. Robbins *et al.* [He *et al.* 1999, He and Robbins 2001, Müser *et al.* 2001, and Rottler and Robbins 2001] have also shown by molecular dynamic simulation that τ_o increases as adhesion or attractive force is increased whereas α does not change. τ_o is the initial shear stress when the contact pressure, $P = 0$.

The adhesion between contacting solids at rest is partially transformed into elastic strain in the cantilever at the onset of lateral sliding motion. The stored elastic energy in the cantilever will be released when the initial friction force measured by the deflection of the cantilever reaches the failure of the adhesion at the contact, also known as static friction. This is the point at which the actual sliding starts giving the lateral force at release (or slip) as the initial friction. τ_o is an important parameter controlling initial friction (also referred to as static friction) which changes with the pull-off force, F_o . Figure 8.5 presents the data for F_o and τ_o for Si_3N_4 ball and UHMWPE film. It is evident that τ_o increases slightly with F_o up to 0.72 mN and beyond this value, τ_o rises exponentially. As we mentioned before, the application of PFPE could affect the frictional behavior of UHMWPE film. It could help to lower the friction in addition to lowering the surface energy. However, when the data of PFPE are removed from Figure 8.5 (a), it is obvious that the relationship between F_o and τ_o is still an exponential curve (see in Figure 8.5 b) with only slight changes in the curve fitting

parameters. Thus, this behavior between F_o and τ_o can be modeled by an exponential curve of the following form,

$$\tau_o = c_1 \exp(n F_o) \quad (8.4)$$

where c_1 and n are constants that depend upon the nature of the surface materials. The values of c_1 and n shown in Figure 8.5 (a) are 9×10^{-5} MPa and 8.4 (mN)^{-1} , respectively.

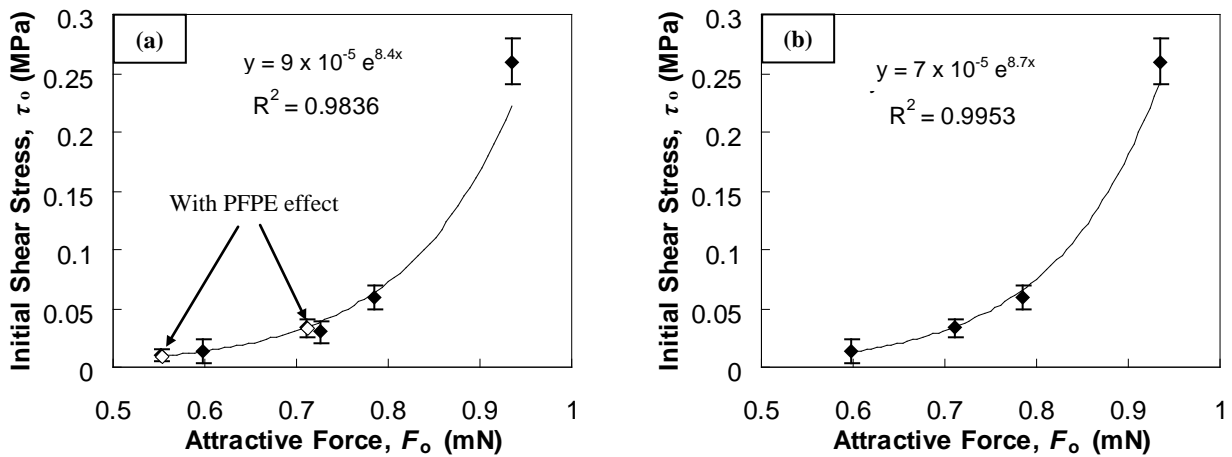


Figure 8.5: The initial shear stress, τ_o as a function of the attractive force, F_o of UHMWPE film (a) with PFPE data and (b) without PFPE data. There is an exponential relation between the two.

8.2.3 The relationship between the initial coefficient of friction and the surface energy of UHMWPE film

Since $\tau = \tau_o + \alpha P$ and the initial friction force, $F_i = \tau A$, we can write as

$$F_i = \tau_o A + \alpha P A \quad (8.5)$$

By dividing Equation (8.5) with applied load, L , we obtain the initial coefficient of friction, μ_i as

$$\mu_i = \left[\frac{\tau_o}{L} \times A \right] + \alpha \quad (8.6)$$

where $P = L/A$. Finally, we can correlate μ_i as a function of attractive or pull-off force, F_o using Equation (8.4) and (8.6) as

$$\mu_i = \left[\frac{c_1 \exp(nF_o)}{L} \times A \right] + \alpha \quad (8.7)$$

For the visco-elastic materials such as UHMWPE film, Bowden and Tabor [1973] suggested that the contact area, A is nearly proportional to $L^{0.75}$. Since $A = c_2 L^{0.75}$ where c_2 is a constant, Equation (8.7) then becomes,

$$\mu_i = \left[\frac{c_1 c_2 \exp(nF_o)}{L^{0.25}} \right] + \alpha \quad (8.8)$$

In order to verify this relationship, we measured μ_i at different F_o on UHMWPE film for different normal applied loads. In Figure 5, the curves show a very similar exponential relation between μ_i and F_o for different applied loads and variations are within experimental errors. In addition, it might be assumed that the highest frictional value at 0.93 mN (F_o) (which represents the ball and UHMWPE film that were given 10 minutes plasma treatment) has additional effect of covalent bonding between oxygen species that were introduced onto the ball and UHMWPE film due to

air-plasma treatment. Despite some additional chemical effects, we observe that the relation between the initial coefficient of friction and the pull-off force due to surface energy is of exponential type.

Similar exponential trend has been shown by Erhard [1983] and Lavielle [1991]. They studied friction between different polymers with different surface energies ($55\text{-}90\text{ mJ/m}^2$) and found that the coefficient of friction was exponential to the surface energies of the sliding polymers. In the present study, we have used a fixed polymer film (UHMWPE) with modified surface energies and similar exponential relation is observed. Another interesting behavior we have seen from this study is that μ_i drops with increasing load (Figures 8.6 a and b) as predicted by Equation 8.8 within the load range adopted here.

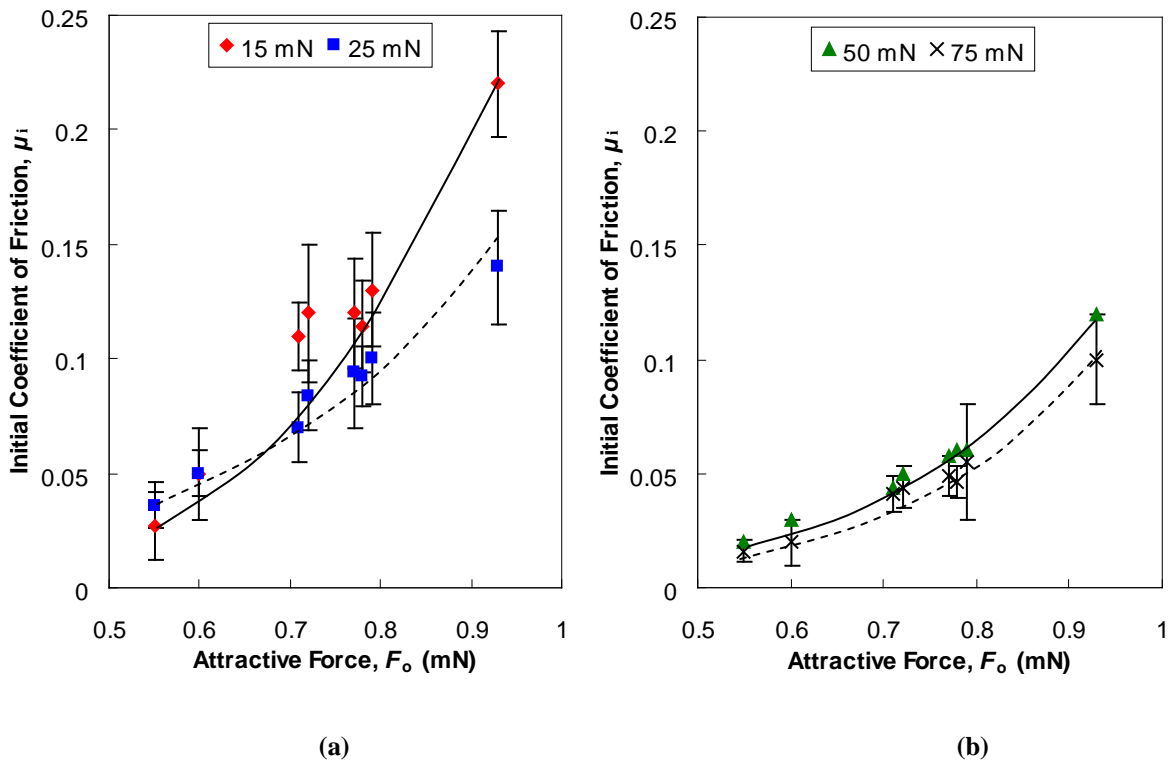


Figure 8.6: The initial coefficient of friction of UHMWPE film versus F_o for different applied loads; (a) low loads and (b) higher loads.

8.2.4 Material transfer between UHMWPE film and different surface energy balls

The tracks on UHMWPE films after two cycles of sliding against PFPE coated Si_3N_4 and untreated Si_3N_4 balls are shown in Figures 8.7 (A1 and B1) respectively. The tests were conducted under an applied load of 15 mN and a rotational speed of 2 rpm. The track on UHMWPE film, which was slid against low surface energy (PFPE coated) ball, shows some orientation of the polymer asperities made by the ball surface. Because of the low adhesion between UHMWPE film and PFPE coated ball, the probability of materials being pulled out, plastically deformed or scratched is very less.

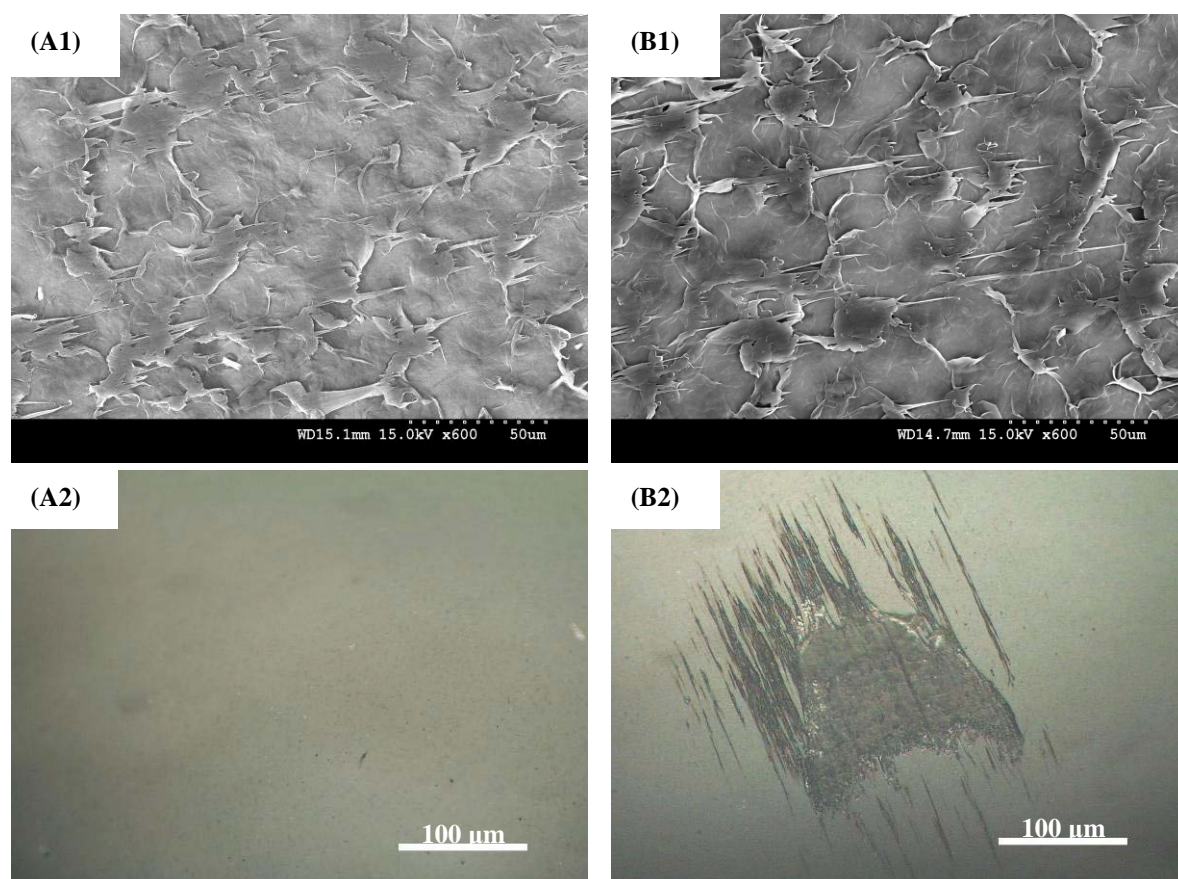


Figure 8.7: (A1) and (B1) are FESEM images of UHMWPE films after sliding against (A2) PFPE coated Si_3N_4 and (B2) bare Si_3N_4 balls respectively, where the applied load is 15 mN.

After the sliding test, the optical images of the ball surface were taken under an optical microscope. From the image, it is obvious that the amount of material transferred to PFPE coated ball was very less if any (Figure 8.7 A2). However when UHMWPE film was slid against high surface energy (untreated) ball, the track shows discontinuous scratches. It proves that high surface energy ball provides strong adhesion and as a result polymer is pulled out when sliding is introduced. The discontinuous nature of the scratch marks on the track suggests the effect of high surface energy in material removal of the counterface rather than scratching by the asperities on the ball surface which is very smooth (5 nm roughness). It is also clear in the optical image (Figure 8.7 B2) that lumps of polymer transfer easily to the ball surface when the surface energy of the ball is high. The microscopic images show the differences in the shear mechanisms when surfaces with different surface energies are involved. This basically governs the materials' wear characteristics.

8.3 Summary

In summary, we have studied the shear stress, τ , with the contact pressure, P on UHMWPE film in conjunction with the effect of attractive or pull-off force, F_o . Data show that τ increases linearly with increasing P as proposed by Bowden and Tabor whereas the pressure-independent initial shear stress, τ_o increases exponentially with F_o . Based on the trends between τ_o and F_o from the experimental data, an exponential relation is proposed. According to this model, the initial coefficient of friction, μ_i , increases exponentially with increasing F_o . Further, μ_i shows a decreasing trend with

increasing applied load, L , at a given F_0 for polymer surface because of its visco-elastic nature.

Since the attractive force is directly proportional to the surface energy (Equation 8.2), we can control friction by modifying the energies of the solids involved. This study will provide a better understanding of the initial friction and nanolubrication in small devices such as MEMS/NEMS where the surface energy of small moving parts can be easily changed and controlled. Surface energy is also directly responsible for the removal of the polymer material as wear debris.

Chapter 9

Conclusions and Future Recommendations

This Chapter will present the main conclusions from the present thesis and will suggest the recommendations for future study.

9.1 General conclusions

The main objectives of this thesis are to develop a new micron meter range polymer coating film that could be useful to industrial applications, to optimize the different coating and modification parameters for enhancing the friction and wear properties of the polymer film, and to understand the frictional behaviors of the polymer film with regards to the effects of sliding directions and surface energy that are inevitable in any actual working environments.

9.1.1 Optimizing the parameters for UHMWPE film

As stated at several places in this thesis, polymers are very promising as coatings because of their better tribological properties in their bulk form. Though polymers have many useful advantages to be used as coatings, there are very limited numbers of research papers that have studied the properties of polymer films. A polymer must be qualified in terms two major properties: low friction and high wear resistance in enhancing the tribological properties. After extensive study on the

tribology of bulk polymers, UHMWPE turned out to be the most suitable polymer for using as a coating film due to its low friction and excellent wear resistance.

In optimizing the parameters of UHMWPE film, this work has focused on the thickness of the UHMWPE film, the hardness of the substrate and the surface wettability of Si substrate which strongly influences the tribology of the UHMWPE film. A summary of the optimizing parameters and their respective wear durability of UHMWPE film are provided in Table 9.1.

9.1.1.1 Effect of thickness on tribology of UHMWPE film with and without DLC interface

1. The bare Si without any coating failed within 5 cycles. After coating 28 μm thickness UHMWPE onto Si, the coefficient of friction reduces to 0.18 and wear durability is increased to 20,000 cycles.
2. The presence of DLC as an intermediate layer provides higher load carrying capacity and better adhesion and as a result, the coefficient of friction decreases to 0.13 and the wear durability extends to 100,000 cycles for Si/DLC/UHMWPE.
3. Overcoating with PFPE as a top layer provides lower coefficient of friction of 0.06 and the wear durability increases to more than 300,000 cycles (test stopped due to long duration) for Si/DLC/UHMWPE/PFPE.
4. In studying the effect of UHMWPE thickness for Si/DLC/UHMWPE, it is observed that the wear lives of thin film (3.4 μm) and thick film (28 μm) are approximately 100,000 cycles. The wear lives of optimum (moderate)

thickness films are 200,000 cycles and more than 300,000 cycles for 6.2 μm and 12.3 μm , respectively.

Table 9.1: The summary of the optimizing parameters of UHMWPE film thickness, interface layer thickness and surface wettability of Si substrate with respect to their wear durability. All tests were conducted with a normal load of 40 mN at a range of sliding (0.052 m/s to 0.1 m/s) except some cases that are mentioned in remarks.

Sample	Thickness of UHMWPE film (μm)	Wear durability (cycles)	Reference	Remarks	
Effect of film thickness					
Si	Nil	5	Minn and Sinha 2008 a		
Si/UHMWPE	28 \pm 1	20000			
Si/UHMWPE/PFPE	28 \pm 1	100000			
Si/DLC57/UHMWPE	28 \pm 1	100000			
Si/DLC57/UHMWPE/PFPE	28 \pm 1	300000			
Si/DLC57/UHMWPE	3.4 \pm 1	100000			
Si/DLC57/UHMWPE	6.2 \pm 1	200000			Optimum thickness range
Si/DLC57/UHMWPE	12.3 \pm 1	300000			
Effect of hard interlayer					
Si/UHMWPE	4~5	1000	Minn and Sinha Submitted		
Si/CrN/UHMWPE		2000			
Si/DLC15/UHMWPE		50000			
Si/TiN/UHMWPE		300000			Best interfacial hardness range
Si/DLC57/UHMWPE		300000			
Si/DLC70/UHMWPE		300000			
Si/TiN/UHMWPE/PFPE		1 million			Applied load is 70 mN
Si/DLC57/UHMWPE/PFPE	1 million				
Si/DLC70/UHMWPE/PFPE	1 million				
Effect of surface energy of the substrate					
Si/UHMWPE	6 \pm 2	1000	Minn and Sinha 2008 b		
heated Si/UHMWPE		60000			
Si/APTMS/UHMWPE		100000			
Si-H/UHMWPE		250000			Optimum surface wettability
Si/OTS/UHMWPE		6500			

9.1.1.2 Effect of hard intermediate layer on tribology of UHMWPE film

1. In this study, it is observed that the wear durability of UHMWPE film is directly related to the hardness of the intermediate layer. The lowest hardness layer, bare Si/UHMWPE (film thickness is 4~5 μm), has a wear life of 1,000 cycles whereas the higher hardness layers, Si/TiN/UHMWPE, Si/DLC57/UHMWPE and Si/DLC70/UHMWPE have shown the wear lives of more than 300,000 cycles.
2. The critical loads from scratch tests are also consistent with the tribological test results, as Si/UHMWPE failed at 20 mN whereas Si/DLC70/UHMWPE with the hardest intermediate layer at 80 mN.
3. When the applied load is increased to 70 mN, the wear lives of Si/TiN/UHMWPE, Si/DLC57/UHMWPE and Si/DLC70/UHMWPE dropped to 8,000 cycles, 22,000 cycles and 120,000 cycles respectively. Thus, Si/DLC70/UHMWPE with the hardest interlayer shows the maximum wear durability.
4. Overcoating with PFPE as the top layer on the best three films further reduces the friction and extends the wear lives to more than one million cycles under an applied load of 70 mN and a sliding speed of 0.052 m/s.

9.1.1.3 Effect of surface wettability on tribology of UHMWPE film

1. The initial coefficients of friction are the same, approximately 0.17 regardless of the surface wettability of interfaces on Si substrate.

2. However, the wear durability of UHMWPE film is directly related to the surface wettability of the interfaces. The most hydrophilic interface, Si/UHMWPE, has a wear life of 1,000 cycles. The most hydrophobic interface, Si/OTS/UHMWPE, has a wear life of 6,500 cycles. Surfaces with intermediate wettability, heated Si/UHMWPE, Si/APTMS/UHMWPE and Si-H/UHMWPE have shown wear lives of 60,000 cycles, 100,000 cycles and 250,000 cycles, respectively.
3. The surface wettability of Si-H is 71° that is the best condition for better adhesion of UHMWPE film to Si substrate. The adhesion strength data studied from scratch test also confirmed that the critical load for Si-H/UHMWPE film was the highest at 70 mN.

9.1.2 Effects of unidirectional dry sliding on the frictional behaviors of UHMWPE film

The following conclusions can be drawn from the study of the frictional behaviors of UHMWPE with different sliding directions with respect to the number of sliding cycles:

1. Depending on the number of initial sliding cycles, the coefficient of friction is greatly different if a new sliding ball is slid in the forward and reverse directions.
2. During the initial sliding up to 50,000 cycles, the surface roughness increases before it finally becomes very smooth at around 50,000 cycles. The nanoindentation results showed that the polymer film becomes harder

because of changing molecular orientation and relative crystallinity effects.

The coefficient of friction remains on the higher side until the top film surface is completely modified.

3. When the sliding direction is reversed after certain number of cycles, because of the changes in the relative crystallinity and molecular orientation during initial sliding, the coefficient of friction in the reverse direction is higher than that in the forward direction.
4. As the sliding starts, the asperities of the top layer are plastically deformed that cover the original crystalline region of the film. Initial plastic deformation of the film leads to a decrease in the relative crystallinity in the middle range of sliding cycles (30,000-50,000 cycles) due to the change in the molecular orientation. Because of the lower crystallinity and higher number of sharp edges, the coefficients of friction in the reverse direction after 30,000 cycles and 50,000 cycles of sliding are higher than the lower and the higher number of initial sliding cycles.
5. After very large number of sliding cycles (100,000 cycles), there is no difference in the friction coefficients for forward and reverse directions.

9.1.3 Effects of surface energy of UHMWPE film on friction, adhesion and wear

In the last part of the thesis, the correlation between the friction of UHMWPE film and the surface energy has been studied. The surface energy or the surface wettability of a film could easily be changed due to many parameters such as temperature, humidity and chemical means etc. The following conclusions are drawn:

1. The higher surface energy promotes the attractive or pull-off force between surfaces which is dominant for soft surfaces at low normal loads
2. The present film of UHMWPE satisfies the Bowden and Tabor relation given as $\tau = \tau_0 + \alpha P$ where τ is the shear stress, τ_0 is the initial shear stress, α is the pressure coefficient of friction and P is the contact pressure.
3. The relation between the attractive force and the initial shear stress is observed to be exponential. Since the initial shear stress (τ_0) is directly proportional to the initial coefficient of friction, we can model the relation between the initial coefficient of friction and the attractive force (F_0) or surface energy by an exponential equation, $\tau_0 = c_1 \exp(n F_0)$ where c_1 and n are 9×10^{-5} MPa and 8.4 (mN)^{-1} , respectively, for UHMWPE film used in this work.
4. The initial coefficient of friction for UHMWPE film decreases with increasing applied load for a given surface energy because of the visco-elastic nature.
5. Since the attractive force is directly proportional to the surface energy, the coefficient of friction could be controlled by modifying the surface energies of the solids.

9.2 Future recommendations

The following recommendations are given for future study:

1. UHMWPE films using other coating techniques such as spin coating, sputtering can be thinner and uniform. The tribological properties of thinner films should be evaluated with different effects: load, speed, hardness etc.
2. The surface wettability of different hard intermediate layers is modified and further studies on the combined effect of hardness and surface wettability on UHMWPE film are necessary to be explored.
3. Chemical constituents can change the frictional behavior of UHMWPE film. Further studies on the friction with the effect of different chemical environments should be revealed.

References

- Advincula, R. C., Brittain, W. J., Caster, K. C. and Ruhe, J.** (2004) *Polymer brushes: synthesis, characterization and applications* (Wiley-VCH Verlag GmbH & Co.).
- Ajayi, O. O., Erdemir, A., Erck, R. A., Fenske, G. R. and Nichols, F. A.** (1991) 'The role of soft (metallic) films in the tribological behavior of ceramic materials', *Wear*, **149**, 221-232.
- Albrecht, T. and Strobl, G.** (1995) 'Temperature-dependent crystalline-amorphous structures in linear polyethylene: surface melting and the thickness of the amorphous layers', *Macromolecules*, **28**, 5827-5833.
- Alves, A. L. S., Nascimento, L. F. C. and Suarez, J. C. M.** (2005) 'Influence of weathering and gamma irradiation on the mechanical and ballistic behavior of UHMWPE composite armor', *Polymer Testing*, **24**, 104-113.
- Armstrong, R. D. and Wright, J. D.** (1993) 'Polymer protective coatings-the distinction between coating porosity and the wetted metal area', *Electrochimica Acta*, **38** (14), 1799-1801.
- Amstutz, H. C., Campbell, P., Kossarsky, N. and Clarke, I. C.** (1991) 'Mechanical and clinical significance of wear debris induced osteolysis', *Clinical Orthopaedics and Related Research*, **276**, 7-17.
- Aoike, T., Yokoyama, D., Uehara, H., Yamanobe, T. and Komoto, T.** (2007) 'Tribology of ultra-high molecular weight polyethylene disks molded at different temperatures', *Wear*, **262**, 742-748.
- Archard, J. F.** (1953) 'Contact and rubbing of flat surfaces', *Journal of Applied Physics*, **24**, 981-988.
- Arkles, B. Theberge, J. and Schireson, M.** (1977) 'Wear behavior of thermoplastic polymer-filled PTFE composites', *Lubrication Engineering*, **33**, 33-38.
- Arnell, R. D.** (1990) 'The mechanics of the tribology of thin film systems', *Surface and Coatings Technology*, **43-44**, 674-687.
- Aubert, A., Nabot, J. P. H., Ernoult, J. and Renaux, Ph.** (1990) 'Preparation and properties of MoS_x films grown by d.c. magnetron sputtering', *Surface and Coating Technology*, **41**, 127-134.
-
- Bahadur, S. and Tabor, D.** (1984) 'The wear of filled polytetrafluoroethylene', *Wear*, **98**, 1-13.
- Bahadur, S. and Gong, D.** (1992) 'The role of copper compounds as fillers in the transfer and wear behavior of polyetheretherketone', *Wear*, **154**, 151-165.
- Bahadur, S., Gong, D. and Anderegg, J. W.** (1993) 'Tribochemical studies by XPS analysis of transfer films of Nylon 11 and its composites containing copper compounds', *Wear*, **165**, 205-212.
- Bahadur, S. and Polineni, V. K.** (1996) 'Tribological studies of glass fabric-reinforced polyamide composites filled with CuO and PTFE', *Wear*, **200**, 95-104.

-
- Bahadur, S.** (2000) 'The development of transfer layers and their role in polymer tribology', *Wear*, **245** (1-2), 92-99.
- Barraud, A., Rosilio, P. H., Legressus, C. Okuzumi, H. and Mogami, A.** (1974) in *Proceedings of 8th International Conference on Electron Microscopy* (The Australian Academy of Science, Canberra), 682.
- Bau, Y., Zhang, T. and Gawne, D. T.** (2005) 'Influence of composition and process parameters on the thermal spray deposition of UHMWPE coatings', *Journal of Materials Science*, **40**, 77-85.
- Bijwe, J. and Tewari, U. S.** [1989] 'Friction and wear studies of a short glass-fibre-reinforced polyetherimide composite', *Wear*, **132**, 247-264.
- Bijwe, J. and Tewari, U. S.** [1990] 'Friction and wear studies of polyetherimide composites', *Wear*, **138**, 61-76.
- Bijwe, J., Logan, C. N. and Tewari, U. S.** [1990] 'Influence of fillers and fibre reinforcement on abrasive wear resistance of some polymeric composites', *Wear*, **138**, 77-92.
- Bijwe, J. and Rattan, R.** [2007 a] 'Carbon fabric reinforced polyetherimide composites: Optimization of fabric content for best combination of strength and adhesive wear performance', *Wear*, **262**, 749-758.
- Bijwe, J. and Rattan, R.** [2007 b] 'Influence of weave of carbon fabric in polyetherimide composites in various wear situations', *Wear*, **263**, 984-991.
- Blanchet, T., Kennedy, F. and Jayne, D.** (1993) 'XPS analysis of the effect of fillers on PTFE transfer film development in sliding contacts', *Tribology Transactions*, **36**, 535.
- Blanchet T. A.** (1997) *Friction, wear and PV limits of polymers and their composites*, in *Tribology data handbook*, (CRC Press, Boca Raton, New York), 547-562.
- Booser, E. R.** (1997) *Solid lubricants*, in *Tribology data handbook*, (CRC Press, Boca Raton, New York), 156-158.
- Bowden, F. P and Tabor, D.** (1943) 'The lubrication by thin metallic films and the action of bearing metals', *Journal of Applied Physics*, **14**, 141-151.
- Bowden, F.P. and Tabor, D.** (1973) *Friction: An introduction to tribology* (Anchor Books, New York).
- Bowden, F.P. and Tabor, D.** (1986) *The friction and lubrication of solids* (Clarendon Press, Oxford).
- Bradley, R. S.** (1932) *Philosophical Magazine*, **13**, 583.
- Briscoe, B. J., Scruton, B. and Willis, R. F.** (1973) 'The shear strength of thin lubricant films', *Proceedings of the Royal Society of London. Series A*, **333**, 99-114.
- Briscoe, B. J., Pogosian, A. K. and Tabor, D.** (1974) 'The friction and wear of high density polythene: The action of lead oxide and copper oxide fillers', *Wear*, **27**, 19-34.
- Briscoe, B. J. and Tabor. D.** (1975) 'The effect of pressure on the frictional properties of polymers', *Wear*, **34**, 29-38.
- Briscoe, B. J., Steward, M. D. and Groszek, A.** (1977) 'The effect of carbon aspect ratio on the friction and wear of PTFE', *Wear*, **42**, 99-107.
- Briscoe, B. J.** (1978) *Adhesion of elastomers in surface properties of polymers* (Plenum, London).
-

-
- Briscoe, B. J. and Tabor, D.** (1978 a) 'Shear properties of thin polymeric film', *Journal of Adhesion*, **9**, 145-155
- Briscoe, B. J. and Tabor, D.** (1978 b) *Friction and wear of polymers in surface properties* (Plenum, London).
- Briscoe, B. J.** (1981) 'Wear of polymers: An essay on fundamental aspects', *Tribology International*, **14** (4), 231-243.
- Briscoe, B. J., Pelillo, E. and Sinha, S. K.** (1996) 'Scratch hardness and deformation maps for polycarbonate and polyethylene', *Polymer Engineering and Science*, **36** (24), 2996-3005.
- Briscoe, B. J., Chateauminis, A., Lindley, T. C. and Parsonage, D.** (1998) 'Fretting wear behaviour of polymethylmethacrylate under linear motions and torsional contact conditions', *Tribology International*, **31**, 701-711.
- Briscoe, B. J. and Sinha, S. K.** (2002) 'Wear of polymers', *Proceedings of the Institution of Mechanical Engineers, Part J: Journal of Engineering Tribology*, **216**, 401-413.
- Buckle, H.** (1973) *The Science of Hardness Testing and Its Research Applications* (Metals Park, OH: American Society for Materials), 453.
- Burris, D. and Sawyer, W.** (2006) 'Improved wear resistance in alumina-PTFE nanocomposites with irregular shaped nanoparticles', *Wear*, **260**, 915-918.
- Callister, W. D. Jr.** (2007) *Materials Science and Engineering: An Introduction, Seventh Edition* (John Wiley & Sons, New Jersey).
- Clauss, F. J.** (1972) *Solid lubricants and self-lubricating solids* (Academic Press, New York).
- Cole, K. C., Ajji, A., Ward, I. M., Coated, P. D. and Dumoulin, M. M.** (2000) *Characterization of orientation in solid phase processing of polymers* (Carl Hanser Publications, Munich).
- Corwin, A. D. and de Boer, M. P.** (2004) 'Effect of adhesion on dynamic and static friction in surface micromachining', *Applied Physics Letters*, **84**, 2451-2453.
- Davey, S.M., Orr, J.F., Buchanan, F.J., Nixon, J.R., Bennett, D. B.** (2004) 'Measurement of molecular orientation in retrieved ultra-high-molecular-weight polyethylene (UHMWPE) hip sockets using fourier-transform infrared spectroscopy', *Strain*, **40**, 203-210.
- Derjaguin, B. V., Muller, V. M. and Toporov, Y. P.** (1975) 'Effect of contact deformations on the adhesion of particles', *Journal of Colloid and Interface Science*, **53**, 314-326.
- Devine, M. J.** (1976) *Proceedings of a workshop on wear control to achieve product durability AD-A055712* (Naval Air Development Center, Warminster, PA).
- Dowson, D.** (1998) *History of Tribology* (Longman, London and New York).
- Dunbar, C.** (1994) Surface preparation for continuously applied coatings, **Vol. 5**, *Surface Engineering* (ASM Handbook, USA), 1051.
-

-
- Edidin, A. A., Pruitt, L., Jewett, C. W., Crane, D. J., Roberts, D. and Kurtz, S. M.** (1999) 'Plasticity-induced damage layer is a precursor to wear in radiation-cross-linked UHMWPE acetabular components for total hip replacement', *The Journal of Arthroplasty*, **14** (5), 616-627.
- Edidin, A. A. and Kurtz, S. M.** (2000) 'The influence of mechanical behavior on the wear of four clinically relevant polymeric biomaterials in a hip simulator', *Journal of Arthroplasty*, **15**, 321-331.
- Eleiche, A. M. and Amin, G. M.** (1986) 'The effect of molecular orientation through uniaxial prestraining in poly(vinyl chloride) and polycarbonate on their friction and wear characteristics', *Wear*, **112**, 57-66.
- Elliott, A.** (1969) *Infra-red spectra and structure of organic long-chain polymers* (Edward Arnold (Publishers) Ltd, London), 48.
- Erdemir, A. and Donnet, C.** (2000) *Modern Tribology Handbook*, (CRP Press, Boca Ranton).
- Erdemir, A. and Donnet, C.** (2006) 'Tribology of diamond-like carbon films: recent progress and future prospects', *Journal of Physics D: Applied Physics*, **39**, R311-327.
- Erhard, G.** (1983) 'Sliding friction behaviour of polymer-polymer material combinations', *Wear*, **84**, 167-181.
- Ettles, C. M. McC and Shen, J. H.** (1987) 'The influence of frictional heating on the sliding friction of elastomers and polymers', *Rubber Chemistry and Technology*, **61**, 119-136.
- Extrand, C. W., Gent, A. N. and Kaany, S. Y.** (1990) 'Friction of a rubber wedge sliding on glass', *Rubber Chemistry and Technology*, **64**, 108-117.
- Fisher, J., Dowson, D., Hamdzah, H. and Lee, H. L.** (1994) 'The effect of sliding velocity on the friction and wear of UHMWPE for use in total artificial joints', *Wear*, **175**, 219-225.
- Fitzsimmons, V. G. and Zisman, W. A.** (1956) 'Thin films of polytetrafluoroethylene (Teflon) resin as lubricants and preservative coatings for metals', *NRL Report*, **4753**.
- Fitzsimmons, V. G. and Zisman, W. A.** (1958) 'Thin films of polytetrafluoroethylene resin as lubricants and preservative coatings for metals', *Industrial and Engineering Chemistry*, **50** (5), 781-784.
- Friedrich, K.** (1984) *Friction and wear of polymer composites* (VDI-Verlag, Germany)
- Friedrich, K., Cirino, M. and Pipes, R. B.** (1987 a) 'The abrasive wear behaviour of continuous fiber polymer composite', *Journal of Materials Science*, **22**, 2481-2492.
- Friedrich, K. and Voss, H.** (1987 b) 'On the wear behaviour of short-fiber-reinforced PEEK composites', *Wear*, **116**, 1-18.
- Friedrich, K., Cirino, M. and Pipes, R. B.** (1988) 'Evaluation of polymer composites for sliding and abrasive wear applications', *Composites*, **19**, 383-392.
- Friedrich, K., Karger-Kocsis, J. and Lu, Z.** (1991) 'Effects of steel counterface roughness and temperature on the friction and wear of PEEK composites under dry sliding conditions', *Wear*, **148**, 235-247.
-

-
- Friedrich, K., Lu, Z. and Hager, A. M.** (1996) 'Recent advances in polymer composites tribology', *Wear*, **190**, 139-144.
- Fusaro, R. L.** (1982) 'Effect of sliding speed and contact stress on tribological properties of ultra-high-molecular-weight polyethylene', *NASA Technical Paper*, **2059**.
- Gadow, R. and Scherer, D.** (2002) 'Composite coatings with dry lubrication ability on light metal substrates', *Surface and Coatings Technology*, **151-152**, 471-477.
- Ge, S., Wang, Q., Zhang, D., Zhu, H., Xiong, D., Huang, C. and Huang, X.** (2003) 'Friction and wear behavior of nitrogen ion implanted UHMWPE against ZrO₂ ceramic', *Wear*, **255**, 1069-1075.
- Good, R. J.** (1993) in *Contact Angle, Wettability and Adhesion*, Mittal, K. L. (ed.), (VSP International Science).
- Gorokhovskii, G. A. and Agulov, I. I.** (1966) 'Effect of orientation and crystallinity of the friction and wear of polytetrafluoroethylene', *Polymer Mechanics*, **2 (1)**, 87-92.
- Gough, V. E.** (1958 a) 'Friction of rubber, No. 1', *The Engineer*, **31 Oct**, 701-704.
- Gough, V. E.** (1958 b) 'Friction of rubber, No. 2', *The Engineer*, **31 Nov**, 741-743.
- Gracias, D.H. and Somorjai, G.A.** (1998) 'Continuum force microscopy study of the elastic modulus, hardness and friction of polyethylene and polypropylene surfaces', *Macromolecules*, **31**, 1269-1276.
- Gresham, R. M.** (1994) *Bonded solid film lubricants*, in *CRC Handbook of tribology and Lubrication*, **3**, (CRC Press, Boca Raton, Fla), 167-181.
- Grill, A. and Patel, V.** (1993) 'Tribological properties of diamond-like carbon and related materials', *Diamond and Related Materials*, **2**, 597-605.
- Grosch, K. A.** (1963) 'The relation between the friction and visco-elastic properties of rubber', *Proceedings of the Royal Society of London: Series A*, **274**, 21-39.
- Harrop, R. and Harrop, P. J.** (1969) 'Friction of sputtered PTFE films', *Thin Solid Films*, **3**, 109-117.
- He, G., Müser, M. H. and Robbins, M. O.** (1999) 'Adsorbed layers and the origin of static friction', *Science*, **284**, 1650-1652.
- He, G. and Robbins, M. O.** (2001) 'Simulations of the static friction due to adsorbed molecules', *Physical Review B*, **64**, 035413.
- Israelachvili, J. N. and Tabor, D.** (1972) 'The measurement of van der Waals dispersion forces in the range 1.5 to 130 nm', *Proceedings of the Royal Society of London. Series A*, **331**, 19-38.
- Jamison, W. E.** (1994) *Plastics and plastic matrix composites*, in *CRC Handbook of tribology and Lubrication*, **3**, (CRC Press, Boca Raton, Fla), 121-147.
- Jang, D-S. and Kim, D. E.** (1996) 'Tribological behavior of ultra-thin soft metallic deposits on hard substrates', *Wear*, **196**, 171-179.
-

-
- Janssen, A. P., Akhter, P., Harland, C. J. and Venables, J. A.** (1980) 'High spatial resolution surface potential measurements using secondary electrons', *Surface Science*, **93**, 453-470.
- Jiang, W., Malshe, A. P. and Wu, J.-H.** (2007) 'Bio-mimetic surface structuring of coating for tribological applications', *Surface and Coatings Technology*, **201**, 7889-7895.
- Johnson, K. L., Kendall, K. and Roberts, A. D.** (1971) 'Surface Energy and the Contact of Elastic Solids', *Proceedings of the Royal Society of London. Series A*, **324**, 301-313.
- Jost, H. P.** (1966) 'Lubrication (tribology) education and research', *Jost Report*, (Department of Education and Science, HMSO, London) 4.
- Jost, H. P.** (1990) 'Tribology - Origin and future', *Wear*, **136**, 1-17.
- Kanaga Karupiah, K. S., Bruck, A. L., Sundararajan, S., Wang, J., Lin, Z., Xu, Z.-H. and Li, X.** (2008) 'Friction and wear behavior of ultra-high molecular weight polyethylene as a function of polymer crystallinity', *Acta Biomaterialia*, **4** (5), 1401-1410.
- Kar, M. K. and Bahadur, S.** (1974) 'The wear equation for unfilled and filled polyoxymethylene', *Wear*, **30**, 337-348.
- Khonsari, M. M. and Booser, E. R.** (2008) *Applied Tribology: bearing designs and lubrication* (Wiley, England).
- Kitoh, M. and Honda, Y.** (1995) 'Preparation and tribological properties of sputtered polyimide film', *Thin Solid Film*, **271**, 92-95.
- Kurtz, S. M., Muratoglu, O. K., Evans, M. and Edidin, A. A.** (1999) 'Advances in the processing, sterilization, and crosslinking of ultra-high molecular weight polyethylene for total joint arthroplasty', *Biomaterials*, **20**, 1659-1688.
- Lancaster, J. K.** (1968) 'The effect of carbon fibre reinforcement on the friction and wear of polymers', *British Journal of Applied Physics*, **1**, 549-559.
- Lancaster, J. K.** (1969) 'Relationship between the wear of polymers and their mechanical properties', *Tribology Convention*, Institution of Mechanical Engineers, London, 100-108.
- Lancaster, J. K.** (1972) 'Lubrication of carbon fibre-reinforced polymer, Part I, water and aqueous solutions', *Wear*, **20**, 315-333.
- Lancaster, J. K.** (1973) 'Basic mechanisms of friction and wear of polymers', *Plastics and Polymers*, **41**, 297-306.
- Lancaster, J. K.** (1984) *Solid lubricants*, in *CRC Handbook of lubrication*, **2**, (CRC Press, Boca Raton, Fla), 269-299.
- Lavielle, L.** (1991) 'Polymer-polymer friction: relation to adhesion', *Wear*, **151**, 63-75.
- Lebovier, D., Gilormini, P. and Felder, E.** (1989) 'A kinematic model for plastic indentation of a bilayer', *Thin Solid Films*, **172**, 227-239.
- Lee, J.-Y. and Lim, D.-S.** (2004) 'Tribological behavior of PTFE film with nanodiamond', *Surface and Coatings Technology*, **188-189**, 534-538.
-

-
- Lee, L.** (1974) *Recent advances in polymer friction and wear*. (Gordon and Breach, New York).
- Lee, M. C. and Peppas, N. A.** (1993) 'Water transport in epoxy resins', *Progress in Polymer Science*, **18**, 947-961.
- Lei, R. Z., Gellman, A. J. and Jones, P.** (2001) 'Thermal stability of Fomblin Z and Fomblin Zdol thin films on amorphous hydrogenated carbon', *Tribology Letters*, **11** (1), 1-5.
- Lim, S. C. and Ashby, M. F.** (1987) 'Wear-mechanism maps', *Acta Metallurgica*, **35** (1), 1-24.
- Lim, S. C. and Ashby, M. F.** (1990) 'Wear-mechanism maps', *Scripta Metallurgica et Materialia*, **24** (5), 805-10.
- Liu, Z. H., Lemoine, P., Zhao, J. F., Zhou, D. M., Mailley, S., McAdams, E.T., Maguire, P., and McLaughlin, J.** (1998) 'Characterisation of ultra-thin DLC coatings by SEM/EDX, AFM and electrochemical techniques', *Diamond and Related Materials*, **7**, 1059-1065.
- Liu, Z. H., Zhao, J. F. and McLaughlin, J. A.** (1999) 'A study of microstructural and electrochemical properties of ultra-thin DLC coatings on AlTiC substrates deposited using the ion beam technique', *Diamond and Related Materials*, **8**, 56-63.
- Livermore, J., Duane, I. and Murray, B.** (1990) 'Effect of femoral head size on the wear of the polyethylene acetabular component', *Journal of Bone and Joint Surgery*, **72-A**, 518-528.
- Loomis, W. R.** (ed.) (1985) *New directions for solid lubricants in New directions in lubrication, materials, wear and surface interactions*, (Noyes Publications, Park Ridge, New Jersey), 631-733.
- Lubricomp.** (1998) *Internally lubricated reinforce thermoplastics and fluoropolymer composites* (LNP Engineering Plastics, Malvern, PA) 254-688.
- Ludema, K. C. and Tabor, D.** (1966) 'The friction and visco-elastic properties of polymeric solids', *Wear*, **9**, 329-348.
- Luzinov, I., Julthongpiput, D., Gorbunov, V. and Tsukruk, V. V.** (2001) 'Nanotribological behavior of tethered reinforced polymer nanolayer coatings', *Tribology International*, **34**, 327-333.
- Maboudian, R. and Howe, R. T.** (1997) 'Critical review: Adhesion in surface micromechanical structures', *Journal of Vacuum Science and Technology B*, **15**, 1-20.
- Maeda, N., Chen, N., Tirrell, M. and Israelachvili, J. N.** (2002) 'Adhesion and friction mechanisms of polymer-on-polymer surfaces', *Science*, **297**, 379-382.
- Makinson, K. R. and Tabor, D.** (1964) 'The friction and transfer of polytetrafluoroethylene', *Proceedings of the Royal Society of London: Series A*, **281**, 49-61.
- Manika, I. and Maniks, J.** (1992) 'Characteristics of deformation localization and limits to the microhardness testing of amorphous and polycrystalline coatings', *Thin Solid Films*, **208**, 223-227.
-

- Mansfeld, F.** (1995) 'Use of electrochemical impedance spectroscopy for the study of corrosion protection by polymer coatings', *Journal of Applied Electrochemistry*, **25** (3), 187-202.
- Mansfeld, F., Han, L. T., Lee, C. C. and Zhang, G.** (1998) 'Evaluation of corrosion protection by polymer coatings using electrochemical impedance spectroscopy and noise analysis', *Electrochimica Acta*, **43**, 2933-2945.
- Mastrangelo, C. H.** (1997) 'Adhesion-related failure mechanisms in micromechanical devices', *Tribology Letters*, **3**, 223-238.
- Mate, C. M.** (2008) *Tribology on the small scale: A bottom up approach to friction, lubrication and wear* (Oxford University Press, Oxford and New York).
- Mens, J. W. M. and de Gee, A. W. J.** (1991) 'Friction and wear behavior of 18 polymers in contact with steel in environments of air and water', *Wear*, **149**, 255-268.
- Minn, M. and Sinha, S. K.** (2008 a) 'DLC and UHMWPE as hard/soft composite film on Si for improved tribological performance', *Surface & Coatings Technology*, **202**, 3698-3708.
- Minn, M., Leong, J. Y. and Sinha, S.K.** (2008 b) 'Effects of interfacial energy modifications on the tribology of UHMWPE coated Si', *Journal of Physics D: Applied Physics*, **41**, 055307.
- Minn, M. and Sinha, S. K.** (2009) 'Molecular orientation, crystallinity, and topographical changes in sliding and their frictional effects for UHMWPE film', *Tribology Letter*, **34**, 133-140.
- Moy, P. and Karasz, F. E.** (1980) 'Epoxy-water interactions', *Polymer Engineering and Science*, **20**, 315-319.
- Muratoglu, O. K., Bragdon, C. R., O'Connor, D. O., Jasty, M., Harris, W. H., Gul, R. and McGarry, F.** (1999) 'Unified wear model for highly crosslinked ultra-high molecular weight polyethylenes (UHMWPE)', *Biomaterials*, **20**, 1463-1470.
- Muratoglu, O. K., Bragdon, C. R., O'Connor, D. O., Jasty, M. and Harris, W. H.** (2001) 'A novel method of cross-linking ultra-high-molecular-weight polyethylene to improve wear, reduce oxidation, and retain mechanical properties: Recipient of the 1999 HAP Paul Award', *The Journal of Arthroplasty*, **16** (2), 149-160.
- Müser, H. M., Wenning, L. and Robbins, M. O.** (2001) 'Simple microscopic theory of amontons's laws for static friction', *Physical Review Letters*, **86**, 1295-1298.
- Ng, C. B., Schadler, L. S. and Siegel, R. W.** (1999) 'Synthesis and mechanical properties of TiO₂-epoxy nanocomposites', *Nanostructure Materials*, **12**, 507-510.
- Ng, C. B., Ash, B. J., Schadler, L. S. and Siegel, R. W.** (2001) 'A study of the mechanical and permeability properties of nano- and micron-TiO₂ filled epoxy composites', *Advanced Composites Letters*, **10**, 101-111.
- Nogueira, P., Rami'rez, C., Torres, A., Abad, M. J., Cano, J., Lo'pez, J., Lo'pez-Bueno, I. and Barral, L.** (2001) 'Effect of water sorption on the structure and mechanical properties of an epoxy resin system', *Journal of Applied Polymer Science*, **80**, 71-80.

- O'Brien, E. P., White, C. C. and Vogt B. D.** (2006) 'Correlating interfacial moisture content and adhesive fracture energy of polymer coatings on different surfaces', *Advanced Engineering Materials*, **8**, 114-118.
- OECD.** (1969) *Glossary of Terms and Definitions in the Field of Friction, Wear and Lubrication – Tribology* (Research Group on Wear of Engineering Materials, OECD, Paris)
- Opondo, M. N. and Bassell, T. J.** (1982) 'Wear of rigid PVC in relation to water pump designs', *Tribology International*, **15** (2), 75-83.
- Peterson, M. B.** (1979) 'Technical options for conservation of metals: Case studies of selected metals and products', OTA-M-97.
- Petrovicova, E., Knight, R., Schadler, L. and Twardowski, T.** (2000) 'Nylon 11/silica nanocomposite coatings applied by the HVOF process. II. Mechanical and barrier properties', *Journal of Applied Polymer Science*, **78** (13), 2272-2289.
- Pooley, C. M. and Tabor, D.** (1972) 'Friction and molecular structure: the behaviour of some thermoplastics', *Proceedings of the Royal Society of London: Series A*, **329**, 251-274.
- Rabinowicz, E.** (1976) 'Wear', *Materials Science and Engineering*, **25**, 23-28.
- Ratner, S. N., Farberoua, I. I., Radyukeuich, O. V. and Lure, E. G.** (1964) 'Correlation between wear resistance of plastics and other mechanical properties', *Soviet Plastics*, **7**, 37-45.
- Rattan, R., Bijwe, J. and Fahim, M.** [2008] 'Optimization of weave of carbon fabric for best combination of strength and tribo-performance of polyetherimide composites in adhesive wear mode' *Wear*, **264**, 96-105.
- Rauhut, H. W.** (1969) 'Pretreating polyethylene for optimum structural adhesive joints', *Adhesives Age*, **12**, 28-34.
- Ren S, Yang S. R, and Zhao Y. P.** (2004) 'Preparation and tribological studies of C60 thin film chemisorbed on a functional polymer surface', *Langmuir*, **20** (9), 3601-3605.
- Reynaud, E., Jouen, T., Gauthier, C., Vigier, G. and Varlet, J.** (2001) 'Nanofillers in polymeric matrix: a study on silica reinforced PA6', *Polymer*, **42**, 8759-8768.
- Reynolds, O.** (1886) 'On the theory of lubrication and its application to Mr. Beauchamp Tower's experiments, Including an experimental determination of viscosity of olive oil', *Philosophical Transactions of the Royal Society of London*, **177** (1886), 157-234.
- Ricklin, S and Miller, R. R.** (1954) *Materials and Methods*, **112 Oct.**
- Robertson, J.** (1992) 'Mechanical properties and structure of diamond-like carbon', *Diamond and Related Materials*, **1**, 397-406.
- Ross, J. D. J., Pollock, H. M., Pivin, J. C. and Takadoum, J.** (1987) 'Limits to the hardness testing of films thinner than 1 μm ', *Thin Solid Films*, **148**, 171-180.
- Rottler, J. and Robbins, M. O.** (2001) 'Yield conditions for deformation of amorphous polymer glasses', *Physical Review E*, **64**, 051801.
- Ryntz, R. A.** (1994) 'Coating adhesion to low surface free energy substrates', *Progress in Organic Coatings*, **25**, 73-83.

- Sakata, H., Kobayashi, M., Otsuka, H. and Takahara, A.** (2005) 'Tribological properties of poly (methyl methacrylate) brushes prepared by surface-initiated atom transfer radical polymerization', *Polymer Journal*, **37**, 767-775.
- Santner, E. and Czichos, H.** (1989) 'Tribology of polymers', *Tribology International*, **22**, 103-109.
- Satyanarayana, N. and Sinha, S. K.** (2005) 'Tribology of PFPE overcoated self-assembled monolayers deposited on Si surface', *Journal of Physics D: Applied Physics*, **38**, 3512-3522.
- Satyanarayana, N., Sinha, S. K. and Ong, B. H.** (2006) 'Tribology of a novel UHMWPE/PFPE dual film coated onto Si surface', *Sensors and Actuators A: Physical*, **128** (1), 98-108.
- Sawyer, W., Freudenberg, K., Bhimaraj, P. and Schadler, L.** (2003) 'A study on the friction and wear behavior of PTFE filled with alumina nanoparticles', *Wear*, **254**, 573-580
- Schonhorn, H. and Ryan, F. W.** (1969) 'Adhesion of polytetrafluoroethylene', *The Journal of Adhesion*, **1**, 43-47.
- Schwartz, C. J. and Bahadur, S.** (2001) 'The role of filler deformability, filler-polymer bonding, and counterface material on the tribological behavior of polyphenylene sulfide (PPS)', *Wear*, **251**, 1532-1540.
- Sidorenko, A., Ahn, H. S., Kim, D. I., Yang, H. and Tsukruk, V. V.** (2002) 'Wear stability of polymer nanocomposite coatings with trilayer architecture', *Wear*, **252**, 946-955.
- Siegel, R., Chang, S., Ash, B., Stone, J., Ajayan, P., Doremus, R. and Schadler, L.** (2001) 'Mechanical behavior of polymer and ceramic matrix nanocomposites', *Scripta Materialia*, **44**, 2061-2064.
- Sherbinney, M. A. and Halling, J.** (1977) 'Friction and wear of ion-plated soft metallic films', *Wear*, **45**, 211-220.
- Shi, W., Li, X. Y. and Dong, H.** (2001) 'Improved wear resistance of ultra-high molecular weight polyethylene by plasma immersion ion implantation', *Wear*, **250**, 544-552.
- Shipway, P. H. and Ngao, N. K.** (2003) 'Microscale abrasive wear of polymeric materials', *Wear*, **255**, 742-750.
- Simis, K. S., Bistolfi, A., Bellare, A. and Pruitt, L. A.** (2006) 'The combined effects of crosslinking and high crystallinity on the microstructural and mechanical properties of ultra high molecular weight polyethylene', *Biomaterials*, **27**, 1688-1694.
- Shooter, K. V. and Thomas, O. H.** (1949) 'Frictional properties of some plastics', *Research*, **2**, 533-535.
- Solvay Solexis**, (2009)
http://www.solvaysolexis.com/static/wma/pdf/5/4/3/4/fom_thin.pdf
last accessed in July, 2009.
- Spalvins, T. and Buzek, B.** (1981) 'Frictional and morphological characteristics of ion-plated soft metallic films', *Thin Solid Films*, **84**, 267-272.
- Speersneider, C. J. and Li, C. H.** (1962) 'The role of filler geometrical shape in wear and friction of filled PTFE', *Wear*, **5**, 392-399.
- Sperling, L. H.** (2006) *Introduction to physical polymer science* (Wiley, Hoboken, NJ).

-
- Steijn, R. P.** (1968) 'The sliding surface of polytetrafluoroethylene: an investigation with the electron microscope', *Wear*, **41**, 193-212.
- Suh, N. P.** (1986) *Tribophysics* (Prentice-Hall, Englewood Cliffs, New Jersey).
- Sun, C., Zhou, F., Shi, L., Yu, B., Gao, P., Zhang, J. and Liu, W.** (2006) 'Tribological properties of chemically bonded polyimide films on silicon with polyglycidyl methacrylate brush as adhesive layer', *Applied Surface Science*, **253**, 1729-1735.
- Tabor, D. and Williams, D. E. W.** (1961) 'The effect of orientation on the friction of polytetrafluoroethylene', *Wear*, **4**, 391-400.
- Tabor, D.** (1977) 'Surface forces and surface interactions', *Journal of Colloid and Interface Science*, **58**, 2-13.
- Tabor, D.** (1995) 'Tribology - the last 25 years: A personal view', *Tribology International*, **28** (1), 7-10.
- Tanaka, K., Uchiyama, Y. and Toyooka, S.** (1973) 'The mechanism of wear of polytetrafluoroethylene', *Wear*, **23**, 153-172.
- Tanaka, K. and Miyata, T.** (1977) 'Studies on the friction and transfer of semicrystalline polymers', *Wear*, **41**, 383-398.
- Tay, B. K., Sheeja, D., Choong, Y. S., Lau, S. P., and Shi, X.** (2000) 'Pin-on-disk characterization of amorphous carbon films prepared by filtered cathodic vacuum arc technique', *Diamond and Related Materials*, **9**, 819-824.
- Tetrault, D. M. and Kennedy, F. E.** (1989) 'Friction and wear of ultra high molecular weight polyethylene on Co-Cr and titanium alloys in dry and lubricated environments', *Wear*, **133**, 295-307.
- Tewari, U. S. and Bijwe, J.** [1991] 'Comparative studies on sliding wear of polyimide composites', *Composites*, **22** (3), 204-210.
- Tian, H. and Matsudaira, T.** (1993) 'The role of relative humidity, surface roughness and liquid build-up on static friction behavior of the head/disk interface', *ASME Journal of Tribology*, **115** (1), 28-35.
- Tower, B.** (1883) 'First report on friction experiments', *Proceedings of the Institute of Mechanical Engineers*, 632-659.
- Tsuya, Y. and Takagi, R.** (1964) 'Lubricating properties of lead films on copper', *Wear*, **7**, 131-143.
- Turell, M. B. and Bellare, A.** (2004) 'A study of the nanostructure and tensile properties of ultra-high molecular weight polyethylene', *Biomaterials*, **25**, 3389-3398.
- Tyndall, G. W., Leezenberg, P. B. and Castenada, J.** (1998) 'Interfacial interactions of perfluoropolyether lubricants with magnetic recording media', *Tribology Letters*, **4**, 103-108.
- Ulman, A.** (1991) *An introduction to ultrathin organic films* (Academic Press, USA).
- van Oss, C. J.** (1994 a) *Interfacial Force in Aqueous Media* (Marcel Dekker, New York) 20-21.

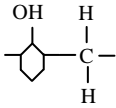
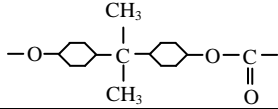
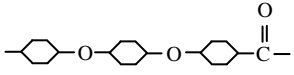
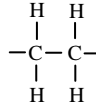
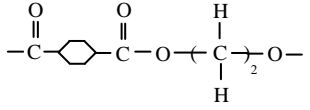
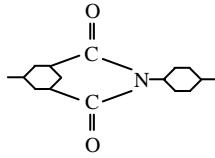
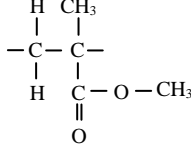
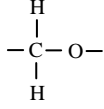
-
- van Oss, C. J.** (1994 b) *Interfacial Force in Aqueous Media* (Marcel Dekker, New York) 171-175.
- Vande Voort, J. and Bahadur, S.** (1995) 'The growth and bonding of transfer film and the role of CuS and PTFE in the tribological behavior of PEEK', *Wear*, **181-183**, 212-221.
- Vogt, B. D., Soles, C. L., Jones, R. L., Wang, C-Y., Lin, E. K., Wu, W-L., Satiji, S. K., Goldfarb, D. L. and Angelopoulos, M.** (2004) 'Interfacial effects on moisture absorption in thin polymer films', *Langmuir*, **20**, 5285-90.
- Wang, A., Sun, D. C., Yau, S. S., Edwards, B., Sokol, M., Essner, A., Polineni, V. K., Stark, C. and Dumbleton, J. H.** (1997) 'Orientation softening in the deformation and wear of ultra-high molecular weight polyethylene', *Wear*, **203**, 230-241.
- Wang, Q., Xu, J., Shen, W. and Liu, W.** (1996) 'An investigation of the friction and wear properties of nanometer Si₃N₄ filled PEEK', *Wear*, **196**, 82-86.
- Weightman, B. and Light, D.** (1986) 'The effect of the surface finish of alumina and stainless steel on the wear rate of UHMWPE', *Biomaterials*, **7**, 20-4.
- Wong, T. C. and Broutman, L. J.** (1985) 'Water in epoxy resins: II. Diffusion mechanism', *Polymer Engineering and Science*, **25**, 529-534.
- Xu, Z. R. and Ashbee, K. H. G.** (1991) 'The radial-distribution of axial stress around a single fiber in epoxy-resin undergoing water-uptake', *Journal of Composite Materials*, **25**, 760-773.
- Xue, Q. and Wang, Q.** (1997) 'Wear mechanisms of polyetheretherketone composites filled with various kinds of SiC', *Wear*, **213**, 54-58.
- Yamada, S.** (2003) 'Layering transitions and tribology of molecularly thin films of poly(dimethylsiloxane)', *Langmuir*, **19**, 7399-7405.
- Yamada, Y. and Tanaka, K.** (1986) 'Effect of the degree of crystallinity on the friction and wear of poly(ethylene terephthalate) under water lubrication', *Wear*, **111**, 63-72.
- Yoshizawa, H., Chen, Y-L. and Israelachvili, J. N.** (1993) 'Fundamental Mechanisms of Interfacial Friction. 1. Relation between Adhesion and Friction', *Journal of Physical Chemistry*, **97**, 4128-4140.
- Yoon, R-H., Flinn, D. H. and Rabinovich, Ya. I.** (1997) 'Hydrophobic interactions between dissimilar surfaces', *Journal of Colloid and Interface Science*, **185**, 363-370.
- Yu, L. and Bahadur, S.** (1998) 'An investigation of the transfer film characteristics and the tribological behaviors of polyphenylene sulfide composites in sliding against tool steel', *Wear*, **214**, 245-251.
- Zeng, K.** (2009) *Nanoindentation and indentation creep of polymeric materials in Polymer tribology* (Imperial College Press, 2009).
-

-
- Zhao, Q. and Bahadur, S.** (1999) 'The mechanism of filler action and the criterion of filler selection for reducing wear', *Wear*, **225-229**, 660-668.

Appendix A

The Tribological Properties of Bulk Polymers

Table A.1: Tribological properties of bulk polymers.

Polymer	Chemical structure	Static friction	Kinetic friction	Wear rate ($10^{-15} \text{m}^3 / \text{Nm}$)	Reference
Phenol-formaldehyde (Phenolic)		-	0.78	29	<i>a</i>
Polycarbonate (PC)		0.31	0.38	50	<i>b</i>
Polyetheretherketone (PEEK)		0.2	0.25	4.0	<i>b</i>
Ultra high molecular weight polyethylene (UHMWPE)		-	0.2	0.1-1.6	<i>c</i>
Polyethylene terephthalate (PET)		-	-	3.2	<i>d</i>
Polyimide (PI)		-	0.65	1.7	<i>a</i>
Polymethylmethacrylate (PMMA)		-	0.55	170	<i>a</i>
Polyoxymethylene (POM, Acetal)		-	0.45	2.1	<i>e</i>

Appendix A: The Tribological Properties of Bulk Polymers

Polystyrene (PS)	$ \begin{array}{cccc} \text{H} & \text{H} & \text{H} & \text{H} \\ & & & \\ -\text{C}- & \text{C}=\text{C}- & \text{C}- & \text{C}- \\ & & & \\ \text{H} & & & \text{C}_6\text{H}_5 \end{array} $	0.28	0.32	60	^b
Polytetrafluoroethylene (PTFE)	$ \begin{array}{cc} \text{F} & \text{F} \\ & \\ -\text{C}- & \text{C}- \\ & \\ \text{F} & \text{F} \end{array} $	0.04	0.05	100	^f

^aLancaster 1968, ^bLubricomp 1998, ^cTetrault 1989, ^dSantner 1989, ^eMens 1991 and ^fArkles 1977.